Spatial Spread of Rabies in Wildlife

by

Hao Liu

A Dissertation Presented in Partial Fulfillment
of the Requirement for the Degree
Doctor of Philosophy

Approved November 2013 by the
Graduate Supervisory Committee:

Yang Kuang, Chair
Zdzislaw Jackiewicz
Nicolas Lanchier
Hal Smith
Horst Thieme

ARIZONA STATE UNIVERSITY

December 2013

ABSTRACT

Rabies disease remains enzootic among raccoons, skunks, foxes and bats in the United States. It is of primary concern for public-health agencies to control spatial spread of rabies in wildlife and its potential spillover infection of domestic animals and humans. Rabies is invariably fatal in wildlife if untreated, with a non-negligible incubation period. Understanding how this latency affects spatial spread of rabies in wildlife is the concern of chapter 2 and 3. Chapter 1 deals with the background of mathematical models for rabies and lists main objectives. In chapter 2, a reaction-diffusion susceptible-exposed-infected (SEI) model and a delayed diffusive susceptible-infected (SI) model are constructed to describe the same epidemic process – rabies spread in foxes. For the delayed diffusive model a non-local infection term with delay is resulted from modeling the dispersal during incubation stage. Comparison is made regarding minimum traveling wave speeds of the two models, which are verified using numerical experiments. In chapter 3, starting with two Kermack and McKendrick's models where infectivity, death rate and diffusion rate of infected individuals can depend on the age of infection, the asymptotic speed of spread c^* for the cumulated force of infection can be analyzed. For the special case of fixed incubation period, the asymptotic speed of spread is governed by the same integral equation for both models. Although explicit solutions for c^* are difficult to obtain, assuming that diffusion coefficient of incubating animals is small, c^* can be estimated in terms of model parameter values. Chapter 4 considers the implementation of realistic landscape in simulation of rabies spread in skunks and bats in northeast Texas. The Finite Element Method (FEM) is adopted because the irregular shapes of realistic landscape naturally lead to unstructured grids in the spatial domain. This implementation leads to a more accurate description of skunk rabies cases distributions.

ACKNOWLEDGEMENTS

I would like to thank my parents for supporting and encouraging me. I also would like to thank my advisor Professor Yang Kuang for so many useful insights and suggestions, and most of all, for his patience, also to Professor Horst Thieme for helping me with the analysis and calculations in Chapter 3, and thanks to all other committee members Professor Hal Smith, Zdzislaw Jackiewicz and Nicolas Lanchier for all the advices. Thanks for the support to all my friends, my colleagues and my cat “Funding”, who must be scratching his head while watching birds outside the window now.

TABLE OF CONTENTS

CHAPTER Page

CHAPTER Page

LIST OF TABLES

LIST OF FIGURES

Figure Page

Figure Page

Figure Page

Figure Page

Chapter 1

MOTIVATION

1.1 Introduction

Rabies virus, a member of the *Lyssavirus* genus and *Rhabdoviridae* family, is a neurotropic, single-stranded and negative-sense RNA virus (Kaplan, 1985). The first case of rabies is found by a Roman physician called Celsus (Jackson and Wunner, 2002a). The rabies virus afflicts humans, domestic and wildlife animals, causing central nervous system infections that lead to quick death (Kaplan, 1985). Rabies is usually transmitted via bite by infected animals, when virus carried in the saliva of infected animals enters the body (Jackson and Wunner, 2002b). Due to advancement of medical technologies, human mortality from rabies is rare nowadays, but rabies still causes thousands of human deaths in a few countries, such as Africa and India (Sterner and Smith, 2006). Usually rabies infection is fatal once the virus already lodges in the central nervous system, so precautionary measure before and immediately after bite by infected animals is vital.

Rabies is also maintained in some wildlife reservoir species, such as raccoons, foxes, skunks and bats (CDC, 2011). Although rabies virus is well understood and effective vaccines exists, it still causes great concerns among epidemiologists, because rabies still persists in wildlife animals, and the economic cost of distributing vaccines to wildlife animals and the potential infections in endangered animals make studies of rabies, in particular spatial dynamics, essential. Attempts to control rabies spread in wildlife animals have been made in various ways. The methods include population reduction and vaccination. Population reduction measures include gassing, trapping, baits and hunting. So far in North America, trapping and distribution of vaccines are most widely used methods (Lyles and

Rupprecht, 2007; Pybus, 1988).

There are three major well-studied rabies epidemic geographic expansions: one in Europe associated with rabies in red fox (*Vulpes vulpes*), one in the US related to rabies spread in raccoon and the last one in Canada associated with rabies in arctic fox, red fox and raccoon (Rupprecht *et al.*, 1995). Currently in the US rabies in terrestrial wildlife is endemic in raccoon in the Eastern US, skunks in the Midwestern US and California, while endemic rabies in red and gray foxes is now uncommon in the US (Jackson, 2011).

1.2 Background of mathematical rabies models

With various control methods at hand and rabies still spreading in wildlife animals, it is important to understand the progression of rabies epizootic wavefront into uninfected geographic areas. There have been various mathematical models developed for studies of rabies, and the development of these models has been mostly guided by the development of mathematical methods for infectious disease problems in general. Early rabies models bore resemblance with early models for other diseases. For epidemiologists the original primary concern was the spread of rabies throughout a population. Hence compartmental systems of ordinary differential equations (ODE) have been proposed (Capasso, 1991; Keeling and Rohani, 2008), where populations of animals are subdivided into susceptible, infectious and recovered/removed classes, and sometimes an exposed class is added that accounts for the incubation period between contraction of rabies and onset of clinical symptoms. These compartmental systems hence followed the basic "SEIR" framework (Anderson and May, 1979, 1981). The dynamics of these rabies models are summarized in the construction of systems of ODEs for either a single population or a network of many populations (metapopulations). Analysis of these models could then translate into prediction or evaluation of temporal or spatial rabies patterns within or between populations.

1.2.1 Early mathematical approach to rabies dynamics

Following World War II, an epizootic expansion of rabies virus in red fox (*V. vulpes*) populations originating from Eastern Europe caught epidemiologists' attention. The epizootic rabies wave traveled at an approximately constant speed towards Western Europe. In order to understand the rabies disease emergence and spread, some earliest mathematical models (Anderson *et al.*, 1981) that used the basic "SEIR" compartmental framework were constructed to derive some important characteristics of the rabies epizootic in red fox, including the basic reproductive number (R_0) for the disease. The basic reproductive number (R_0) stands for the number of secondary infections caused by a single infection placed in a completely susceptible population (Mollison, 1995). Based on this R_0 a critical threshold density for susceptible foxes S_c can be calculated below which a rabies epizootic cannot be established. With the critical threshold S_c, even if the early models were not spatially explicit, it is possible to recommend what level of population control, for example culling, would be required for a given location.

The following system of ODEs was adapted from these earliest compartmental models (Anderson *et al.*, 1981):

$$\begin{aligned} \frac{\mathrm{d}S}{\mathrm{d}t} &= rS - \gamma SN - \beta SI \\ \frac{\mathrm{d}E}{\mathrm{d}t} &= \beta SI - \gamma EN - (\sigma + b)E \\ \frac{\mathrm{d}I}{\mathrm{d}t} &= \sigma E - \gamma IN - (\alpha + b)I \end{aligned} \tag{1.1}$$

where S, E, I are population densities for susceptible, exposed and infected foxes, $N = S + E + I$ is the total population density. $r = a - b$ is the intrinsic population growth rate, with a, b the per capita birth and death rates. Infectious, or rabid, foxes are under greater risk of mortality, which is represented by the additional death rate α. $1/\sigma$ is the average length of time a fox stays in the exposed class before onset of clinical symptoms. γ is the additional competition-induced mortality.

Also note that in (1.1) the recovered class is absent. This is consistent with convention of early rabies models where there was no evidence suggesting development of natural immunity against rabies in the absence of vaccination among infected foxes.

It was also assumed (Anderson *et al.*, 1981) that a few fox rabies infections were introduced in a totally susceptible population at its stable equilibrium r/γ, which is obtained by setting the right hand side of S equation equal to 0 while assuming $E = I = 0$. Solving the system defined in (1.1), it was calculated that the minimum density of foxes for rabies infection to spread was

$$S_c = \frac{(\sigma + a)(\alpha + a)}{\beta\sigma}$$

and the reproductive number R_0 was given as

$$R_0 = \frac{r/\gamma}{S_c} = \frac{r\beta\sigma}{\gamma(\sigma + a)(\alpha + a)}.$$

Based on available ecological data for foxes (MacDonald, 1980), it was determined in (Anderson *et al.*, 1981) that the critical threshold $S_c \approx 0.99$ foxes/km^2.

Since at the time of these early models oral vaccines for rabies had not been invented or produced, these findings suggested population culling for areas with a fox density exceeding $S_c \approx 0.99$ foxes/km^2, which would be a surpassingly difficult and expensive project to manage given the large dimensions of affected areas.

1.2.2 Approaches based on reaction diffusion methods

The system (1.1) of ODEs from (Anderson *et al.*, 1981) was constructed at almost the same time as when fox rabies infection wave front was advancing southwesterly into France and Switzerland. To understand this spatial propagation of rabies virus, MacDonald et al began descriptive studies (MacDonald, 1980; MacDonald *et al.*, 1981) into responsible ecological factors, such as fox densities or habitat properties. Following these studies, Murray et al (Kallen *et al.*, 1985; Murray *et al.*, 1986; Murray, 1989; Murray and Seward, 1992)

performed a series of famous studies into spatial rabies spread. He proposed and analyzed in consecutive papers several reaction diffusion models to describe this persistent propagating wave of rabies infection in red fox. The importance of these studies lies not only in the introduction of an even more sophisticated mathematical tool to the modeling process, but also in allowing the predictive modeling that suggested how transmission barriers could be implemented before the arrival of epizootic wave fronts.

The model used by Murray *et al.* (1986) was formulated using the following system of partial differential equations (PDEs)

$$\begin{aligned}
\frac{\partial S(x,t)}{\partial t} &= rS\left(1-\frac{N}{K}\right) - \beta SI \\
\frac{\partial E(x,t)}{\partial t} &= \beta SI - \frac{rNE}{K} - (\sigma + b)E \\
\frac{\partial I(x,t)}{\partial t} &= \sigma E - \frac{rNI}{K} - (\alpha + b)I + D\frac{\partial^2 I}{\partial x^2}
\end{aligned} \tag{1.2}$$

where most parameters are identical to those in (1.1) except the replacement of γ by r/K and the addition of a diffusion term $D\frac{\partial^2 I}{\partial x^2}$ at the end of the I equation. The diffusion term reflects the random movement of infectious rabid foxes due to rabid clinical symptoms, most notably disorientation. Applying similar parameter values as in (Anderson *et al.*, 1981; MacDonald, 1980), it was estimated in (Andral *et al.*, 1982; Murray *et al.*, 1986) that the rate of movement for rabid red foxes was approximately 50 km^2/year.

Although, different from (1.1) system (1.2) is composed of coupled PDEs and can describe properties of spatial spread, it makes similar assumptions to those from ODEs in (1.1), the most important of which is the assumption that the population is well mixed, homogeneous and all parameters are constant in both time and space. An important consequence of this assumption in the context of reaction diffusion equations defined in (1.2) is that an epidemic wave will maintain its shape and traveling speed v as it propagates through the space. In mathematical terms this translates into a solution of the form $f(z) = f(x+vt)$ with $z = x + vt$. In addition to the diffusion rate D, the traveling wave speed v is another

important quantity to characterize the rabies epizootic wave propagation. But usually solving the resulting system of ODEs for v after substitution of $z = x + vt$ is nontrivial. Also one needs to rule out impractical solutions that generate negative population densities. In the case of (1.2) some solutions of v, however, correspond to oscillations when sufficient time has passed after the initial wave of infection. These secondary oscillations require careful analysis and derivation, but in the analysis of complicated reaction diffusion equations in (1.2), it is possible to ignore secondary oscillations and focus only on the speed of initial wave by reducing (1.2) to a more simplified form.

To simplify (1.2) we note that initial infection wave is primarily caused by infectious foxes, and during a reasonably small time frame Δt fox populations at the infection wave front stays unchanged. So we let $a = b = 0$ and $\frac{\partial E}{\partial t} = 0$, and now in the simplified model

$$\begin{aligned} \frac{\partial S}{\partial t} &= -\beta IS \\ \frac{\partial I}{\partial t} &= \beta IS - \alpha I + D\frac{\partial^2 I}{\partial x^2} \end{aligned} \tag{1.3}$$

The simple system (1.3) ignores the reproduction from fox populations, and assumes that only infectious foxes disperse due to rabies-induced disorientation and the fact that healthy foxes tend to stay within their home ranges (MacDonald, 1980). These are reasonable over a small time interval Δt during the initial infection wave. Now the equation for I in (1.3) has the same form as the Fisher-Kolmogoroff equation. (1.3) still has two important conclusions: rabies epidemic will die out if densities of susceptible foxes drop below a critical value $S_t = \alpha/\beta$, and where densities of susceptible foxes are above this threshold, the rabies epizootic wave front travels at a speed of

$$c = 2\left[D(\beta S_0 - \alpha)\right]^{1/2}$$

where S_0 is the density of susceptible foxes before the arrival of initial infection wave.

From the standpoint of management of rabies epizootic, the formulas for S_t and c provide ample explanations as to how the first infection wave can be controlled. S_t suggests

the level of fox population culling to prevent the further advancement of infection wave, and estimation of D from c can indicate the width of vaccination buffer zones to be implemented, provided vaccines for rabies are available.

More detailed and complicated analysis of the wave speed v can be found in Murray's works (Murray *et al.*, 1986; Murray and Seward, 1992; Murray, 1989). Some nice summaries of ODE and PDE models used for early studies of rabies in red fox can also be found in (Shigesada and Kawasaki, 1997).

1.2.3 Methods using nonlocal delayed reaction diffusion equations

The reaction time lag is common among many ecological models, for example, the maturation time from juvenile class to adult class. In the transmission of infectious diseases, such as rabies, the latency in transmission caused by disease incubation time, can also be viewed as a reaction time lag. Spatial movement is also an important feature in ecological and epidemiological models. It is then of interest to consider both spatial movement and reaction time lag in ecological and epidemiological models concerning spatiotemporal dynamics for a single species. It turns out, however, that modeling the interplay of these two factors is highly nontrivial, and from recent literature we can see that nonlocal delayed reaction diffusion equations naturally arise. These systems were studied first in early works of Yamada (1984), Pozio (1980, 1983) and Redlinger (1984, 1985). Later, works from Britton (1990), Gourley and Britton (1996), Smith and Thieme (1991) started systematic investigation of this new class of nonlinear differential equations motivated by biological realities. For general work in this area we refer to a series of reviews by Gourley (Gourley *et al.*, 2004; Gourley and Wu, 2006; Gourley *et al.*, 2008).

It was observed that juvenile foxes tend to leave their home territory in the fall in search of new territory, with typical traveling distance up to 10 times the usual territory size. It was also noted in (Murray *et al.*, 1986) that it is likely for juvenile foxes to contract rabies

during this time, resulting in additional spatial propagation of rabies infection. To address this phenomenon, Ou and Wu (2006) started with the general framework that assumes individuals' spatial movement characteristics depend on their maturation level. They showed that nonlocal delayed reaction diffusion equations arise naturally.

Let $S(x,t,a), I(x,t,a)$ be the population densities at location $x \in \mathbb{R}$, time t and age $a \geq 0$ for the susceptible and infectious foxes. Let $\tau > 0$ be the fixed maturation time for juvenile foxes. It was shown that the density of adult susceptible foxes $M(x,t) = \int_\tau^\infty S(x,t,a)\,\mathrm{d}a$ and the population density of the infectious foxes $J(x,t) = \int_0^\infty I(x,t,a)\,\mathrm{d}a$ satisfy

$$\begin{aligned} \frac{\partial J}{\partial t} &= D_I \frac{\partial^2 J}{\partial x^2} + \beta M J - d_I J + \beta J \int_0^\tau S(x,t,a)\,\mathrm{d}a \\ \frac{\partial M}{\partial t} &= -\beta M J - d_S M + S(x,t,\tau), \end{aligned} \tag{1.4}$$

where D_I, d_I, β, d_S are diffusion coefficient, death rate for infectious foxes, and transmission rate, death rate for susceptible foxes respectively. $S(x,t,a)$ is governed by

$$\begin{aligned} &\frac{\partial S}{\partial t} + \frac{\partial S}{\partial a} = D_Y \frac{\partial^2 S}{\partial x^2} - \beta S J - d_Y S \\ &S(x,t,0) = b(M(t,x)), \end{aligned} \tag{1.5}$$

where D_Y, d_Y are the diffusion coefficient and death rate for the juvenile susceptible foxes and b is the birth function that is dependent on matured susceptible foxes. It was shown in (Ou and Wu, 2006), from analysis of this system of partial differential equations with nonlocal and delayed terms which are implicitly defined by a hyperbolic-parabolic equation, that the minimal traveling wave speed is a decreasing function of the maturation period.

1.2.4 Methods for modeling landscape heterogeneities

The ODE and PDE approaches, however complicated they are, all assume that population and disease dynamics occur over a homogeneous landscape and all parameter values

remain constant throughout time and space. This might not be a problem if problems are restricted within a local area, but since rabies transmission usually occurs over a large geographical region, spatial or landscape heterogeneities can be of great importance. Furthermore, due to seasonal migration of animals, spatial movement of animals can have major effects on the transmission of disease. Modeling landscape heterogeneities might not be possible in the past when early works were limited by scarce data at fine resolution or local scale, but as refined data become more and more available, it becomes more and more important to model landscape heterogeneities. For example, modeling and data showed in (Russel *et al.*, 2004; Smith *et al.*, 2002) that rivers are effective barriers for rabies epizootic wave, reducing by sevenfold rabies transmission across rivers.

Early attempts at incorporating landscape heterogeneity were based on the ODE and PDE models by considering additionally some parameter variation, stochasticity, or environmental heterogeneity. For example, a stochastic dispersal process was used in (Mollison and Kuulasmaa, 1985) that showed good agreement with estimated fox rabies propagation speed. Shigesada and Kawasaki (1997) allowed some variations in diffusion coefficients between classes of individuals and between different habitats.

Agent-based modeling was also used in early models incorporating landscape heterogeneities. For example, Voigt *et al.* (1985) and MacInnes *et al.* (1988) used agent-based models that are parametrized for the Ontario region in Canada and obtained insights into rabies epidemic processes.

Many recent works that describe movement of individuals across a region follow the procedure of discretizing the population and the geography into geopolitical units, such as townships, and then considering the movement of individuals between units (Keeling and Rohani, 2008; Smith *et al.*, 2002). This approach has two inherent issues. First, geopolitical units might help collect and categorize case data, but the spatial movement of animals does not either follow geopolitical units, or fit the scale of geopolitical units. Therefore

in these models using geopolitical units we see introduction of so-called long distance translocations (Smith *et al.*, 2005). Moreover, when models require implementation of heterogeneities of landscapes, geopolitical units are not of much help.

It is commonplace in realistic landscapes for irregular shapes of regions or boundaries to occur. In these circumstances, simple finite difference schemes, like those used in (Neilan and Lenhart, 2011), are not sufficient to incorporate these realistic geographic features. Sometimes modelers need refer to unstructured grids to discretize space, which naturally leads to the use of finite element methods to simulate models. There are population models (Milner, 1990; Ayati and Dupont, 2002; Gerardo-Giorda, 2008; Cusulin and Gerardo-Giorda, 2010) that use finite element methods to model diffusion but perform numerical experiments only on simple geometries, such as rectangles. Finite element methods are considered in an epidemiological context in (Kim and Park, 1998) only in terms of stability and convergence of the scheme. Numerical simulation is carried out and finite element schemes are applied in (Keller *et al.*, 2012) to model the diffusion of raccoon rabies in the state of New York. Note that only a single species is considered in this work.

1.2.5 Optimal control and stochastic models

Recently the framework of the Gillespie method (Gillespie, 1977) and interacting network (Kampen, 2001) are used in constructing stochastic ODEs of rabies models. Similar to (Smith *et al.*, 2002; Russel *et al.*, 2006), subpopulations distributed over a network are each represented by set of ODEs and coupled with each other by parameters for local spread or long distance translocation. The rates of events happening in each subpopulation, for example birth, death, infection and movement, are chosen according to some distribution. Therefore, different from traditional deterministic equations where events and population densities are continuous, events in these stochastic models happen in discrete times and densities change in integer increments, which gives these models a sense of realism.

Duke-Sylvester *et al.* (2010) constructed a stochastic rabies model to study the role of seasonality in dynamics of the rabies virus in raccoon along the East coast in the United States. In this paper a north-south latitudinal gradient in the seasonal demography of raccoon birth rates is implemented, which allows for simulation of variance in the timing of birth pulses for raccoons from Southern and Northern United States. It is found that narrow birth pulses associated with raccoons from Northern United States contribute to irregular rabies epidemics that are not spatially synchronized; however, in southern populations greater variance in birth pulses of raccoons leads to spatial synchronization of epidemics. This has potential implications for smart allocation of resources for surveillance of southern and northern raccoon populations. Due to synchronization in epidemics in southern raccoon populations, it might be reasonable to free up some resources for other purposes, for example vaccination programs.

Similar to Smith and Harris (1991), Duke-Sylvester *et al.* (2010) constructed stochastic simulation models that include spatial dynamics but no age structure. However, as a disease spreads through a host population over a large geographical range it may encounter significant variation in demographical structure. There are also some stochastic models that incorporate both age structure and spatial dynamics. For example, Allen *et al.* (2002) developed a spatially explicit, age-structured, stochastic and discrete-time Markov chain model for rabies spread. The population is subdivided according to juveniles and adults, susceptible, infected and vaccinated individuals, and individuals move between adjacent patches. And an estimation for the probability of disease elimination is given for the stochastic model.

Another more realistic aspect concerns the management of rabies spread in wildlife using vaccination, which is used extensively to avoid spillover to humans, domestic animals, or prevent existing rabies epizootics from further spreading into other wildlife populations (Jackson and Wunner, 2002a). Because usually public health resources for pro-

duction, distribution and maintenance of rabies vaccines are limited, it is helpful for strategies for vaccination in wildlife populations to incorporate the effects of landscapes, such as mountains, rivers, on the movement of wildlife populations. Indeed, there are studies (Smith *et al.*, 2002) that show rivers, in particular, slow down the advance of rabies due to decrease in local short distance dispersal rate across rivers. Therefore, it has become a popular trend to incorporate factors of landscape features in optimal control models for rabies (Russel *et al.*, 2006). So, in addition to limited public health resources, the spatial distribution of rabies vaccines is directed by landscape features (Stark *et al.*, 2006). Landscape effects on rabies spatial spread, the limited public health resources, and various kinds of rabies management objectives, combine to place a premium on obtaining the best outcome.

It is a newly formed trend in infectious disease modeling that spatial dynamics of infectious disease are considered in optimal control models. There are a few recent works that focus on combine spatial rabies spread and formulation of optimal rabies vaccination strategies. For example, Russel *et al.* (2006) compared optimal spatial vaccination policies with and without spatial barriers. Ding *et al.* (2007) discussed a model that incorporates the natural attrition of vaccine baits. It is likely that vaccines distributed are consumed by other non-target animals, degrade in natural environment. In this paper, optimal control model was constructed that showed how optimal control strategies are shaped by possibilities of natural attrition. Asano *et al.* (2008) considered a compartmental model with susceptible, infectious, exposed classes that incorporates spatial heterogeneities in the disease-free population, which in turn were shown to influence optimal spatial vaccination strategies.

1.2.6 Objectives

Traveling wavefront solutions arise naturally from reaction diffusion equations like (1.3). In these models the existence of traveling wavefront solutions and their minimum

speed are of primary concern. The existence of traveling wave fronts in various epidemic models described by reaction-diffusion systems has been extensively studied. We refer to the monographs of Murray (2002), Rass and Radcliffe (2003) and a survey by Ruan (2007). Recent development also abounds in exploring traveling wave solutions to delay reaction diffusion equations and their minimum wave speeds (Gourley and Kuang, 2005; Wu and Zou, 2001). To incorporate incubation period for rabies we can either choose to explicitly assign an exposed class of animals, or implicitly include it in a delay. The explicit model results in a susceptible-exposed-infective system of reaction diffusion equations, and the implicit method gives rise to a susceptible-infective system of delay reaction diffusion equations. We intend to compare the modeling processes behind these two models and their respective minimum traveling wave speeds.

It is important that mathematical models capture dynamics of realistic processes. For example, the simple system (1.3) proposed by Murray *et al.* (1986) has implications that are qualitatively in accordance with realistic observations. However, sometimes to this end, the simplicity of mathematical models need to be sacrificed. Nowadays with the help of improving computing capabilities and numerical schemes the difficulties of treating complicated mathematical models are partially relieved by computer simulations. Then the simulation outputs can be examined and compared with actual data. Useful insights can subsequently be drawn about realistic concerns, for instance, how rabies in wildlife would spread over a realistic landscape. Hence there are two layers of realities in modeling here, one coming from the model itself, for example, incorporation of spatial dispersal or delay, and the other from data, where outputs of realistic models can be checked with the actual observations or facts.

1.3 Outline

In chapter 2, we take into account the incubation period from initial rabies infection to onset of clinical symptoms. To do that we can add an exposed class in model (1.3). We can also include a delay to model the incubation period. This leads to a delay reaction diffusion model that only accounts for susceptible and infective classes. Murray also considered the first option without considering dispersals of exposed animals. For our models we assume the exposed animals disperse too. This assumption serves as an important connection between the SEI system of reaction diffusion equations and the SI system of delay reaction diffusion equations. Then we compare the SEI reaction diffusion model with the SI delay reaction diffusion model using the same set of parameters values. In particular we look at their minimum traveling wavefront speeds.

In chapter 3, we use an alternative modeling approach by incorporating the infection age. We consider the idealized situation where a single infection is placed in a naive uniform susceptible population. This can produce an initial wave of infection. Since this is the first wave front, we make the simplifying assumption that population turnover is ignored. When considering wave fronts in ensuing infections after the first wave, population turnover is important, otherwise the susceptible animals would simply decline monotonically without regenerating and there would be no second wave of infections. We consider two approaches of applying infection age dependent modeling, both of which result in an integral equation that can be analyzed for the asymptotic speed of spread. Then we show that under the appropriate initial condition the asymptotic speed of spread c^* exists and give its estimate.

In chapter 4, we consider rabies spatial spread over a realistic landscape. In most theoretical and mathematically tractable models, individual movement is governed by diffusion equations in homogeneous domains, meaning no spatial dependence in parameters and dif-

fusion is isotropic, but most realistic landscapes cause heterogeneities in the model. Rivers, for example, may significantly hinders transmission process of rabies epidemic by altering the direction of diffusion from rabid animals. In this chapter, we consider an irregular two-dimensional domain of interest that incorporates geographic features such as rivers and city limits. To simulate our model over this domain requires the use of finite element method. The model of interest is a rabies model for skunk and bat interactions. Model is defined over a $(300 \text{ km})^2$ region in northeastern Texas. Model parameter values are estimated from literatures.

Chapter 2

SPATIAL SPREAD OF RABIES – TRAVELING WAVES

2.1 Spatial Spread of Rabies in Foxes: Comparison Between Two Models

The simple models in the previous chapter involve only susceptible and infectious classes of animals. While they are able to capture certain aspects of an epizootic rabies wavefront, they are still elementary in terms of neglecting the key incubation period between initial infection and subsequent onset of clinical rabid symptoms. For foxes, for example, the incubation period generally lasts from 12 to 150 days. The movement and dispersal of animals during this time span could influence the dynamics of epidemic wavefronts significantly. Therefore it is of practical and realistic importance to implicate the factor of incubation period in our models.

In the following sections we consider and compare two models both of which describe the same underlying rabies infection process over an infinite one-dimensional domain $-\infty < x < \infty$. One is a simple susceptible-exposed-infected model featuring reaction diffusion equations, and the other is a simple susceptible-infected model of delayed reaction diffusion equations. From both models we seek traveling wave solutions, and by comparing them analytically and numerically we hope to obtain insights into dependence of system dynamics on parameters.

The underlying disease transmission process is rabies epizootic among a single type of terrestrial animals, raccoons or foxes for example. For this work we consider foxes. So far we don't restrict ourselves within certain closed spatial domain and we only consider an infinite one-dimensional spatial domain $-\infty < x < \infty$. In addition, the spatial range is considered homogeneous and there is no dependence of system parameter values on

spatial element, which means that all parameters are necessarily constants. We assume the following for our modeling work

(1) reproduction occurs only in susceptible class, and growth dynamics of susceptibles is modeled by logistic terms;

(2) from inoculation to onset of clinical rabid symptoms, there is an incubation period of an average length $1/\sigma$; animals in this phase are grouped in the exposed class, E;

(3) infectious animals, I, invariably die after a short time of an average length $1/\mu$; since rabies is fatal, we don't consider background mortality in infectious class;

(4) rabies virus is able to cause either furious rabid symptoms, where virus enters central nervous system leading to abnormalities in animal behaviors such as disorientation and randomly attacking and biting other animals, or paralysis, which is caused by virus lodging in spinal cords; as a result, we assume that both exposed and infectious animals disperse because of rabies infection;

(5) susceptible class, S, tend to stick to their home ranges, for example foxes, so we assume that susceptibles don't disperse.

(6) although young animals sometimes disperse out of their home range while they search for new territory, we opt to ignore the possibility of them being bitten by infectious animals during their search, since there have been some observations given by Artois and Aubert (1982) and MacDonald (1980) where rabies is much less common in the young than adults. The influence of age structures and maturation is considered in the form of a system of delayed reaction diffusion equations with nonlocal interactions by Ou and Wu (2006).

2.2 Models

The SEI reaction diffusion model is readily obtained by adding diffusion terms for both exposed and infectious classes

$$\begin{aligned}
\frac{\partial S}{\partial t} &= rS\left(1-\frac{S}{K}\right)-\beta IS \\
\frac{\partial E}{\partial t} &= \beta IS - bE - \sigma E + D_2\frac{\partial^2 E}{\partial x^2} \\
\frac{\partial I}{\partial t} &= \sigma E - \mu I + D_1\frac{\partial^2 I}{\partial x^2}
\end{aligned} \tag{2.1}$$

with initial conditions

$$S(x,0)=S_0(x), \quad E(x,0)=E_0(x), \quad I(x,0)=I_0(x)$$

where S_0, E_0, I_0 are smooth functions, r, K, β, b, σ are intrinsic growth rate, carrying capacity, infection rate, death rate for exposed animals and progression rate from exposed to infectious class respectively, $D_1, D_2 > 0$ are diffusion coefficients for infectious and exposed classes while we assume that $D_1 > D_2$.

While the derivation of SEI reaction diffusion model (2.1) seems straightforward, the deduction of delayed reaction diffusion model is complicated by the fact that because of diffusion when an exposed animal becomes infectious it might emerge at a location different from where it initially was infected. Therefore a more careful and deliberate design is needed.

Let $T = 1/\sigma$ be the fixed incubation time. For the following we intend to use delayed reaction diffusion equations to model the same rabies infection process described by (2.1), and reduce the SEI structure to an SI system

$$\begin{aligned}
\frac{\partial S}{\partial t} &= rS\left(1-\frac{S}{K}\right)-\beta IS \\
\frac{\partial I}{\partial t} &= -\mu I + D_1\frac{\partial^2 I}{\partial x^2} + \{\text{rate of recruitment from exposed class}\}
\end{aligned} \tag{2.2}$$

In order to fill out those in curly braces, we will use an age structure way similar to those in (Gourley and Kuang, 2005; So *et al.*, 2001; Thieme and Zhao, 2001, 2003).

Let $p(x,t,a)$ denote the density of exposed animals at time t, location x and infection age $a \in [0,T]$.

Following the convention of age structure modeling (Metz and Diekmann, 1986; So *et al.*, 2001), assume that p satisfies equation

$$\frac{\partial p}{\partial t} + \frac{\partial p}{\partial a} = D_2 \frac{\partial^2 p}{\partial x^2} - bp. \tag{2.3}$$

where D_2 is diffusion coefficient and b is death rate for E.

Note that the initial condition, when $a = 0$, is

$$p(x,t,0) = \beta S(x,t) I(x,t). \tag{2.4}$$

Total density of exposed animals at time t and location x is thus

$$E(x,t) = \int_0^T p(x,t,a)\,\mathrm{d}a.$$

Let $p^r(x,a) = p(x,a+r,a)$. Then

$$\frac{\partial p^r}{\partial a} = \left[\frac{\partial p}{\partial t} + \frac{\partial p}{\partial a}\right]_{t=a+r} = \left[D_2 \frac{\partial^2 p}{\partial x^2} - bp\right]_{t=a+r} = D_2 \frac{\partial^2 p^r}{\partial x^2} - bp^r.$$

$p^r(x,a)$ can be solved using the Gaussian kernel, the fundamental solution associated with partial differential operator $\partial_t - \Delta_x$

$$\Gamma(t,x) = \frac{1}{\sqrt{4\pi t}} e^{-\frac{x^2}{4t}}$$

so that

$$p^r(x,a) = \int_{-\infty}^{\infty} \beta S(y,r) I(y,r) e^{-ba} \Gamma\left(D_2 a, x-y\right)\,\mathrm{d}y.$$

Let $t = a + r$, then $r = t - a$ and

$$p(x,t,a) = \int_{-\infty}^{\infty} \beta S(y,t-a) I(y,t-a)\, e^{-ba} \Gamma\left(D_2 a, x-y\right)\,\mathrm{d}y.$$

Hence the total density of exposed animals is

$$E(x,t) = \int_0^T \int_{-\infty}^{\infty} \beta S(y,t-a) I(y,t-a)\, e^{-ba} \Gamma\left(D_2 a, x-y\right)\, \mathrm{d}y\, \mathrm{d}a$$
$$= \int_{t-T}^{t} \int_{-\infty}^{\infty} \beta S(y,\tau) I(y,\tau)\, e^{-b(t-\tau)} \Gamma\left(D_2(t-\tau), x-y\right)\, \mathrm{d}y\, \mathrm{d}\tau$$

the last equation is by a change of variable $\tau = t - a$.

Now for convenience let

$$G(x,t,\tau) = e^{-b(t-\tau)} \Gamma\left(D_2(t-\tau), x\right).$$

Then

$$E(x,t) = \int_{t-T}^{t} \int_{-\infty}^{\infty} \beta S(y,\tau) I(y,\tau) G(x-y,t,\tau)\, \mathrm{d}y\, \mathrm{d}\tau.$$

Note that

$$\frac{\partial E}{\partial t} = \int_{-\infty}^{\infty} \beta S(y,t) I(y,t)\, G(x-y,t,t)\, \mathrm{d}y$$
$$- \int_{-\infty}^{\infty} \beta S(y,t-T) I(y,t-T)\, G(x-y,t,t-T)\, \mathrm{d}y$$
$$+ \int_{t-T}^{t} \int_{-\infty}^{\infty} \beta S(y,\tau) I(y,\tau)\, \frac{\partial G}{\partial t}\left(x-y,t,\tau\right)\, \mathrm{d}y\, \mathrm{d}\tau. \qquad (2.5)$$

To simplify (2.5) we find that

$$G(x-y,t,t) = \lim_{\tau \to t} e^{-b(t-\tau)} \Gamma\left(D_2(t-\tau), x-y\right) = \delta(x-y)$$

where δ is the Dirac delta distribution concentrated at 0. Also

$$G(x-y,t,t-T) = e^{-bT}\, \Gamma\left(D_2 T, x-y\right)$$

$$\frac{\partial G}{\partial t}\left(x-y,t,\tau\right) = \frac{\partial}{\partial t}\left(e^{-b(t-\tau)} \Gamma\left(D_2(t-\tau), x-y\right)\right)$$

$$= -bG\left(x-y,t,\tau\right) + D_2 \frac{\partial^2}{\partial x^2} G(x-y,t,\tau) \qquad \text{by property of } \Gamma(t,x).$$

Therefore

$$\begin{aligned}
\frac{\partial E}{\partial t} &= \int_{-\infty}^{\infty} \beta S(y,t) I(y,t)\, \delta(x-y)\, \mathrm{d}y \\
&\quad - \int_{-\infty}^{\infty} \beta S(y,t-T) I(y,t-T)\, e^{-bT}\, \Gamma\left(D_2 T, x-y\right)\, \mathrm{d}y \\
&\quad + \int_{t-T}^{t} \int_{-\infty}^{\infty} \beta S(\tau,y) I(\tau,y) \left[-bG + D_2 \frac{\partial^2 G}{\partial x^2}\right] \mathrm{d}y\, \mathrm{d}\tau \\
&= \beta S(x,t) I(x,t) - bE + D_2 \frac{\partial^2 E}{\partial x^2} \\
&\quad - \beta e^{-bT} \int_{-\infty}^{\infty} S(y,t-T) I(y,t-T) \Gamma\left(D_2 T, x-y\right)\, \mathrm{d}y.
\end{aligned}$$

It is then clear from the definition and formulation of exposed class that the last term in previous equation is the rate of recruitment for the infectious class. Now the simple SI delayed reaction diffusion equations are as follows

$$\begin{aligned}
\frac{\partial S}{\partial t} &= rS\left(1 - \frac{S}{K}\right) - \beta SI \\
\frac{\partial I}{\partial t} &= D_1 \frac{\partial^2 I}{\partial x^2} - \mu I + \beta e^{-bT} \int_{-\infty}^{\infty} S(y,t-T) I(y,t-T) \frac{e^{-(x-y)^2/(4D_2 T)}}{2\sqrt{\pi D_2 T}}\, \mathrm{d}y
\end{aligned} \tag{2.6}$$

where $T = 1/\sigma$ is the incubation period, b is death rate for exposed animals and D_2 the diffusion rate for exposed class.

The simple SI delayed reaction diffusion system (2.6) is complete with proper initial conditions

$$S(x,t) = S_0(x,t), \qquad I(x,t) = I_0(x,t)$$

with $t \in [-T, 0]$, $x \in (-\infty, \infty)$ and S_0, I_0 smooth functions.

While mathematical analysis is important, realistic perspectives, for instance typical parameter values of fox ecology, could also provide key observations in guiding mathematical analysis as well as numerical experiments. For considerations of our models (2.1) and (2.6), typical parameter values for foxes, except for the important D_1, D_2, are given in Table 2.1.

Table 2.1: Parameter values for rabies in foxes (see Anderson *et al.* (1981)).

Meaning	Parameter	Value
Growth rate	r	0.5 fox year^{-1}
Average death rate	b	0.5 fox year^{-1}
Average duration of infectious/rabid phase	$1/\mu$	5 days
Average incubation time	$1/\sigma$	28 days
Transmission coefficient	β	80 km^{2}year^{-1}
Carrying capacity	K	0.25–4 foxes km^{-2}

In the following sections we intend to seek traveling wave solutions for both models (2.1) and (2.6) and compare their minimum traveling wave speeds. Throughout the discussions we mainly focus on traveling wave fronts connecting the disease-free steady state and endemic steady state. As a result the existence of endemic or positive steady state must be ensured.

2.3 Traveling wavefronts for SEI reaction diffusion model

Two steady states for system (2.1) are trivial, extinction steady state $(0, 0, 0)$ and disease-free steady state $(K, 0, 0)$. The endemic or positive steady state is given by setting the right hand side of (2.1) to zero and solving for positive solutions (S^*, E^*, I^*). They are

$$\begin{aligned} S^* &= \frac{\mu}{\beta}\frac{b+\sigma}{\sigma} \\ E^* &= \frac{\mu r}{\sigma\beta}\left(1-\frac{\mu}{\beta K}\frac{b+\sigma}{\sigma}\right) \\ I^* &= \frac{r}{\beta}\left(1-\frac{\mu}{\beta K}\frac{b+\sigma}{\sigma}\right) \end{aligned} \tag{2.7}$$

Positive steady state given in (2.7) exists if and only if

$$1-\frac{\mu}{\beta K}\frac{b+\sigma}{\sigma} > 0 \Leftrightarrow K > \frac{\mu}{\beta}\frac{b+\sigma}{\sigma} =: K_c \tag{2.8}$$

where $K_c > 0$ is defined as the critical carrying capacity. If $K < K_c$ the rabies endemic steady state does not exist.

To reduce the amount of parameters considered, we introduce the following nondimensional quantities

$$\begin{aligned}
&\tilde{S} = \frac{S}{K}, \quad \tilde{E} = \frac{E}{K}, \quad \tilde{I} = \frac{I}{K}, \\
&\tilde{r} = \frac{r}{\beta K}, \quad \tilde{b} = \frac{b}{\beta K}, \quad \tilde{\sigma} = \frac{\sigma}{\beta K}, \quad \tilde{\mu} = \frac{\mu}{\beta K} \\
&\tilde{x} = \sqrt{\frac{\beta K}{D_1}} x, \quad \tilde{t} = \beta K t, \quad \epsilon = \frac{D_2}{D_1}.
\end{aligned} \tag{2.9}$$

With the scalings defined in (2.9), (2.1) becomes, on removing tildes for simplicity

$$\begin{aligned}
\frac{\partial S}{\partial t} &= rS\left(1 - S\right) - IS \\
\frac{\partial E}{\partial t} &= IS - bE - \sigma E + \epsilon \frac{\partial^2 E}{\partial x^2} \\
\frac{\partial I}{\partial t} &= \sigma E - \mu I + \frac{\partial^2 I}{\partial x^2}
\end{aligned} \tag{2.10}$$

To revert to dimensionalized variables, we only need to refer to scalings defined in (2.9).

Then steady states in dimensionless model (2.10) are extinction steady state $(0, 0, 0)$, disease-free steady state $(1, 0, 0)$ and positive steady state (S^*, E^*, I^*) defined by

$$\begin{aligned}
S^* &= \frac{b + \sigma}{\sigma} \mu \\
E^* &= \frac{\mu r}{\sigma} \left(1 - \frac{b + \sigma}{\sigma} \mu\right) \\
I^* &= r \left(1 - \frac{b + \sigma}{\sigma} \mu\right)
\end{aligned} \tag{2.11}$$

with the positive steady state defined above possible if and only if

$$\frac{b + \sigma}{\sigma} \mu < 1. \tag{2.12}$$

For considerations of realistic values for dimensionless variables we refer to Table 2.1 for values of dimensionalized variables for foxes in Europe. If we set $K = 2$ then for

dimensionless parameters

$$r = 0.003 = b, \quad \sigma = 0.08, \quad \mu = 0.453. \tag{2.13}$$

where we can observe that dimensionless $r \ll 1$ and $b \ll 1$ are small compared with dimensionless σ, μ, which reflects the fact that death rate for rabies is much greater than natural growth and death rates.

From here on in this section, for convenience we refer to the dimensionless parameter and variables with their names. Dimensionless parameters and variables are distinguished from dimensionalized ones only when necessary.

2.3.1 Minimum wave speed for SEI reaction diffusion model

We look for epizootic wave solutions to (2.10), which travels at a constant velocity $v > 0$ into a rabies free region corresponding to disease-free steady state $(1, 0, 0)$. Thus, let

$$z = x + vt$$

we look for $(S(z), E(z), I(z))$ that satisfy

$$\begin{aligned} vS' &= rS(1 - S) - IS \\ vE' &= IS - bE - \sigma E + \epsilon E'' \\ vI' &= \sigma E - \mu I + I'' \end{aligned} \tag{2.14}$$

We assume that $(S(-\infty), E(-\infty), I(-\infty)) = (1, 0, 0)$ and $(S'(-\infty), E'(-\infty), I'(-\infty)) = (0, 0, 0)$. Also assume that threshold condition (2.12) holds, so that traveling wave solutions are likely to go to either extinction steady state $(0, 0, 0)$ or endemic steady state (S^*, E^*, I^*).

Write (2.14) as a 5-dimensional first order ODE system in (S, E, P, I, Q) where we let

$P = E'$ and $Q = I'$, where $'$ denotes differentiation with respect to z

$$\begin{aligned} S' &= \frac{r}{v}S(1-S) - \frac{1}{v}IS \\ E' &= P \\ P' &= \frac{v}{\epsilon}P - \frac{1}{\epsilon}IS + \frac{b+\sigma}{\epsilon}E \\ I' &= Q \\ Q' &= vQ - \sigma E + \mu I \end{aligned} \tag{2.15}$$

In the neighborhood of disease-free equilibrium $(1, 0, 0)$ the system behavior is determined by linearized system, and solutions of the linearized system is determined by linear combinations of eigensolutions in the form of $\mathbf{w}e^{\lambda z}$, where $\mathbf{w}$ and λ are eigenvector and corresponding eigenvalue of Jacobian matrix (2.16) evaluated at disease-free equilibrium $(1, 0, 0)$.

The Jacobian matrix for (2.15) is

$$J = \begin{pmatrix} \frac{r}{v} - 2\frac{r}{v}S - \frac{1}{v}I & 0 & 0 & -\frac{1}{v}S & 0 \\ 0 & 0 & 1 & 0 & 0 \\ -\frac{1}{\epsilon}I & \frac{b+\sigma}{\epsilon} & \frac{v}{\epsilon} & -\frac{1}{\epsilon}S & 0 \\ 0 & 0 & 0 & 0 & 1 \\ 0 & -\sigma & 0 & \mu & v \end{pmatrix} \tag{2.16}$$

After calculating the characteristic equation it is revealed that eigenvalues of Jacobian matrix (2.16) at $(1, 0, 0)$ is $\lambda_1 = -r/v$ and roots of the following degree 4 polynomial

$$f(\lambda) = g(\lambda) - \frac{\sigma}{\epsilon} \tag{2.17}$$

where

$$g(\lambda) = \left(\lambda^2 - v\lambda - \mu\right)\left(\lambda^2 - \frac{v}{\epsilon}\lambda - \frac{b+\sigma}{\epsilon}\right). \tag{2.18}$$

Now we observe that

$$\begin{aligned} f(0) &= g(0) - \frac{\sigma}{\epsilon} \\ &= \mu\frac{b+\sigma}{\epsilon} - \frac{\sigma}{\epsilon} \\ &= \frac{\sigma}{\epsilon}\left(\frac{b+\sigma}{\sigma}\mu - 1\right) < 0 \qquad \text{by } (2.12) \end{aligned}$$

$$\begin{aligned} f'(0) &= g'(0) \\ &= -v\left(-\frac{b+\sigma}{\epsilon}\right) + \left(-\frac{v}{\epsilon}\right)(-\mu) \\ &= \frac{v}{\epsilon}(b+\sigma+\mu) > 0 \qquad \text{since } v > 0. \end{aligned}$$

The graph of $f(\lambda)$ is obtained by shifting downward the graph of $g(\lambda)$ by $\frac{\sigma}{\epsilon}$. From the equation for $g(\lambda)$ we know that $g(\lambda)$ has two distinct positive real roots and two distinct negative real roots. Additionally, we obtain above that $f(0) < 0$ and $f'(0) > 0$, so the graph of $f(\lambda)$ can only look like one of three cases described in Figure 2.1. In other words, the middle part where the hump is located can cross the λ axis, just touch λ axis, or stay below it, which correspond to respectively two distinct positive real roots, a double positive root at λ_c, and two complex roots with positive real parts. Furthermore, it is readily seen that as v increases, the middle hump rises gradually from below λ axis and eventually touches and crosses it.

When the velocity v is such that $f(\lambda)$ has two complex roots, with Im $\lambda \neq 0$, these represent oscillatory solutions in the neighborhood of disease-free steady state $(1, 0, 0, 0, 0)$, which imply negative populations, and hence physical waves cannot travel with such velocities. Thus we seek the exact λ_c and v_c such that middle part of $f(\lambda)$ just touches the

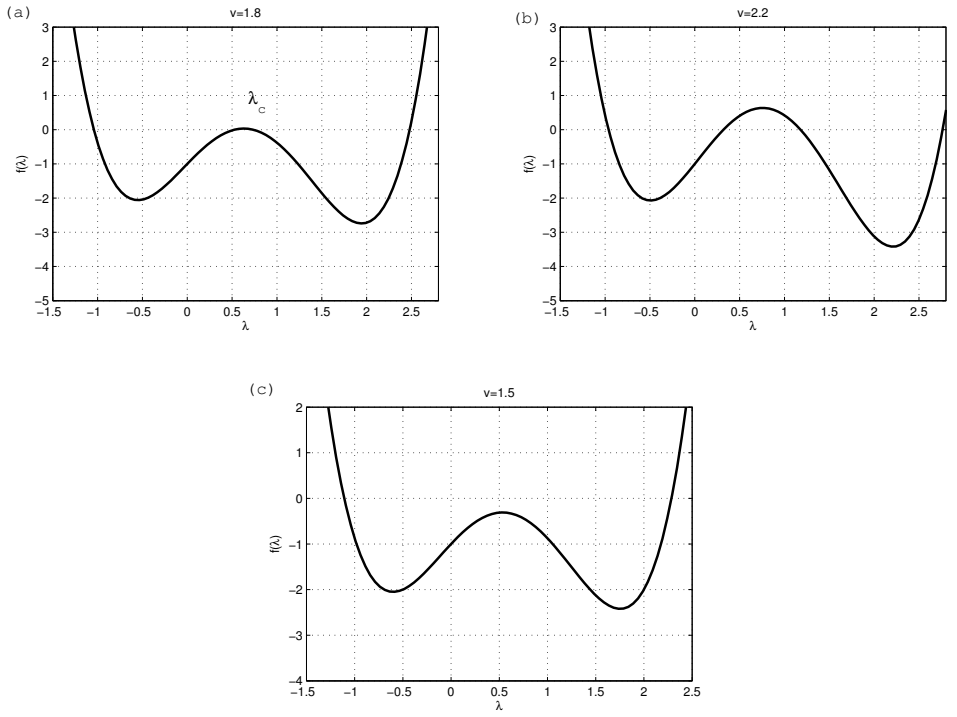

Figure 2.1: The profiles for a hypothetical degree 4 polynomial $f(\lambda) = (\lambda^2 - v\lambda - 1)(\lambda^2 - \frac{v}{2}\lambda - 1) - 2$ with different values for v. In general the polynomial is obtained from characteristic polynomial for Jacobian (2.16) about $(1, 0, 0)$. Then $f(\lambda)$ definitely has one positive real and negative real roots, but additionally could have (a) double root at λ_c, (b) two distinct positive real roots or (c) two complex roots with positive real parts.

horizontal axis, which corresponds to a double root. And this v_c corresponds to the minimum wave speed of an epidemic wavefront.

In order to find such a v_c, we need to set $f(\lambda) = 0$ and $f'(\lambda) = 0$, from which we have the following system of nonliner equations for v, λ

$$\begin{aligned} &\lambda^4 - \left(\tfrac{v}{\epsilon} + v\right)\lambda^3 + \left(\tfrac{v^2}{\epsilon} - \tfrac{b+\sigma}{\epsilon} - \mu\right)\lambda^2 + \tfrac{v}{\epsilon}\left(b + \sigma + \mu\right)\lambda + \tfrac{\sigma}{\epsilon}\left(\tfrac{b+\sigma}{\sigma}\mu - 1\right) = 0 \\ &4\lambda^3 - 3\left(\tfrac{v}{\epsilon} + v\right) + 2\left(\tfrac{v^2}{\epsilon} - \tfrac{b+\sigma}{\epsilon} - \mu\right)\lambda + \tfrac{v}{\epsilon}\left(b + \sigma + \mu\right) = 0. \end{aligned} \tag{2.19}$$

We can solve for the positive pair (v_0, λ_0) that corresponds to the middle hump of $f(\lambda)$ where the graph just touches the λ-axis. The solution can be obtained numerically using Newton method. Note that with this pair of solution (v_0, λ_0), corresponding to the middle

hump, we have $f''(\lambda_0) < 0$.

Proposition 2.1 *If traveling wave solutions of (2.10) exist with*

$$\lim_{z\to-\infty}(S(z), E(z), I(z)) = (1, 0, 0) \quad \textit{and} \quad \lim_{z\to-\infty}(S'(z), E'(z), I'(z)) = (0, 0, 0)$$

then the minimum wave front speed v_0 of the dimensionless system (2.10) is given by solving the positive solution (v_0, λ_0) in (2.19) such that $f''(\lambda_0) < 0$.

Proof See previous discussions in this section.

Now that we have the minimum wave front speed, it follows from the next proposition that trajectories corresponding to this wave front cannot connect the disease-free steady state $(1, 0, 0, 0, 0)$ and the extinction equilibrium $(0, 0, 0, 0, 0)$.

Proposition 2.2 *If the threshold condition (2.12) holds, and traveling wave solutions of (2.10) exist with*

$$\lim_{z\to-\infty}(S(z), E(z), I(z)) = (1, 0, 0) \quad \textit{and} \quad \lim_{z\to-\infty}(S'(z), E'(z), I'(z)) = (0, 0, 0)$$

then the traveling wave solutions cannot have extinction equilibrium as asymptotic state.

Proof First we consider the system (2.15) linearized about the origin in the 5-dimensional space (S, E, P, I, Q). The Jacobian matrix evaluated at the origin is thus

$$J(\mathbf{0}) = \begin{pmatrix} \frac{r}{v} & 0 & 0 & 0 & 0 \\ 0 & 0 & 1 & 0 & 0 \\ 0 & \frac{b+\sigma}{\epsilon} & \frac{v}{\epsilon} & 0 & 0 \\ 0 & 0 & 0 & 0 & 1 \\ 0 & -\sigma & 0 & \mu & v \end{pmatrix}$$

The eigenvalues of $J(\mathbf{0})$ is $\frac{r}{v}$ and roots of

$$p(\lambda) = \left(\lambda^2 - \frac{v}{\epsilon}\lambda - \frac{b+\sigma}{\epsilon}\right)\left(\lambda^2 - v\lambda - \mu\right)$$

with

$$\lambda_{2,3} = \frac{v \pm \sqrt{v^2 + 4\epsilon(b+\sigma)}}{2\epsilon}, \qquad \lambda_{4,5} = \frac{v \pm \sqrt{v^2 + 4\mu}}{2}.$$

In the neighborhood of the origin, trajectories that approach it correspond to linear combinations of eigensolutions with negative eigenvalues

$$\lambda_3 = \frac{v - \sqrt{v^2 + 4\epsilon(b+\sigma)}}{2\epsilon}, \qquad \lambda_5 = \frac{v - \sqrt{v^2 + 4\mu}}{2}.$$

It is also readily obtained from plugging λ_3, λ_5 back to solve for their corresponding eigenvectors

$$\phi_3 = \begin{pmatrix} 0 \\ 1 \\ \lambda_3 \\ 0 \\ 0 \end{pmatrix}, \qquad \phi_5 = \begin{pmatrix} 0 \\ 0 \\ 0 \\ 1 \\ \lambda_5 \end{pmatrix}$$

i.e. trajectories that approach the origin $(0, 0, 0, 0, 0)$ are linear combinations in the form of

$$c_3 e^{\lambda_3 z}\phi_3 + c_5 e^{\lambda_5 z}\phi_5$$

where c_3, c_5 are constants and $z = x + vt$.

Since both ϕ_3, ϕ_5 have zero in the first entry, all trajectories that approach the origin are in the $S = 0$ plane, meaning that every trajectory approaching the origin in the (S, E, P, I, Q) space in forward time would stay in the $S = 0$ plane throughout both backward and forward time. This is a contradiction.

Going back to the three-dimensional space of (S, E, I), it is therefore not possible for traveling wave solutions of (2.10) to have $(0, 0, 0)$ as asymptotic state, if they start from $(1, 0, 0)$.

2.3.2 Behavior of traveling wave solutions near positive steady state

Proposition 2.2 implies that if (2.12) holds, i.e. endemic steady state exists, a traveling wave can only occur if there is a trajectory from the disease-free steady state $(1, 0, 0)$ to the critical point (S^*, E^*, I^*).

Next we consider the behavior of the wave as it approaches the critical point (S^*, E^*, I^*).

First note that $b, r \ll 1$. This suggests an asymptotic analytical procedure. With the endemic steady state defined in (2.11), if (2.12) holds, these values are given, up to the first order in b and r, by

$$\begin{aligned} S^* &= \mu + \frac{\mu}{\sigma} b \\ E^* &= \frac{\mu(1-\mu)}{\sigma} r \\ I^* &= (1-\mu) r \end{aligned} \tag{2.20}$$

Sufficiently close to the endemic steady state, solutions of (2.15) follow those of the linearized form. So we can determine the solution behavior near the endemic steady state by considering all possible linear combinations of the eigensolutions. If $\mathrm{Re}\,\lambda_i < 0$, then $\mathbf{w}_i \exp(\lambda_i z) \to 0$ as $z \to \infty$, where $\mathbf{w}_i$ and λ_i are the five eigenvectors and eigenvalues of the corresponding coefficient matrix evaluated at the endemic steady state, whereas if $\mathrm{Re}\,\lambda_i > 0$ the trajectory comes out of the endemic steady state. Trajectories leaving the critical point thus correspond to linear combinations of those eigensolutions $\mathbf{w}_i \exp(\lambda_i z)$ with $\mathrm{Re}\,\lambda_i > 0$. And similarly trajectories entering the critical point correspond to linear combinations of those eigensolutions with $\mathrm{Re}\,\lambda_i < 0$.

We now substitute (2.20) in the Jacobian (2.16)

$$J = \begin{pmatrix} -\frac{\mu r}{v}(1+\frac{2}{\sigma}b) & 0 & 0 & -\frac{\mu}{v}(1+\frac{b}{\sigma}) & 0 \\ 0 & 0 & 1 & 0 & 0 \\ -\frac{1-\mu}{\epsilon}r & \frac{\sigma}{\epsilon}+\frac{b}{\epsilon} & \frac{v}{\epsilon} & -\frac{\mu}{\epsilon}-\frac{\mu}{\epsilon\sigma}b & 0 \\ 0 & 0 & 0 & 0 & 1 \\ 0 & -\sigma & 0 & \mu & v \end{pmatrix}. \tag{2.21}$$

After some algebra, we arrive at the characteristic equation

$$\begin{aligned} &\lambda^5 - \left(v + \frac{v}{\epsilon} - \frac{\mu}{v}r - \frac{2\mu}{\sigma v}br\right)\lambda^4 \\ &\quad - \left(\mu + \frac{\sigma}{\epsilon} - \frac{v^2}{\epsilon} + \frac{1}{\epsilon}b + \left(1+\frac{1}{\epsilon}\right)\mu r + \frac{2\mu}{\sigma}\left(1+\frac{1}{\epsilon}\right)br\right)\lambda^3 \\ &\quad + \left(\frac{\mu v}{\epsilon} + \frac{\sigma v}{\epsilon} + \frac{v}{\epsilon}b - \frac{\mu}{v}\left(\frac{\sigma}{\epsilon} - \frac{v^2}{\epsilon} + \mu\right)r - \frac{2\mu}{\sigma v}\left(\frac{3\sigma}{2\epsilon} - \frac{v^2}{\epsilon} + \mu\right)br - \frac{2\mu}{\epsilon\sigma v}b^2 r\right)\lambda^2 \\ &\quad + \left(\frac{\mu}{\epsilon}(\mu+\sigma)r + \frac{\mu}{\epsilon}\left(3 + \frac{2\mu}{\sigma}\right)br + \frac{2\mu}{\epsilon\sigma}b^2 r\right)\lambda \\ &\quad + \frac{\sigma\mu(1-\mu)}{\epsilon v}r + \frac{\mu(1-\mu)}{\epsilon v}br = 0. \end{aligned} \tag{2.22}$$

Let

$$\lambda = c_0 + c_1 b^\alpha + c_2 r^\beta$$

where c_0, c_1, c_2 are constants, $0 < \alpha, \beta \leq 1$.

Substitute this in (2.22), up to order $O(1)$

$$c_0^5 - \left(v + \frac{v}{\epsilon}\right)c_0^4 - \left(\mu + \frac{\sigma}{\epsilon} - \frac{v^2}{\epsilon}\right)c_0^3 + \left(\frac{\mu v}{\epsilon} + \frac{\sigma v}{\epsilon}\right)c_0^2 = 0. \tag{2.23}$$

It is easy to see that two roots of (2.23) are 0, so two eigenvalues are small in amplitude compared with the others. There are two positive roots, one in $(v, \frac{v}{\epsilon})$ and the other in $(\frac{v}{\epsilon}, \infty)$. There is also a negative root, which we denote as λ_1.

Now in order to get the two small eigenvalues, which we denote as λ_2, λ_3, we assume that

$$\lambda_{2,3} = c_1 b^\alpha + c_2 r^\beta.$$

Substitute it again in (2.22). After some algebra, first we note that terms in lowest order of r need to be balanced. So

$$\left(\frac{\mu v}{\epsilon}+\frac{\sigma v}{\epsilon}\right) c_2^2 r^{2\beta}+\frac{\sigma\mu(1-\mu)}{\epsilon v} r = 0.$$

Solving this equation

$$\beta = \frac{1}{2}, \qquad c_2 = \pm\frac{i}{v}\left(\frac{\sigma\mu(1-\mu)}{\sigma+\mu}\right)^{1/2}. \tag{2.24}$$

Notice that $c_1 = 0$, since with a nonzero c_1 there is always a term

$$\left(\frac{\mu v}{\epsilon}+\frac{\sigma v}{\epsilon}\right) b^{2\alpha}$$

that cannot be balanced.

Now let the two small eigenvalues be instead

$$\lambda_{2,3} = c_2 r^{\beta} + c_3 r^{\gamma}$$

where c_2, r are given by (2.24) and c_3 constant, $1/2 < \gamma \leq 1$.

The next lowest term in r is $r^{3/2}$, so $\gamma = 1$, and setting coefficient of $r^{3/2}$ to 0

$$-\left(\mu+\frac{\sigma}{\epsilon}-\frac{v^2}{\epsilon}\right) c_2^2 + \left(\frac{\mu v}{\epsilon}+\frac{\sigma v}{\epsilon}\right) 2c_3 + \frac{\mu}{\epsilon}(\mu+\sigma) = 0.$$

Solving this equation gives

$$c_3 = -\frac{\mu}{2v^3(\mu+\sigma)^2}\left[v^2\left((\mu+\sigma)^2-\sigma(1-\mu)\right)+\sigma(\epsilon\mu+\sigma)(1-\mu)\right]. \tag{2.25}$$

Notice that in (2.25) the polynomial in σ, $(\mu+\sigma)^2-\sigma(1-\mu)$ has a discriminant

$$(1-\mu)(1-5\mu) < 0$$

for the parameter value μ of our choice in (2.13).

So $c_3 < 0$ and

$$\begin{aligned}\lambda_{2,3} = \pm\frac{i}{v}&\left(r\,\frac{\sigma\mu(1-\mu)}{\sigma+\mu}\right)^{1/2} \\ &-\frac{r\,\mu}{2v^3(\mu+\sigma)^2}\left[v^2\left((\mu+\sigma)^2-\sigma(1-\mu)\right)+\sigma(\epsilon\mu+\sigma)(1-\mu)\right].\end{aligned} \tag{2.26}$$

up to first order in r.

So near the endemic steady state (S^*, E^*, I^*), any solution that approaches it as $z \to \infty$ is a linear combination of the eigensolutions corresponding to $\lambda_{1,2,3}$, since they have negative real parts. Since $|\lambda_1| \gg |\text{Re}\,\lambda_{2,3}|$, the amplitude of eigensolution corresponding to λ_1 decays much faster than that of the eigensolutions corresponding to complex $\lambda_{2,3}$. Therefore, sufficiently far back at the tail of the wave, i.e. for sufficiently large z, the eigensolutions corresponding to $\lambda_{2,3}$ govern the behaviors of the traveling wave.

2.3.3 Existence of traveling wave solutions

We have excluded the traveling wave solutions from disease-free steady state to the origin by proposition 2.2, however for the first order system (2.15) the existence of traveling wave solutions that satisfy

$$\lim_{z\to-\infty}(S,E,I) = (1,0,0), \quad \lim_{z\to-\infty}(S',E',I') = (0,0,0)$$

and

$$\lim_{z\to\infty}(S,E,I) = (S^*,E^*,I^*), \quad \lim_{z\to\infty}(S',E',I') = (0,0,0)$$

have not been discussed. Let us briefly discuss the intuitive reason that traveling wave solutions satisfying the above conditions exist.

The traveling wave solutions correspond to orbits in phase space connecting one critical point to another. For our first order system in (2.15) the task is to find a trajectory connecting $(1,0,0,0,0)$ to $(S^*,0,E^*,0,I^*)$ in $\mathbb{R}^5$, with $S, E, I > 0$.

Many studies exist that concern the existence of traveling wave solutions to reaction diffusion equations (see for instance the monograph by Volpert *et al.* (1994) and references citepd therein). However the traveling waves found are shown using quasi-monotone dynamical system theories and constructing upper and lower solutions to set up proofs using fixed point theorems. In our case, the system (2.15) is not necessarily quasi-monotone.

From our linearized analysis near the disease-free steady state, we find that unstable manifold at $(1, 0, 0, 0, 0)$ is three dimensional, since there are three eigenvalues with positive real parts for Jacobian matrix at $(1, 0, 0, 0, 0)$. In previous section, we show that the stable manifold of $(S^*, 0, E^*, 0, I^*)$ is three dimensional, since there are three eigenvalues with negative real parts for the corresponding Jacobian matrix. Roughly speaking, the traveling wave solutions are identified as the intersection of the three dimensional unstable manifold at $(1, 0, 0, 0, 0)$ and the three dimensional stable manifold at $(S^*, 0, E^*, 0, I^*)$ in $\mathbb{R}^5$ with $S, E, I > 0$. This induces topological arguments that are similar to those employed in Dunbar (1984).

2.4 Traveling wavefronts for delayed SI reaction diffusion model

For system (2.6) we do not look for nondimensionalization. The possible equilibriums are extinction equilibrium $(0, 0)$, disease-free equilibrium $(K, 0)$ and endemic equilibrium $(\hat{S}, \hat{I})$ where

$$\begin{aligned} \hat{S} &= \frac{\mu}{\beta} e^{bT} \\ \hat{I} &= \frac{r}{\beta}\left(1 - \frac{\mu}{\beta K} e^{bT}\right) \end{aligned} \tag{2.27}$$

And (2.27) are positive if and only if

$$1 - \frac{\mu}{\beta K} e^{bT} > 0 \Leftrightarrow K > \frac{\mu}{\beta} e^{bT} =: \hat{K_c} \tag{2.28}$$

where $\hat{K_c}$ is defined as the critical carrying capacity for (2.6), similar to K_c. Note that we let $T = 1/\sigma$.

2.4.1 Minimum wave speed for delayed SI reaction diffusion model

Here we only look for traveling wave solutions of (2.6) connecting the disease-free steady state $(K, 0)$ with the endemic equilibrium $(\hat{S}, \hat{I})$ given by (2.27). We also assume that (2.28) holds so that the endemic equilibrium exists.

The traveling wave solution describes the invasion process by the rabies virus into a group of susceptible animals. To study the minimum traveling wave speed, we let $z = x + vt$, where $v \geq 0$ without loss of generality. Then system (2.6) becomes

$$\begin{aligned} vS' &= rS\left(1 - \frac{S}{K}\right) - \beta SI \\ vI' &= D_1 I'' - \mu I + \beta e^{-bT} \int_{-\infty}^{\infty} S(z - vT - y) I(z - vT - y) \frac{e^{-y^2/(4D_2T)}}{2\sqrt{\pi D_2 T}} \, \mathrm{d}y \end{aligned} \tag{2.29}$$

where differentiation is with respect to z, and the second equation is the result of a change of variable $\tilde{y} = x - y$ in the integral and getting rid of the tilde.

We need to solve (2.29) for $(S(z), I(z))$ subjected to

$$\lim_{z \to -\infty} (S, I) = (K, 0) \qquad \text{and} \qquad \lim_{z \to \infty} (S, I) = (\hat{S}, \hat{I}).$$

Assume that the solution exist and we will focus on the speed $v \geq 0$ at which endemic wave front can spread. Primarily we seek the minimum wave front speed that gives biologically reasonable solutions, i.e. $S(z), P(z) \geq 0$. As a result, we require that as $z \to -\infty$, the convergence of $I(z)$ to 0 is non-oscillatory.

As we linearize the second equation of (2.29) about $(K, 0)$, we obtain

$$vI' = D_1 I'' - \mu I + \beta K e^{-bT} \int_{-\infty}^{\infty} I(z - vT - y) \frac{e^{-y^2/(4D_2T)}}{2\sqrt{\pi D_2 T}} \, \mathrm{d}y$$

which has solutions $I(z) = e^{\lambda z}$ if λ satisfies the following

$$v\lambda = D_1 \lambda^2 - \mu + \beta K e^{-bT} e^{-vT\lambda} \int_{-\infty}^{\infty} e^{-\lambda y} \frac{e^{-y^2/(4D_2T)}}{2\sqrt{\pi D_2 T}} \, \mathrm{d}y.$$

Note that in the integral we have the Gaussian kernel or the fundamental solution associated with partial differential operator $\partial_t - \Delta_x$

$$\Gamma(t, x) = \frac{1}{\sqrt{4\pi t}} e^{-\frac{x^2}{4t}}$$

where t is replaced by $D_2 T$.

The following proposition will be used

Proposition 2.3 (Proposition 4.2 in (Thieme and Zhao, 2003)) *Let $\Gamma(t,x)$ be the fundamental solution associated with the partial differential operator $\partial_t - \Delta_x$. Then*

$$\int_{\mathbb{R}^n} e^{-\lambda y_1}\,\Gamma(s,y)\,\mathrm{d}y = e^{\lambda^2 s}$$

with y_1 the first coordinate of y.

Therefore by proposition 2.3

$$\int_{-\infty}^{\infty} e^{-\lambda y}\frac{e^{-y^2/(4D_2T)}}{2\sqrt{\pi D_2 T}}\,\mathrm{d}y = \int_{\mathbb{R}} e^{-\lambda y}\,\Gamma\left(D_2T,y\right)\,\mathrm{d}y = e^{D_2T\lambda^2}.$$

It then follows that λ needs to satisfy

$$-D_1\lambda^2 + v\lambda + \mu = \beta K e^{T\left(D_2\lambda^2 - v\lambda - b\right)} \tag{2.30}$$

Let

$$f(\lambda) = -D_1\lambda^2 + v\lambda + \mu \quad \text{and} \quad g(\lambda) = \beta K e^{T\left(D_2\lambda^2 - v\lambda - b\right)}$$

Define

$$p(\lambda) = f(\lambda) - g(\lambda).$$

Rewriting both left and right-hand sides of (2.30), we have

$$-D_1\left(\lambda - \frac{v}{2D_1}\right)^2 + \frac{v^2}{4D_1} + \mu = \beta K e^{-bT} e^{D_2\left(\lambda - \frac{v}{2D_2}\right)^2 - \frac{v^2}{4D_2}} \tag{2.31}$$

To find the minimum traveling wave speed, it is necessary to make sure that there is at least one positive real root of $p(\lambda)$ and no complex roots exist with positive real parts so that $I(z)$ will converge to 0 in a non-oscillatory way. As we can see from Figure 2.2 plots of both left and right-hand sides of (2.31), if v is small there are no real positive roots, and as v increases, there is a critical value $\hat{v_c}$ at which the left and right-hand sides of (2.31) just touch and are tangent to each other, which corresponds to a positive double root for $p(\lambda)$. Further increase in $v > \hat{v_c}$ will lead to two distinct positive real roots for $p(\lambda)$.

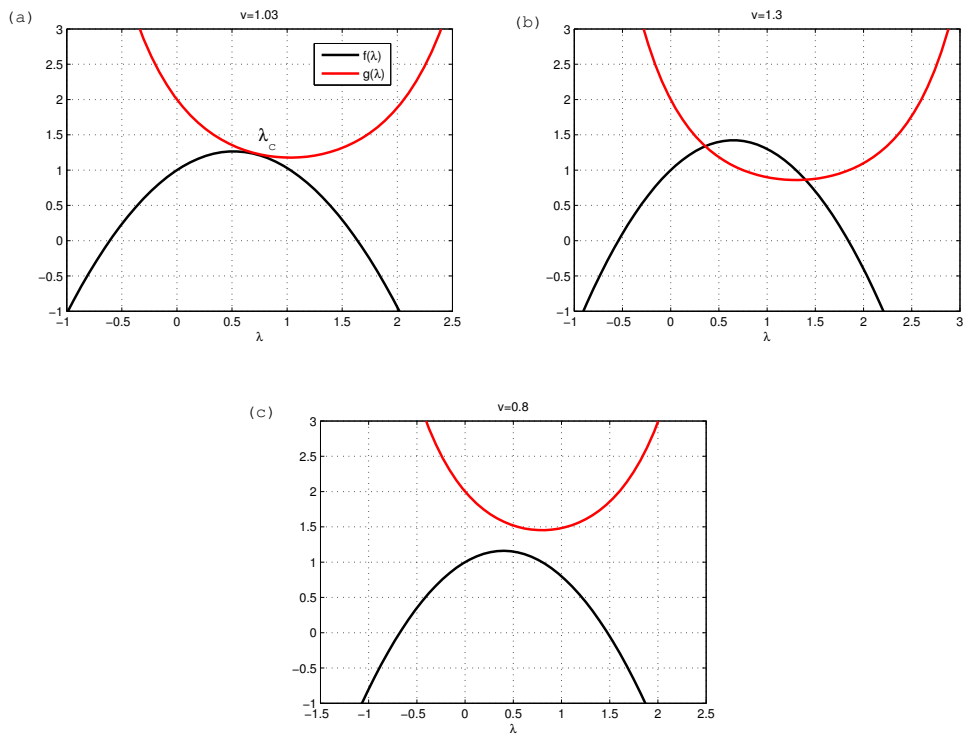

Figure 2.2: The profiles for typical left and right hand-side functions in (2.31) with various values of v. Here $f(\lambda) = -(\lambda - v/2)^2 + v^2/4 + 1$ and $g(\lambda) = 2e^{(\lambda-v)^2/2-v^2/2}$. $p(\lambda) = f(\lambda) - g(\lambda)$ is obtained from linearization of second equation in (2.29) about $(K, 0)$. Then $f(\lambda)$ and $g(\lambda)$ could have (a) a double root at λ_c, (b) two distinct positive real roots or (c) two complex roots with positive real parts.

To find the critical wave speed $\hat{v_c}$ we only need to solve for $\lambda > 0$ from

$$p(\lambda) = 0 \qquad \text{and} \qquad p'(\lambda) = 0$$

which gives us

$$\begin{aligned} -D_1\lambda^2 + v\lambda + \mu &= \beta K e^{-bT} e^{D_2 T\lambda^2 - vT\lambda} \\ -2D_1\lambda + v &= \beta K e^{-bT} e^{D_2 T\lambda^2 - vT\lambda} \left(2D_2 T\lambda - vT\right) \end{aligned} \tag{2.32}$$

Combining two equations in (2.32) gives us

$$q(\lambda) = T(2D_2\lambda - v)(D_1\lambda^2 - v\lambda - \mu) - (2D_1\lambda - v) = 0. \tag{2.33}$$

We note that

$$q\left(\frac{v}{2D_1}\right) = T\left(\frac{D_2}{D_1} - 1\right)\lambda\left(-\frac{v^2}{4D_1} - \mu\right) > 0 \quad \text{since } D_2 < D_1$$
$$q\left(\frac{v+\sqrt{v^2+4D_1\mu}}{2D_1}\right) = -\sqrt{v^2+4D_1\mu} < 0$$
$$q\left(\frac{v}{2D_2}\right) = -\left(\frac{D_1}{D_2} - 1\right)v < 0 \quad \text{since } D_2 < D_1.$$

Hence there exists a unique positive real root λ_c for $q(\lambda)$ in

$$\left(\frac{v}{2D_1}, \min\left\{\frac{v}{2D_2}, \frac{v+\sqrt{v^2+4D_1\mu}}{2D_1}\right\}\right)$$

Note that there is also another positive root $\bar{\lambda} > \lambda_c$ in (2.33), but since

$$\bar{\lambda} > \frac{v+\sqrt{v^2+4D_1\mu}}{2D_1}$$

the left hand side of the first equation at $\lambda = \bar{\lambda}$ in (2.32) is negative while the right hand side is always positive. This is a contradiction, so it follows that λ_c, the smaller of two positive roots in (2.33), is the unique positive real root of (2.32).

Proposition 2.4 *If the condition (2.28) holds and traveling wave solutions* $(S(z), I(z))$ *exist for system (2.6) such that*

$$\lim_{z\to-\infty}(S, I) = (K, 0) \qquad \textit{and} \qquad \lim_{z\to\infty}(S, I) = (\hat{S}, \hat{I})$$

where $\hat{S}, \hat{I}$ *are given by (2.27), then the minimum traveling wavefront speed* $\hat{v}_c$ *can be calculated first by solving for unique positive root* λ_c *of (2.33) in the interval*

$$\left(\frac{v}{2D_1}, \min\left\{\frac{v}{2D_2}, \frac{v+\sqrt{v^2+4D_1\mu}}{2D_1}\right\}\right)$$

then substituting λ_c *back into either equation of (2.32) to solve for the minimum traveling wave speed* $\hat{v}_c$*.*

Proof See previous discussions in this section.

2.4.2 Estimation of $\hat{v}_c$ for delayed SI system

From proposition 2.4 we know how to solve for the minimum traveling wave speed $\hat{v}_c$, but unfortunately it cannot be computed explicitly. However, when $T = 0$ (2.32) becomes

$$\begin{aligned} -D_1\lambda^2 + v\lambda + \mu &= \beta K \\ -2D_1\lambda + v &= 0 \end{aligned} \tag{2.34}$$

from which we obtain its solutions

$$v_0 = 2\left(D_1\left(\beta K - \mu\right)\right)^{1/2}, \qquad \lambda_0 = \left(\frac{\beta K - \mu}{D_1}\right)^{1/2}. \tag{2.35}$$

Hence when $T = 0$ the minimum speed is given by v_0 in (2.35).

Observe that from Table 2.1

$$T = \frac{1}{\sigma} \approx 0.08.$$

So T is small, and it is possible to estimate $\hat{v}_c$ from (2.32) using perturbation analysis. Also it is of interest to inquire whether the minimum wave speed will decrease or increase when delay is introduced. With a small T we can gain useful information on this using perturbation analysis.

Notice that λ_c depends on T too. Therefore

$$\begin{aligned} \hat{v}_c &= v_0 + Tv_1 + T^2v_2 + \cdots \\ \lambda_c &= \lambda_0 + T\lambda_1 + T^2\lambda_2 + \cdots \end{aligned}$$

where v_0, λ_0 are given in (2.35).

Equating coefficients of order $O(T)$ in both equations for (2.32)

$$\begin{aligned} (-2D_1\lambda_0 + v_0)\lambda_1 + \lambda_0 v_1 &= \beta K\left(-b + D_2\lambda_0^2 - v_0\lambda_0\right) \\ -2D_1\lambda_1 + v_1 &= \beta K\left(2D_2\lambda_0 - v_0\right). \end{aligned} \tag{2.36}$$

After some algebra, we find that

$$v_1 = \beta K\left(\frac{\beta K - \mu}{D_1}\right)^{1/2}\left(D_2 - D_1\left(2 + \frac{b}{\beta K - \mu}\right)\right)$$

so that for small delays, the minimum wave speed is given by

$$\hat{v}_c = 2\left(D_1\left(\beta K-\mu\right)\right)^{1/2} + T\beta K\left(\frac{\beta K-\mu}{D_1}\right)^{1/2}\left(D_2 - D_1\left(2+\frac{b}{\beta K-\mu}\right)\right)+\cdots. \tag{2.37}$$

Thus, whether the minimum wave speed is increased or reduced by a small delay T depends on the sign of $D_2 - D_1\left(2+\frac{b}{\beta K-\mu}\right)$. As we mentioned before, we consider the case $D_2 \ll D_1$ to be relevant, i.e. the dispersal of incubating animals is small. With the set of parameter values in Table 2.1, we find that $v_1 < 0$, so that the wave is slowed down by the delay. More generally, it is slowed down when

$$D_2 < D_1\left(2+\frac{b}{\beta K-\mu}\right).$$

2.5 Numerical experiments of two models

In this section, using the parameter values for European foxes given in Table 2.1, first we can calculate the minimum traveling wave speed v_c and $\hat{v_c}$ by theorem 2.1 and 2.4. After that, we look at numerical verification of minimum traveling wave speeds given in propositions 2.1 and 2.4. Then we consider numerical simulation of both models (2.1) and (2.6) to observe traveling wave fronts.

2.5.1 Comparison between two models

Assume that $D_1 = 40$ and $D_2 = 10$, and $K = 2$.

To compute v_c, based on Table 2.1 we have the following dimensionless parameters

$$r = b = \frac{1}{320}, \quad \sigma = \frac{365}{4480}, \quad \mu = \frac{365}{800}, \quad \epsilon = \frac{1}{4}$$

By proposition 2.1, we need to solve the system defined in (2.19) for the positive pair (v_0, λ_0) such that $f''(\lambda_0) < 0$. Then we have

$$v_0 = 0.3531$$

which has no unit and is the critical wave speed for dimensionless variables X, T. For the normal x, t the minimum wave speed is calculated as

$$v_c = \sqrt{40 \cdot 80 \cdot 2} \cdot 0.3531 = 28.25 \text{ km per year.}$$

On the other hand, by proposition 2.4, the minimum wave speed for the delayed SI system (2.6) is

$$\hat{v}_c = 21.97 \text{km per year.}$$

The minimum wave speed computed for delayed SI system is slower than that for SEI reaction diffusion model.

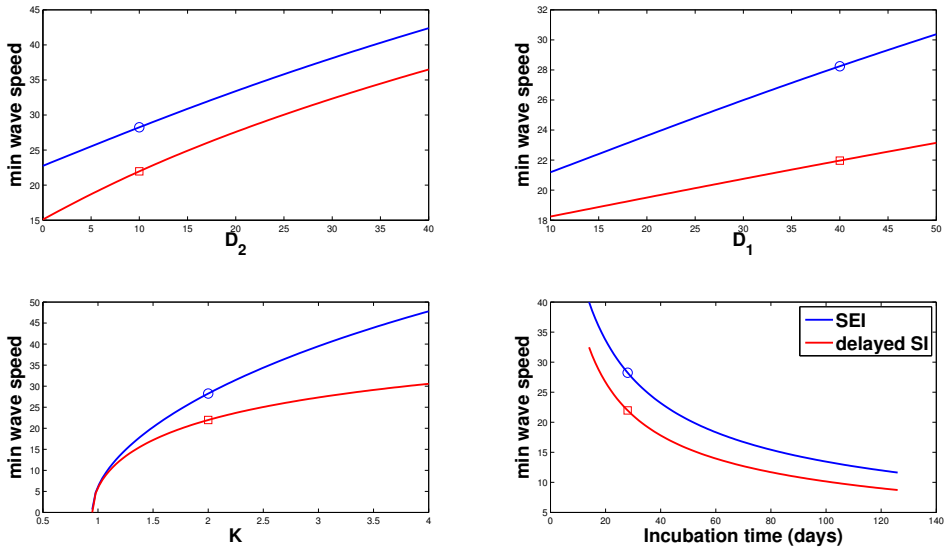

Figure 2.3: Numerical experiments on sensitivity of minimum traveling wave speeds. All parameters values are consistent with Table 2.1. (a) $D_1 = 40$ with D_2 varying. (b) $D_2 = 10$ with D_1 varying. (c) Varying K. Note that equations (2.8) and (2.28) have to be satisfied. (d) Varying incubation length from 14 to 126 days. Also note that minimum wave speeds computed in the illustrative example with $D_1 = 40, D_2 = 10$ are marked as a circle and square in the plot.

To understand how the minimum wave speeds given by propositions 2.1 and 2.4 are affected by parameter values, we perform numerical experiments. Results are presented in Figure 2.3. It is clear that both minimum speeds are increasing functions of D_1, D_2 and K but decreasing functions of incubation length. The relationship between minimum traveling wave speeds and incubation period in both SEI and delayed SI models appears to be an inverse relationship. And it appears that consistently the minimum wave speed computed for the delayed nonlocal SI reaction diffusion equations is lower than that for the SEI reaction diffusion equations. Note that as D_2 approaches 0, the SEI model converges to the model presented and studied in Murray and Seward (1992) and proved to have traveling wave solutions.

2.5.2 SEI reaction diffusion equations

First we consider the numerical verification of the existence of traveling wave solutions and minimum traveling wave speed for the SEI reaction diffusion system (2.1). Specifically, with the traveling wave solution assumption $z = x + vt$, the original SEI system (2.1) becomes a system of first order ODEs

$$\begin{aligned} vS' &= rS(1 - \tfrac{S}{K}) - \beta SI \\ vE' &= \beta SI - bE - \sigma E + D_2 E'' \\ vI' &= \sigma E - \mu I + D_1 I'' \end{aligned} \tag{2.38}$$

where differentiation is with respect to z.

The traveling wave solutions are assumed to connect the disease free equilibrium and positive steady state. Hence

$$\lim_{z\to-\infty} (S(z), E(z), I(z)) = (K, 0, 0), \qquad \lim_{z\to+\infty} (S(z), E(z), I(z)) = (S^*, E^*, I^*)$$

where S^*, E^*, I^* are given in (2.7).

To find the minimum traveling wave speed for (2.1), we can find the traveling wave

speed for the dimensionless system (2.10) and convert it back to the original units using scalings defined in (2.9).

For the simulation results, we use parameters

$$D_1 = 10, D_2 = 1, K = 2$$

and all other relevant parameter values given in Table 2.1. Hence the dimensionless parameter values are

$$\epsilon = \frac{D_2}{D_1} = 0.1,\ r = b = \frac{1}{320},\ \sigma = \frac{365}{4480},\ \mu = \frac{365}{800}.$$

By proposition 2.4, it is readily obtained that the minimum wave speed is

$$\hat{v} = 0.2903$$

which, converted to original units, becomes $v_c = 11.6124$ kilometers per year.

Figure 2.4 shows simulation results for system (2.38) when $v = 13$, higher than our numerically computed minimum traveling wave speed $v_c = 11.6124$. The results indicate the positivity of solution profiles for system (2.38) in both cases. Note that the traveling wave front is not monotone. As v decreases so that $v = 9 < v_c = 11.6124$ in Figure 2.5, proposition 2.1 and its proof suggest that traveling wave solutions are unlikely, since oscillations around $E = 0$ and $I = 0$, as observed in Figure 2.5, lead to negative population densities.

Figure 2.6 shows the simulation of system (2.1) with $D_1 = 10,\ D_2 = 1,\ K = 2$ and other parameter values consistent with those given in Table 2.1. A rough estimation in the overhead view of traveling profiles in Figure 2.7 gives a minimum traveling wave speed around 12 kilometers per year. This is consistent with our observations in the numerical verification of minimum traveling wave speed for system (2.1) and (2.38).

See Appendix for detailed implementation for numerical experiments.

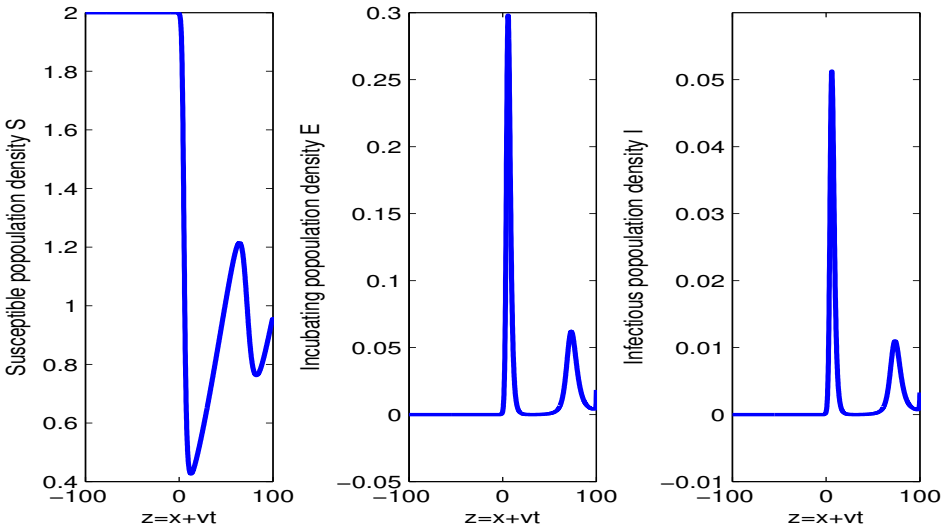

Figure 2.4: Traveling wave profiles generated from (2.38) for susceptible, incubating and infectious animals from left to right. Assuming that $v = 13 > v_c = 11.6124$, there is a traveling wave front with speed $v = 13$.

2.5.3 Delayed SI equations

Now we numerically investigate the existence of traveling wave solutions of the simple delayed SI reaction diffusion model (2.6). The traveling wave solution is assumed to connect the disease free equilibrium and endemic equilibrium. In other words, with $z = x+vt$, we assume that

$$\lim_{z\to-\infty} S(z) = K, \quad \lim_{z\to-\infty} I(z) = 0$$

and

$$\lim_{z\to\infty} S(z) = \hat{S}, \quad \lim_{z\to\infty} I(z) = \hat{I}$$

with $\hat{S}, \hat{I}$ defined in (2.27).

Notice that the simple delayed SI model contains a time delay of incubation period, and a non-local infection term resulted from dispersal of incubating animals. The numerical verification of existence of traveling wave solutions and the minimum traveling wave speed

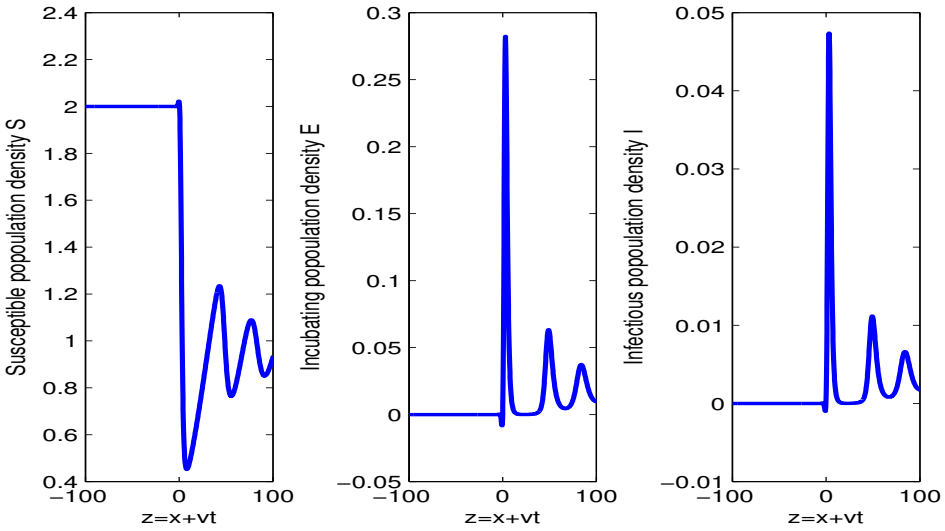

Figure 2.5: Solution profiles generated from (2.38) for susceptible, incubating and infectious animals from left to right. Assuming that $v = 9 < \hat{v} = 11.6124$, traveling wave front does not exist because oscillations near $I = 0$ and $E = 0$ lead to negative population densities.

are non-trivial, and the details of numerical methods used are given in the Appendix. In this section we only look at the results from numerical simulations.

In particular, we plug in $z = x + vt$ to (2.6) and obtain

$$\begin{aligned} vS' &= rS\left(1 - \frac{S}{K}\right) - \beta SI \\ vI' &= D_1 I'' - \mu I + \beta e^{-bT} \int_{\mathbb{R}} S(y + v(t-T))I(y + v(t-T)) \frac{e^{-\frac{(x-y)^2}{4D_2T}}}{2\sqrt{\pi D_2 T}} \, \mathrm{d}y \end{aligned} \tag{2.39}$$

where differentiation is with respect to z.

To find an appropriate $v > 0$ such that the above delayed differential equations have solutions S, I that satisfy the asymptotic boundary conditions above is essentially an eigenvalue problem, which is very complicated because of the non-local term indicated by the integral and the latency of incubation period.

We can use numerical simulations to verify appropriate $v > 0$ such that traveling wave solution to (2.6) exist. Specifically we can perform numerical verification of proposition

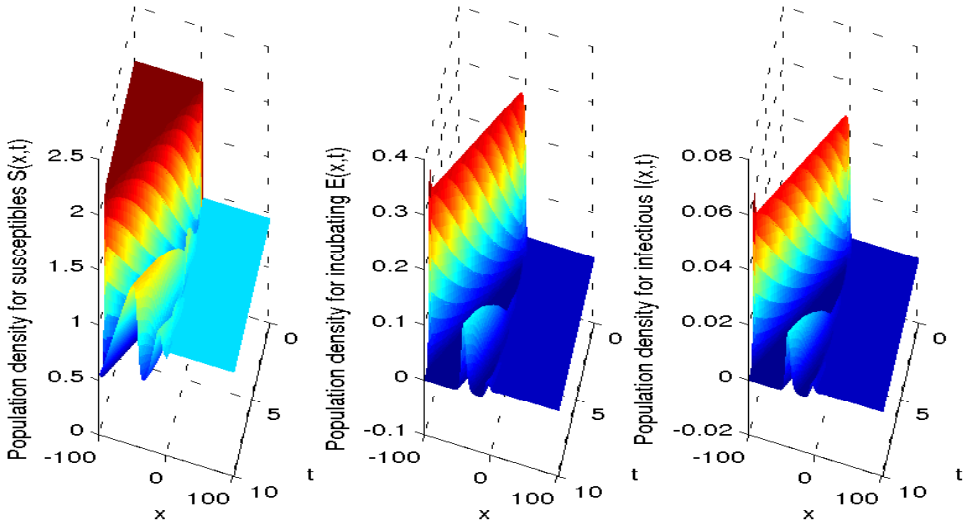

Figure 2.6: Traveling wave profiles observed for system (2.1) with $D_1 = 10,\ D_2 = 1,\ K = 2$ and all other parameter values consistent with Table 2.1. Observe the oscillations after the fist wave of infection. From a rough estimation in the overhead view in Figure 2.7, the minimum traveling wave speed is about 12 kilometers per year.

2.4 by simulating the system (2.39) with varying v.

For the following simulation results, we use parameters

$$D_1 = 10,\ D_2 = 1,\ K = 2 \tag{2.40}$$

in addition to parameters for foxes given in Table 2.1, i.e.

$$r = 0.5,\ b = 0.5,\ T = 28/365,\ \mu = 365/5,\ \beta = 80.$$

The units for space and time are kilometers and years. With these parameter values, proposition 2.4 gives the minimum traveling wave speed

$$\hat{v}_c = 9.003 \text{ km per year.}$$

Figure 2.9 shows simulation results generated for system (2.39) when $v = 13$, which is greater than $\hat{v}_c = 9.003$. It clearly indicates the existence of positive solutions to (2.39), and

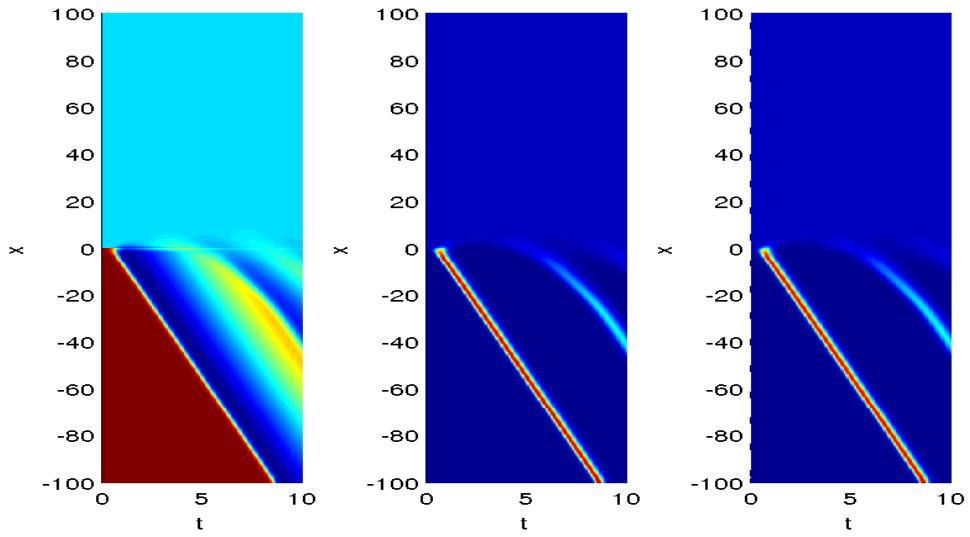

Figure 2.7: Overhead view of traveling wave profiles observed for system (2.1) with $D_1 = 10,\ D_2 = 1,\ K = 2$ and all other parameter values consistent with Table 2.1. The minimum traveling wave speed is about 12 kilometers per year.

thus existence of traveling wave solutions. Comparing the traveling wave solution profiles in Figure 2.9 with that presented for the SEI case (2.38) from Figure 2.4, we find that timing and magnitude for first two infection waves are similar for both the SEI model (2.38) and the delayed SI model (2.39). Also we observe that as v decreases past $\hat{v}_c = 9.003$, when $v = 5$, our discussions from the proposition 2.4 suggest that positive solutions to (2.39) are impossible. This is reflected in the negative infectious population densities observed in Figure 2.8.

Next we present the simulation results for simple delayed SI system (2.6). The details of numerical methods used for this part can be seen in the Appendix. For comparison purposes, we choose parameter values to be the same as those used in the numerical verification of existence of traveling wave solutions for (2.39). In particular

$$D_1 = 10,\ D_2 = 1,\ K = 2,\ T = \frac{28}{365}.$$

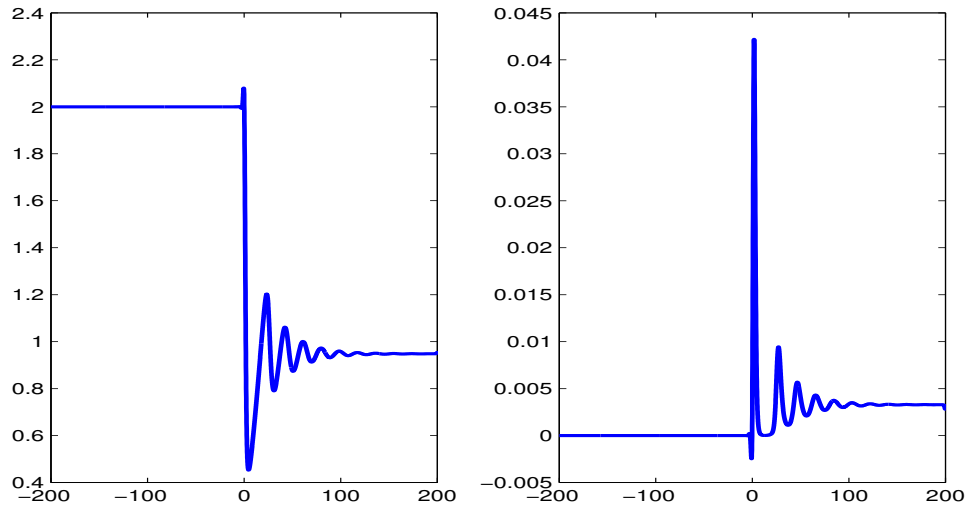

Figure 2.8: Solution profiles generated from (2.39) for susceptible and infectious animals from left to right. Assuming that $v = 5 < \hat{v} = 9.003$, traveling wave solution does not exist, since solution for infectious animals, I, oscillates around $I = 0$ before increasing up to $\hat{I}$.

Note that for convenience, the time step size Δt is chosen so that

$$\frac{T}{\Delta t} = B$$

where B is an integer. In the numerical experiment, we chose $B = 40$.

Figure 2.10 is the simulation result of system (2.6) with $D_1 = 10$, $D_2 = 1$, $K = 2$ and all other parameter values consistent with Table 2.1. Observe that the simulation results clearly show existence of traveling wave solutions. With overhead view of the traveling waves in Figure 2.11, we can estimate the traveling wave speed to be approximately 9 kilometers per year.

In Figure 2.12 we show the simulation results when $D_2 = 10$, i.e the diffusion rate of incubating animals is increased to be the same as that of infectious animals $D_1 = 10$. The persistent oscillations after the first wave of infection still exist, but from Figure 2.13 it is clear that increase in D_2 results in increase in the traveling wave speed.

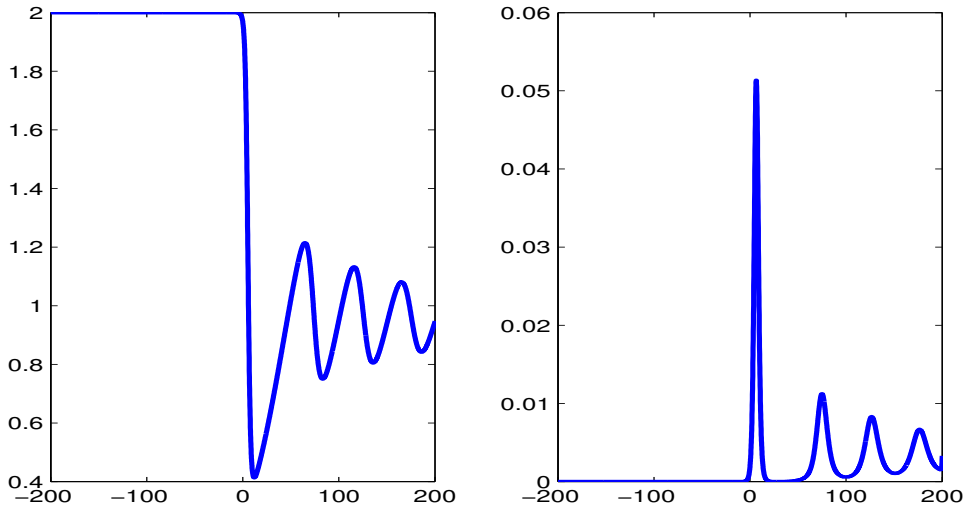

Figure 2.9: Solution profiles generated from (2.39) for susceptible and infectious animals from left to right. Assuming that $v = 13 > \hat{v} = 9.003$, traveling wave solution exists, since solutions stay positive.

2.6 Conclusion and Discussion

In this chapter we have focused on the modeling of incubation period in wildlife rabies models with an application to foxes. We start with an explicit approach where the incubating animals are described by an exposed class in a reaction-diffusion susceptible-exposed-infected (SEI) model. Alternatively we can model the incubating period by a fixed delay between infection and onset of clinical rabid symptoms. Tracking the dispersal of latent individuals and making use of the classical age structure modeling, we have obtained a delayed reaction-diffusion susceptible-infected (SI) system which contains, in addition to the diffusion term, a non-local infection term. The non-local term reflects the mobility of individuals during incubation period.

For both models, we do not focus on theoretically proving the existence or non-existence of traveling wave solutions, instead we seek to numerically verify and compare their traveling wave solutions and the minimum wave speeds. From the numerical experimentation we

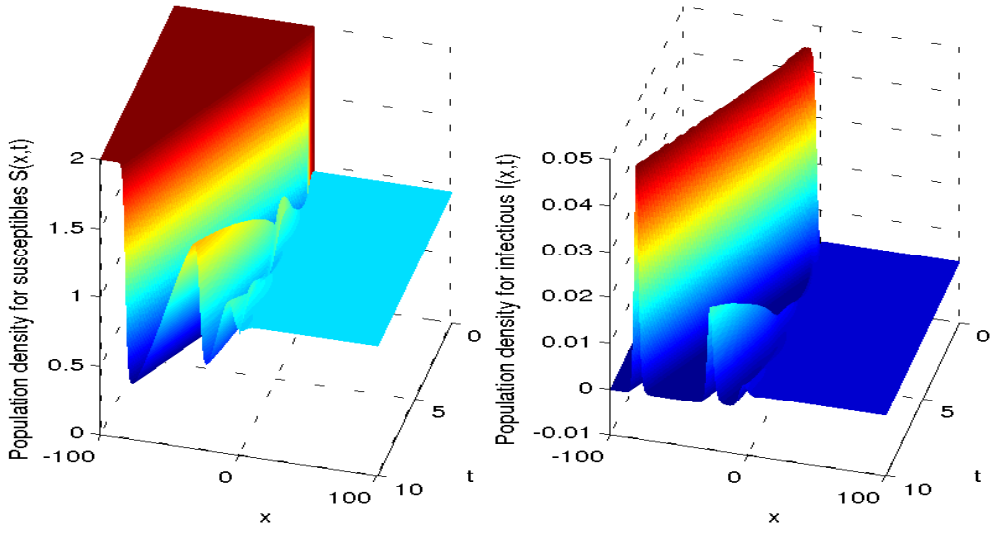

Figure 2.10: The traveling wave observed for the system (2.6) with $D_1 = 10$, $D_2 = 1$, $K = 2$ and all other parameter values consistent with Table 2.1. Note the persistent oscillations after the initial wave.

find that both models generate traveling wave solutions and their corresponding minimum wave speeds agree with our calculations, although consistently the minimum wave speed calculated from the delayed diffusive SI model is lower than that of reaction-diffusion SEI model.

The main difference between the SEI and delayed SI models is the assumption about the distribution of incubation period. In the reaction-diffusion SEI model, it is implicitly assumed that the latency period is exponentially distributed, whereas in the delayed SI model, the incubation period is a fixed constant. More precisely, for the SEI model, the exponential function

$$p_E(s) = e^{-\sigma s}$$

has been used to describe the probability of remaining in the incubation stage and the mean duration of latent state is

$$T_E = \int_0^\infty p_E(s)\,\mathrm{d}s = \frac{1}{\sigma}.$$

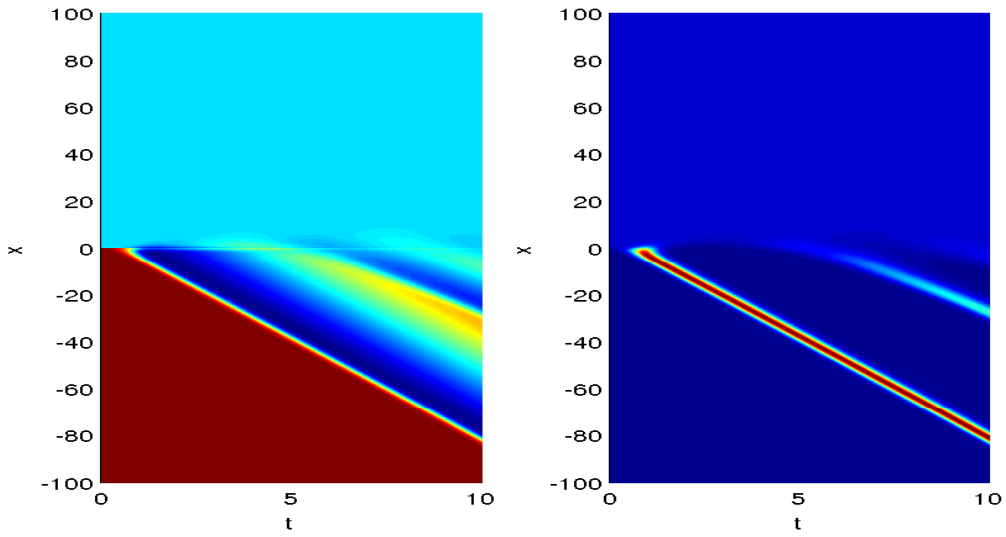

Figure 2.11: The overhead view of traveling wave observed for the system (2.6) with $D_1 = 10$, $D_2 = 1$, $K = 2$ and all other parameter values consistent with Table 2.1. From a rough estimation of the traveling wave speed, it is about 9.

A fundamental property of the exponential distribution is the memory-less property, meaning the remaining expected sojourn time in the exposed (E) class is independent of the time spent in this class. This property of exponential distribution might be in disagreement with the nature of rabies infection. In reality, if an infected fox, for example, already spends some time in the exposed class, the virus must have spread within its central nervous system, resulting in a smaller expected sojourn time in the exposed class. Therefore this implicit exponential distribution assumption might conflict biological realities.

On the other hand, assuming a fixed incubation period in the delayed SI model is questionable by similar arguments. It is documented (Anderson *et al.*, 1981) that the incubation period for foxes, for example, varies with individuals, ranging from 12 to 150 days. Uniformly setting the incubation period for every individual in the population to be the same might be an over-generalized approach.

Therefore both models have weakness in terms of their assumptions about incubation

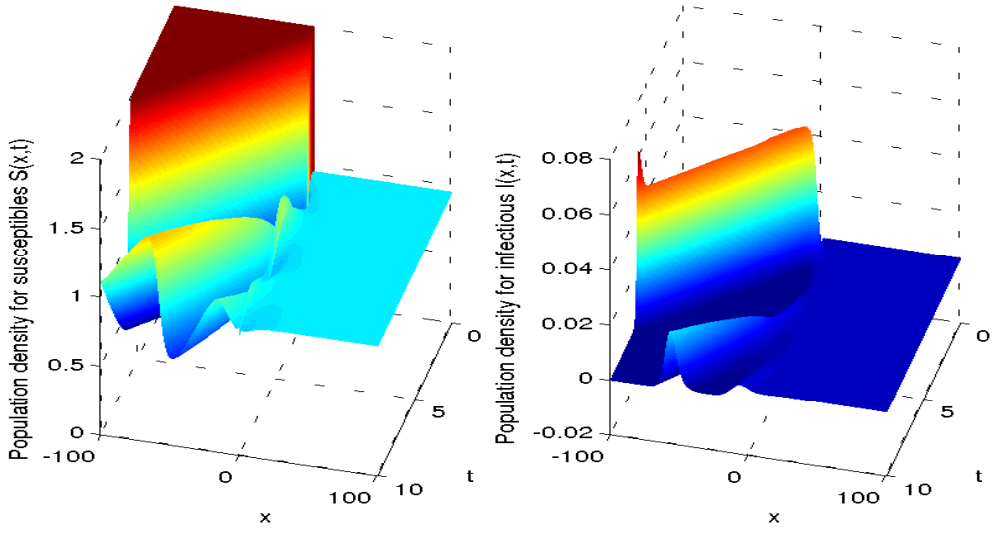

Figure 2.12: The traveling wave observed for the system (2.6) with $D_1 = 10$, $D_2 = 10$, $K = 2$ and all other parameter values consistent with Table 2.1. Note the persistent oscillations after the initial wave.

period distribution. Although both of the two models generate numerically similar results, both can be improved so that more realistic incubation stage distribution can be considered. Epidemiological models with non-exponential distributions such as gamma distribution have been previously discussed (see, for example, Lloyd (2001a,b)). However, for rabies, there has been little evidence so far regarding a general incubation period distribution for any wildlife species.

It is interesting to observe the similarity between numerical results from both models. We have observed traveling wave solutions generated from both, with wave speeds both decreasing in the incubation period, increasing in diffusion rates for incubating D_2 and infectious individuals D_1, and increasing in carrying capacity K. Both wave profiles have actual spread speed coinciding with the minimum traveling wave speed. Theoretical questions may be raised as to why these two types of modeling lead to similar system behaviors.

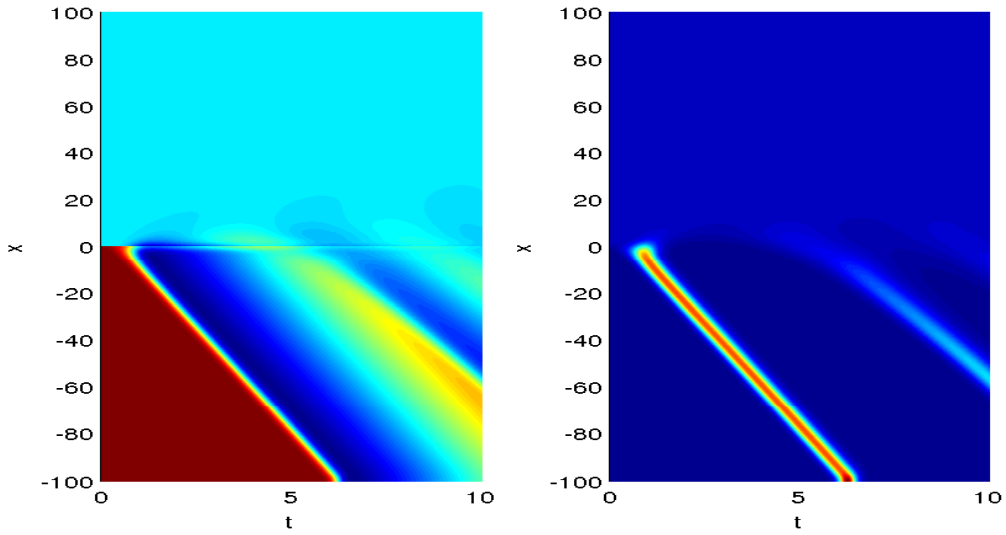

Figure 2.13: The overhead view of traveling wave observed for the system (2.6) with $D_1 = 10$, $D_2 = 10$, $K = 2$ and all other parameter values consistent with Table 2.1. It is clear that increase in $D2$ leads to increase of traveling wave speed.

Chapter 3

AN ALTERNATIVE RABIES MODEL INCORPORATING INFECTION AGE

This chapter continues the investigation of diffusive rabies epidemic models incorporating incubation period. In previous two models in chapter 2, the incubation phenomenon was considered by either adding an exposed class or introducing a delay into the partial differential equations, the latter of which leads to complicated delayed nonlocal reaction diffusion equations. In this chapter we will treat the incubation period by introducing instead an age variable "a", which represents the time elapsed since contracting rabies. Basically there are the following advantages in using this approach

(1) simpler expressions for the relationship between subclasses of the model (no exposed class);

(2) less information needed for initial conditions;

(3) allowing the modeling of infection-age structure of the population.

The apparent disadvantage to this age-dependent approach, however, is the first partial derivatives with respect to "a", adding analytical complexities to the model.

Kermack and McKendrick (1927, 1932, 1933, 1937, 1939) provided a general framework for the analysis of infectious diseases which allows the infectivity of individuals to depend on age of infection. But the general form of Kermack and McKendrick model was largely neglected until around 1970s (Hoppensteadt, 1974; Reddingius, 1971). The age of infection approach has been applied extensively in epidemic models for HIV/AIDS (Thieme and Castillo-Chavez, 1993; Feng and Thieme, 2000). Diffusive models with infection-age-dependent structures can been seen in early works by Gurtin and MacCamy (1974,

1979), Webb (1980). Recently the diffusive models with infection-age-dependent structures have been studied for infection of bacteria by phage (Smith, 2008; Jones *et al.*, 2013). We refer to Webb (2008) for a general review on diffusive age-dependent epidemiological models.

In sections 1 and 2, we introduce infection-age-dependent diffusion rate, infectivity and death rate in the model. In section 1 both infectious and incubating individuals are lumped in an infective class, whose infectivity is a function of infection age, while in section 2, infectious individuals are differentiated from incubating ones by letting only the incubating class be dependent on infection age. Two modeling approaches result in different model structures but both lead to the same integral equation in the special case of fixed incubation length which can be analyzed using theories developed in Thieme (1979), Thieme and Zhao (2003). In section 3 a sufficient admissibility condition is given for the initial condition and the asymptotic speed of spread c^* is estimated.

3.1 A rabies model with infection age dependent diffusion and infectivity

We make the following simplifying assumptions first. We assume that susceptible animals do not move around while infected animals do. We also ignore the natural population turnover of animals. Also we assume that the diffusion rate and infectivity of an infected animal depends on its infection age a, where a is the time that has passed since the moment of infection.

We consider one-dimensional domain of $\mathbb{R}$. Let $S(x,t)$ be the density of susceptible animals at location $x \in \mathbb{R}$ and time $t \geq 0$, and $\mathcal{I}(x,t)$ be the density of infected animals at location x and time t. We stratify the infected animals along infection age a,

$$\mathcal{I}(x,t) = \int_0^\infty I(x,t,a)\,\mathrm{d}a, \tag{3.1}$$

where $I(x,t,a)$ is the density of infected animals at location x and time t with infection

age a. The use of infection age (or age at infection) goes as far back as the classical work of Kermack and McKendrick (1927, 1932, 1933, 1937, 1939).

With the above simplifying assumptions, the susceptibles obey the following differential equations

$$\begin{aligned} &\partial_t S(x,t) = -S(x,t)J(x,t) =: -B(x,t) \\ &J(x,t) = \int_0^\infty \eta(a) I(x,t,a)\,\mathrm{d}a \\ &S(x,0) = S_0(x) \end{aligned} \tag{3.2}$$

where $x \in \mathbb{R}$ and $t \geq 0$. Here we denote

$$B(x,t) = S(x,t)J(x,t)$$

as the incidence at location x and time t, i.e. the number of new infections per unit of time. $\eta(a)$ is the infectivity of an infected animal with infection age a, and $J(x,t)$ is the infection force at location x and time t.

To model the infected population, we first let $D(a)$ be the infection age dependent diffusion rate of an infected animal, and $\mu(a)$ be infection age dependent per capita death rate of an infected animal.

In age dependent models, similar to Thieme and Zhao (2003), the density of infected animals at location x and time t with infection age a can be modeled by

$$\partial_t\, I(x,t,a) + \partial_a\, I(x,t,a) = D(a)\,\partial_x^2\, I(x,t,a) - \mu(a)\, I(x,t,a). \tag{3.3}$$

For initial conditions, we have

$$I(x,t,0) = B(x,t) \quad \text{and} \quad I(x,0,a) = I_0(x,a).$$

Let

$$v(x,r,a) = I(x,r+a,a) \tag{3.4}$$

be the density at location x and time $r+a$ of infected animals with infection age $a \geq 0$ that have been infected at time $r \geq 0$.

Now we can integrate along characteristics in (3.3). We consider $r \geq 0$ as a parameter and x, a as independent variables in the following partial differential equation

$$\begin{aligned} &\partial_a v(x,r,a) = D(a)\,\partial_x^2 v(x,r,a) - \mu(a) v(x,r,a), \\ &v(x,r,0) = I(x,r,0) = B(x,r). \end{aligned} \tag{3.5}$$

From the properties of the Gaussian kernel we derive a solution to (3.5) that is given by

$$\begin{aligned} v(x,r,a) &= \int_{\mathbb{R}} \Gamma(\theta(a), x-y) B(y,r) \mathcal{F}(a)\,\mathrm{d}y, \\ \theta(a) &= \int_0^a D(s)\,\mathrm{d}s, \\ \mathcal{F}(a) &= \exp\left(-\int_0^a \mu(s)\,\mathrm{d}s\right) \end{aligned} \tag{3.6}$$

where the Gaussian kernel is given by

$$\Gamma(t,x) = \frac{1}{\sqrt{4\pi t}} e^{-\frac{x^2}{4t}}$$

and $\mathcal{F}(a)$ is the probability of an infected individual not having died from rabies infection at infection age a.

In fact, since by the chain rule

$$\partial_a\,\Gamma(\theta(a),x) = \theta'(a)\,\partial_t\,\Gamma(\theta(a),x) = D(a)\,\partial_x^2\,\Gamma(\theta(a),x)$$

we can derive that (3.6) is indeed a solution of (3.5). With $a > 0$

$$\begin{aligned} \partial_a\, v(x,r,a) &= \partial_a \left(\int_{\mathbb{R}} \Gamma(\theta(a), x-y) B(y,r) \mathcal{F}(a)\,\mathrm{d}y\right) \\ &= \int_{\mathbb{R}} \partial_a\,\Gamma(\theta(a), x-y) B(y,r) \mathcal{F}(a)\,\mathrm{d}y + \int_{\mathbb{R}} \Gamma(\theta(a), x-y) B(y,r) \mathcal{F}'(a)\,\mathrm{d}y \\ &= \int_{\mathbb{R}} D(a) \partial_x^2\,\Gamma(\theta(a), x-y) B(y,r) \mathcal{F}(a)\,\mathrm{d}y \\ &\qquad + \int_{\mathbb{R}} \Gamma(\theta(a), x-y) B(y,r) \mathcal{F}(a)\,(-\mu(a))\,\mathrm{d}y \\ &= D(a)\,\partial_x^2\, v(x,r,a) - \mu(a) v(x,r,a) \end{aligned}$$

and

$$v(x, r, 0) = B(x, r)$$

by property of the Gaussian kernel.

Also we consider

$$w(x, t, r) = I(x, t, t + r) \tag{3.7}$$

be the density of animals at location x and time t that already had infection age r at time 0. Hence at time t these animals have infection age $t + r$. Once again, we consider $r \geq 0$ as a parameter and x, t as independent variables of the following partial differential equation,

$$\begin{aligned} &\partial_t\, w(x, t, r) = D(t + r)\, \partial_x^2\, w(x, t, r) - \mu(t + r)\, w(x, t, r) \\ &w(x, 0, r) = I_0(x, r) \end{aligned} \tag{3.8}$$

where D, μ is evaluated at infection age $t + r$.

One readily checks that a solution of (3.8) is given by

$$w(x, t, r) = \frac{\mathcal{F}(t + r)}{\mathcal{F}(r)} \int_{\mathbb{R}} \Gamma\left(\theta(t + r) - \theta(r), x - y\right) I_0(y, r)\, \mathrm{d}y. \tag{3.9}$$

In fact for $t > 0$

$$\begin{aligned} \partial_t\, w(x, t, r) =& \partial_t \left(\frac{\mathcal{F}(t + r)}{\mathcal{F}(r)} \int_{\mathbb{R}} \Gamma\left(\theta(t + r) - \theta(r), x - y\right) I_0(y, r)\, \mathrm{d}y \right) \\ =& \frac{\partial_t\, \mathcal{F}(t + r)}{\mathcal{F}(r)} \int_{\mathbb{R}} \Gamma\left(\theta(t + r) - \theta(r), x - y\right) I_0(y, r)\, \mathrm{d}y \\ &+ \frac{\mathcal{F}(t + r)}{\mathcal{F}(r)} \int_{\mathbb{R}} \partial_t\, \Gamma\left(\theta(t + r) - \theta(r), x - y\right) I_0(y, r)\, \mathrm{d}y \\ =& \frac{-\mu(t + r)\mathcal{F}(t + r)}{\mathcal{F}(r)} \int_{\mathbb{R}} \Gamma\left(\theta(t + r) - \theta(r), x - y\right) I_0(y, r)\, \mathrm{d}y \\ &+ D(t + r) \frac{\mathcal{F}(t + r)}{\mathcal{F}(r)} \int_{\mathbb{R}} \partial_x^2\, \Gamma\left(\theta(t + r) - \theta(r), x - y\right) I_0(y, r)\, \mathrm{d}y \\ =& -\mu(t + r) w(x, t, r) + D(t + r) \partial_x^2\, w(x, t, r) \end{aligned}$$

while by property of the Gaussian kernel

$$w(x, 0, r) = I_0(x, r).$$

Therefore with the formula for $I(x,t,a)$ defined in (3.6) and (3.9), we can express the infection force $J(x,t)$ in terms of $v(x,r,a)$ and $w(x,t,r)$,

$$J(x,t) = \underbrace{\int_0^t \eta(a)v(x,t-a,a)\,\mathrm{d}a}_{J_1(x,t)} + \underbrace{\int_t^\infty \eta(a)w(x,t,a-t)\,\mathrm{d}a}_{J_0(x,t)}. \tag{3.10}$$

Substituting (3.6) and (3.9) we find that

$$\begin{aligned} J_1(x,t) &= \int_0^t \eta(a)\mathcal{F}(a) \int_{\mathbb{R}} \Gamma(\theta(a), x-y)B(y,t-a)\,\mathrm{d}y\,\mathrm{d}a \\ J_0(x,t) &= \int_t^\infty \eta(a)\frac{\mathcal{F}(a)}{\mathcal{F}(a-t)} \int_{\mathbb{R}} \Gamma\left(\theta(a)-\theta(a-t), x-y\right) I_0(y,a-t)\,\mathrm{d}y\,\mathrm{d}a. \end{aligned} \tag{3.11}$$

Solving the system of ordinary differential equations for $S(x,t)$ in (3.2), we arrive at

$$\begin{aligned} S(x,t) &= S_0(x)e^{-u(x,t)} \\ u(x,t) &= \int_0^t J(x,s)\,\mathrm{d}s. \end{aligned} \tag{3.12}$$

This gives us the idea to derive a single equation for $u(x,t)$ (see also Diekmann (1977, 1978); Thieme (1977)),

$$u(x,t) = u_1(x,t) + u_0(x,t) \tag{3.13}$$

where using results from (3.11)

$$\begin{aligned} u_1(x,t) &= \int_0^t J_1(x,s)\,\mathrm{d}s \\ &= \int_0^t \left(\int_0^s \eta(a)\mathcal{F}(a) \int_{\mathbb{R}} \Gamma(\theta(a), x-y)B(y,s-a)\,\mathrm{d}y\,\mathrm{d}a \right) \mathrm{d}s. \end{aligned} \tag{3.14}$$

Interchanging the order of integration in (3.14) we find

$$u_1(x,t) = \int_0^t \eta(a)\mathcal{F}(a) \int_{\mathbb{R}} \Gamma(\theta(a), x-y) \left(\int_a^t B(y,s-a)\,\mathrm{d}s \right) \mathrm{d}y\,\mathrm{d}a. \tag{3.15}$$

By our assumptions we ignore natural turnover of the animal population, so from (3.2) we have $B(x,t) = -\partial_t S(x,t)$. Therefore in (3.15), by fundamental theorem of calculus we have

$$\begin{aligned} \int_0^t B(y,s-a)\,\mathrm{d}s &= -\int_0^t \partial_s S(y,s-a)\,\mathrm{d}s \\ &= S_0(y) - S(y,t-a). \end{aligned} \tag{3.16}$$

By (3.12) and (3.16), the equation in (3.15) becomes

$$u_1(x,t) = \int_0^t \int_{\mathbb{R}} \eta(a)\mathcal{F}(a)\Gamma\left(\theta(a), x-y\right) S_0(y) \left(1 - e^{-u(y,t-a)}\right) \,\mathrm{d}y\,\mathrm{d}a. \tag{3.17}$$

If we let

$$k(a,x,y) = \eta(a)\mathcal{F}(a)\Gamma\left(\theta(a), y\right) S_0(x-y) \tag{3.18}$$

and

$$f(u) = 1 - e^{-u} \tag{3.19}$$

then with a change of variable (3.17) can be written as

$$u_1(x,t) = \int_0^t \int_{\mathbb{R}} k(a,x,y) f(u(x-y,t-a)) \,\mathrm{d}y\,\mathrm{d}a. \tag{3.20}$$

The formula for $u_0(x,t)$ can be determined by initial condition $I_0(x,a)$. But to write down the formula for $u_0(x,t)$, we make a substitution in (3.11),

$$J_0(x,t) = \int_0^\infty \eta(a+t)\frac{\mathcal{F}(a+t)}{\mathcal{F}(a)} \int_{\mathbb{R}} \Gamma\left(\theta(a+t) - \theta(a), x-y\right) \, I_0(y,a) \,\mathrm{d}y\,\mathrm{d}a.$$

Hence

$$\begin{aligned} u_0(x,t) &= \int_0^t J_0(x,s)\,\mathrm{d}s \\ &= \int_0^\infty \int_{\mathbb{R}} \left(\int_0^t \eta(a+s)\frac{\mathcal{F}(a+s)}{\mathcal{F}(a)} \Gamma\left(\theta(a+s) - \theta(a), x-y\right) \,\mathrm{d}s \right) I_0(y,a)\,\mathrm{d}y\,\mathrm{d}a. \end{aligned} \tag{3.21}$$

Therefore we obtain that

$$u(x,t) = u_0(x,t) + \int_0^t \int_{\mathbb{R}} k(a,x,y) f(u(x-y,t-a)) \,\mathrm{d}y\,\mathrm{d}a, \tag{3.22}$$

where $u_0(x,t)$ is defined in (3.21) and $k(a,x,y)$, $f(u)$ are defined in (3.18) and (3.19).

If we assume that S_0 is constant, then since Γ is the Gaussian kernel

$$k(a,x,y) = k(a,|y|) = \eta(a)\mathcal{F}(a)\Gamma(\theta(a),y)S_0.$$

Hence we can write (3.22) as

$$u(x,t) = u_0(x,t) + \int_0^t \int_{\mathbb{R}} k(a,|y|) f(u(x-y,t-a))\,\mathrm{d}y\,\mathrm{d}a. \tag{3.23}$$

The equation in (3.23) is in a form that can be analyzed for spreading speeds and traveling wave solutions by the theory developed in (Thieme, 1979; Thieme and Zhao, 2003). This theory has recently been applied in Jones *et al.* (2012, 2013).

We consider the special case that there is a fixed incubation period of length $\tau > 0$. Then $\eta(a) = 0$ for $a \in (0,\tau)$ and $\eta(a) = \eta$ for $a > \tau$. Further $\mu(a) = \nu$ for $a > \tau$ and $D(a) = \tilde{D}$ for $a > \tau$. Assuming S_0 is constant, we have

$$k(a,|y|) = \begin{cases} 0 & 0 \le a < \tau \\ \eta\,\mathcal{F}(\tau) e^{-\nu(a-\tau)}\,\Gamma\left(\theta(\tau) + \tilde{D}(a-\tau), y\right) S_0, & a \ge \tau \end{cases} \tag{3.24}$$

3.2 A rabies model with distributed infection period

In the last section, we interpret $I(x,t,a)$ as the density of infected animals of infection age a at location x and time t, and assign infection age dependent infectivity function $\eta(a)$, diffusion rate function $D(a)$ and death rate function $\mu(a)$ to infected animals. While this is a general enough approach, it is still difficult to use this model to incorporate distributed incubation period τ. To consider distributed incubation period, we make changes in the model (3.2), (3.5) and (3.8).

We now consider $I(x,t,a)$ as the density of infected animals at location x and time t with infection age a that are not yet infective. Further $J(x,t)$ are the infective animals at location x and time t. In this model we make similar assumptions as last model. We assume only incubating and infective animals disperse. We ignore the natural population turnover

of both susceptible and infected yet not infective animals. Now the model becomes

$$\begin{aligned}
&\partial_t S(x,t) = -S(x,t)\eta J(x,t) =: -B(x,t),\\
&S(x,0) = S_0(x),\\
&\partial_t J(x,t) = \tilde{D}\,\partial_x^2 J(x,t) + \int_0^\infty I(x,t,a)P(\,\mathrm{d}a) - \nu\, J(x,t),\\
&J(x,0) = J^\circ(x).
\end{aligned} \tag{3.25}$$

Here $\tilde{D}, \nu$ describe fixed diffusion rate and per capita death rate of infective animals. Also the probability measure P represents the distribution of the length of the incubation period. Now let

$$h(x,t) = \int_0^\infty I(x,t,a)P(\,\mathrm{d}a). \tag{3.26}$$

Then

$$h(x,t) = h_1(x,t) + h_0(x,t) \tag{3.27}$$

with

$$h_1(x,t) = \int_0^t I(x,t,a)P(\,\mathrm{d}a) = \int_0^t v(x,t-a,a)P(\,\mathrm{d}a) \tag{3.28}$$

and

$$h_0(x,t) = \int_t^\infty I(x,t,a)P(\,\mathrm{d}a) = \int_t^\infty w(x,t,a-t)P(\,\mathrm{d}a). \tag{3.29}$$

Similar to (3.4) and (3.7), $v(x,t,r)$ represents the density of incubating animals at location x that have infection age r and have been infected at time t, and $w(x,t,r)$ is defined as the density of incubating animals at location x and time t that already had infection age r at time 0. But since we interpret $I(x,t,a)$ as infected animals that are not yet infective, now the partial differential equations for $v(x,t,r)$ and $w(x,t,r)$, as defined in (3.5) and (3.8), should in general be followed with a loss term, because incubating individuals will become eventually infective after an incubation period, which is described by the probability measure P.

We want to ensure that it is reasonable to use equations defined for $I(x,t,a)$ in (3.6) and (3.9) to replace the I in (3.25), even if $I(x,t,a)$ defined in (3.6) and (3.9) mean infected animals while $I(x,t,a)$ in (3.25) represents incubating animals.

Let $\tilde{I}(x,t,a)$ and $\tilde{J}(x,t)$ for now be density for incubating animals and density for fully infective animals. Consider the infection age dependent transition rate $\beta(a)$ from incubating class to fully infective class. We impose a few assumptions on $\beta(a)$.

(M) $\beta : \mathbb{R}_+ \to [0,1]$ is a continuously differentiable function such that

$(M1)$ $\beta(0) = 0$, i.e. it is impossible for a newly infected animal to turn infective,

$(M2)$ $\beta'(a) \geq 0$, and $\lim_{a\to\infty} \beta(a) = 1$, i.e. longer incubation translates into higher rate of becoming infective,

$(M3)$ $\displaystyle\int_0^\infty \beta(a)\,\mathrm{d}a = \infty.$

Similar to (3.3) we use the following system to model the transition from incubating class to infective class

$$\begin{aligned}
&\partial_t \tilde{I}(x,t,a) + \partial_a \tilde{I}(x,t,a) = D(a)\,\partial_x^2 \tilde{I}(x,t,a) - \mu(a)\,\tilde{I}(x,t,a) - \beta(a)\,\tilde{I}(x,t,a)\\
&\partial_t \tilde{J}(x,t) = \tilde{D}\,\partial_x^2 \tilde{J}(x,t) + \int_0^\infty \beta(a)\,\tilde{I}(x,t,a)\,\mathrm{d}a - \nu\,\tilde{J}(x,t).
\end{aligned} \tag{3.30}$$

Let $G(a) = \exp\left(\displaystyle\int_0^a \beta(s)\,\mathrm{d}s\right)$. Multiply the $\tilde{I}(x,t,a)$ equation in (3.30) by $G(a)$,

$$\partial_t\left(G(a)\partial_t\tilde{I}\right) + \partial_a\left(G(a)\partial_a\tilde{I}\right) = D(a)\,\partial_x^2\left(G(a)\tilde{I}\right) - \mu(a)\left(G(a)\tilde{I}\right).$$

Set

$$U(x,t,a) = G(a)\tilde{I}(x,t,a).$$

It follows that

$$\partial_t U(x,t,a) + \partial_a U(x,t,a) = D(a)\,\partial_x^2 U(x,t,a) - \mu(a)\,U(x,t,a). \tag{3.31}$$

Similar to $v(x,r,a)$ in (3.4) and $w(x,t,r)$ in (3.7), we can stratify $U(x,t,a)$ so that

$$\begin{aligned}\bar{v}(x,r,a) &= U(x,a+r,a) = G(a)\tilde{I}(x,a+r,a)\\ \bar{w}(x,t,r) &= U(x,t,t+r) = G(t+r)\tilde{I}(x,t,t+r)\end{aligned} \tag{3.32}$$

Notice that initial conditions for $\bar{v}$ and $\bar{w}$ here are

$$\begin{aligned}\bar{v}(x,r,0) &= G(0)\tilde{I}(x,r,0) = B(x,r)\\ \bar{w}(x,0,r) &= G(r)\tilde{I}(x,0,r) = G(r)I_0(x,r)\end{aligned} \tag{3.33}$$

where I_0 is now the initial profile of incubating animals.

Similar to (3.6) and (3.9), we integrate along characteristics.

$$\begin{aligned}\bar{v}(x,r,a) &= \int_{\mathbb{R}} \Gamma\left(\theta(a), x-y\right) B(y,r)\mathcal{F}(a)\,\mathrm{d}y\\ \bar{w}(x,t,r) &= \frac{\mathcal{F}(t+r)}{\mathcal{F}(r)}\,G(r)\int_{\mathbb{R}} \Gamma\left(\theta(t+r)-\theta(r), x-y\right) I_0(y,r)\,\mathrm{d}y\end{aligned} \tag{3.34}$$

where $\mathcal{F}(a)$ and $\theta(a)$ are as defined in (3.6).

Therefore, in the equation for $\tilde{J}$ in (3.30),

$$\begin{aligned}&\int_0^\infty \beta(a)\tilde{I}(x,t,a)\,\mathrm{d}a\\ &= \int_0^\infty \frac{\beta(a)}{G(a)}\,U(x,t,a)\,\mathrm{d}a\\ &= \int_0^t \frac{\beta(a)}{G(a)}\,\bar{v}(x,t-a,a)\,\mathrm{d}a + \int_t^\infty \frac{\beta(a)}{G(a)}\,\bar{w}(x,t,a-t)\,\mathrm{d}a\\ &= \int_0^t \frac{\beta(a)}{G(a)}\left(\int_{\mathbb{R}} \Gamma\left(\theta(a), x-y\right) B(y,t-a)\mathcal{F}(a)\,\mathrm{d}y\right)\mathrm{d}a\\ &\quad + \int_t^\infty \frac{\beta(a)}{G(a)}\left(\frac{\mathcal{F}(a)}{\mathcal{F}(a-t)}\,G(a-t)\int_{\mathbb{R}} \Gamma\left(\theta(a)-\theta(a-t), x-y\right) I_0(y,a-t)\,\mathrm{d}y\right)\mathrm{d}a\end{aligned} \tag{3.35}$$

Compare (3.35) with equations for $I(x,t,a)$ in (3.6) and (3.9). We see that we can still use solutions to $I(x,t,a)$ in (3.3) without resorting to the model (3.30). All we need is for the set of initial conditions for (3.3) to be replaced by (3.33).

So

$$\int_0^\infty \beta(a)\tilde{I}(x,t,a)\,\mathrm{d}a = \int_0^\infty P(a)\,I(x,t,a)\,\mathrm{d}a \tag{3.36}$$

where $P(a) \geq 0$ such that

$$P(a) = \frac{\beta(a)}{G(a)} = \beta(a)\,\exp\left(-\int_0^a \beta(a)\,\mathrm{d}s\right) \tag{3.37}$$

and $I(x,t,a)$ is density of incubating animals calculated from (3.3) with modified initial conditions defined in (3.33).

Note that in (3.37)

$$\begin{aligned}\int_0^\infty P(a)\,\mathrm{d}a &= \int_0^\infty \beta(a)\,\exp\left(-\int_0^a \beta(s)\,\mathrm{d}s\right)\,\mathrm{d}a \\ &= -\left(\exp\left(-\int_0^a \beta(s)\,\mathrm{d}s\right)\right)\Big|_0^\infty = 1\end{aligned}$$

where we use property $(M3)$ of $\beta(a)$.

Hence $P(a)$ is a probability density function. Because $\beta(a)$ is generally unknown, we can assume that in (3.25), $P(\,\mathrm{d}a)$ is an arbitrary probability measure.

Also for the calculation of $I(x,t,a)$ in (3.25) we use (3.33) as our initial conditions.

Realizing this we still use (3.6) and (3.9) to replace $v(x,t,r)$ and $w(x,t,r)$. And throughout our discussion we keep the general form of P.

Now (3.28) becomes

$$h_1(x,t) = \int_0^t P(\,\mathrm{d}a)\mathcal{F}(a)\int_{\mathbb{R}} \Gamma(\theta(a), x-y)B(y,t-a)\,\mathrm{d}y \tag{3.38}$$

and (3.29) is determined by initial data

$$h_0(x,t) = \int_t^\infty P(\,\mathrm{d}a)\frac{\mathcal{F}(a)}{\mathcal{F}(a-t)}\int_{\mathbb{R}} \Gamma\left(\theta(a)-\theta(a-t), x-y\right) I_0(y,a-t)\,\mathrm{d}y. \tag{3.39}$$

By the variation of constants formula,

$$\begin{aligned}J(x,t) \;&= \int_0^t \int_{\mathbb{R}} \Gamma\left(\tilde{D}(t-s), x-z\right) e^{-\nu(t-s)} h(z,s)\,\mathrm{d}z\,\mathrm{d}s \\ &\quad + \int_{\mathbb{R}} \Gamma\left(\tilde{D}t, x-y\right) e^{-\nu t} J^\circ(y)\,\mathrm{d}y.\end{aligned} \tag{3.40}$$

To see this, from (3.25)

$$\partial_t J(x,t) + \nu J(x,t) = \tilde{D}\partial_x^2 J(x,t) + h(x,t).$$

Multiplying both sides by $e^{\nu t}$ it becomes

$$\partial_t \left(e^{\nu t} J(x,t)\right) = \tilde{D}\partial_x^2 \left(e^{\nu t} J(x,t)\right) + h(x,t)e^{\nu t}.$$

Let $A(x,t) = e^{\nu t} J(x,t)$. Then $A(x,0) = J^\circ$ and

$$\begin{aligned} A(x,t) = &\int_0^t \int_{\mathbb{R}} \Gamma\left(\tilde{D}(t-s), x-y\right) h(y,s) e^{\nu s} \,\mathrm{d}y \,\mathrm{d}s \\ &+ \int_{\mathbb{R}} \Gamma\left(\tilde{D}t, x-y\right) J^\circ(y) \,\mathrm{d}y. \end{aligned}$$

Then multiplying both sides by $e^{-\nu t}$ we obtain (3.40).

So by (3.27), (3.38) and (3.39)

$$J(x,t) = J_0(x,t) + \int_0^t \int_{\mathbb{R}} \Gamma\left(\tilde{D}(t-s), x-z\right) e^{-\nu(t-s)} h_1(z,s) \,\mathrm{d}z \,\mathrm{d}s \tag{3.41}$$

where

$$\begin{aligned} J_0(x,t) \;&= \int_{\mathbb{R}} \Gamma\left(\tilde{D}t, x-y\right) e^{-\nu t} J^\circ(y) \,\mathrm{d}y \\ &\quad + \int_0^t \int_{\mathbb{R}} \Gamma\left(\tilde{D}(t-s), x-z\right) e^{-\nu(t-s)} h_0(z,s) \,\mathrm{d}z \,\mathrm{d}s \end{aligned} \tag{3.42}$$

which is determined by initial data $J^\circ(x)$ and $I_0(x,a)$, initial density of infective animals and initial profile of incubating animals respectively. We fit (3.38) into (3.41),

$$\begin{aligned} &J(x,t) - J_0(x,t) \\ = \;& \int_0^t \int_{\mathbb{R}} \Gamma\left(\tilde{D}(t-s), x-z\right) e^{-\nu(t-s)} \\ &\left(\int_0^s P(\,\mathrm{d}a)\mathcal{F}(a) \int_{\mathbb{R}} \Gamma\left(\theta(a), z-y\right) B(y, s-a) \,\mathrm{d}y\right) \mathrm{d}z \,\mathrm{d}s. \end{aligned} \tag{3.43}$$

We change the order of integration

$$\begin{aligned} &J(x,t) - J_0(x,t) \\ &= \int_0^t e^{-\nu(t-s)} \,\mathrm{d}s \int_0^s P(\,\mathrm{d}a)\mathcal{F}(a) \int_{\mathbb{R}} B(y, s-a) \,\mathrm{d}y \\ &\qquad \left(\int_{\mathbb{R}} \Gamma\left(\tilde{D}(t-s), x-z\right) \Gamma\left(\theta(a), z-y\right) \,\mathrm{d}z\right). \end{aligned} \tag{3.44}$$

By a change of variable $z \to z + y$ and the Chapman-Kolmogorov equation for Γ,

$$\begin{aligned}\int_{\mathbb{R}} \Gamma\left(\tilde{D}(t-s), x-z\right) \Gamma\left(\theta(a), z-y\right)\, \mathrm{d}z \\ &= \int_{\mathbb{R}} \Gamma\left(\tilde{D}(t-s), x-y-z\right) \Gamma\left(\theta(a), z\right)\, \mathrm{d}z \\ &= \Gamma\left(\tilde{D}(t-s) + \theta(a), x-y\right).\end{aligned} \tag{3.45}$$

So

$$\begin{aligned}&J(x,t) - J_0(x,t) \\ &= \int_0^t P(\,\mathrm{d}a)\mathcal{F}(a) \int_a^t e^{-\nu(t-s)} \int_{\mathbb{R}} \Gamma\left(\tilde{D}(t-s) + \theta(a), x-y\right) B(y, s-a)\,\mathrm{d}y\,\mathrm{d}s.\end{aligned} \tag{3.46}$$

We make a change of variables, $t - s = r - a$,

$$\begin{aligned}&J(x,t) - J_0(x,t) \\ &= \int_0^t P(\,\mathrm{d}a)\mathcal{F}(a) \int_a^t e^{-\nu(r-a)} \int_{\mathbb{R}} \Gamma\left(\tilde{D}(r-a) + \theta(a), x-y\right) B(y, t-r)\,\mathrm{d}y\,\mathrm{d}r.\end{aligned} \tag{3.47}$$

Now we set

$$u(x,t) = \eta \int_0^t J(x,s)\,\mathrm{d}s, \qquad u_0(x,t) = \eta \int_0^t J_0(x,s)\,\mathrm{d}s. \tag{3.48}$$

Then from (3.47)

$$\begin{aligned}&u(x,t) - u_0(x,t) \\ &\qquad = \eta \int_0^t \mathrm{d}s \int_0^s P(\,\mathrm{d}a)\mathcal{F}(a) \int_a^s e^{-\nu(r-a)} \\ &\qquad\qquad \left(\int_{\mathbb{R}} \Gamma\left(\tilde{D}(r-a) + \theta(a), x-y\right) B(y, s-r)\,\mathrm{d}y\right) \mathrm{d}r.\end{aligned}$$

We change the order of integration a few times,

$$\begin{aligned}&u(x,t) - u_0(x,t) \\ &\quad = \eta \int_0^t P(\,\mathrm{d}a) \int_a^t \mathrm{d}s \int_a^s \mathcal{F}(r) \left(\int_{\mathbb{R}} \Gamma\left(\theta(r), x-y\right) B(y, s-r)\,\mathrm{d}y\right) \mathrm{d}r \\ &\quad = \eta \int_0^t P(\,\mathrm{d}a) \int_a^t \mathcal{F}(r)\,\mathrm{d}r \int_{\mathbb{R}} \Gamma\left(\theta(r), x-y\right) \left(\int_r^t B(y, s-r)\,\mathrm{d}s\right) \mathrm{d}y.\end{aligned}$$

Now by (3.25) and fundamental theorem of calculus

$$\int_r^t B(y, s-r)\,\mathrm{d}s = -\int_r^t \partial_s S(y, s-r)\,\mathrm{d}s = S_0(y) - S(y, t-r) = S_0(y) f(u(y, t-r))$$

where

$$f(u) = 1 - e^{-u}.$$

Then

$$\begin{aligned} &u(x,t) - u_0(x,t) \\ &\quad = \eta \int_0^t P(\,\mathrm{d}a) \int_a^t \mathcal{F}(r)\,\mathrm{d}r \int_{\mathbb{R}} \Gamma\left(\theta(r), x-y\right) S_0(y) f(u(y, t-r))\,\mathrm{d}y. \end{aligned} \tag{3.49}$$

So with a change of variable

$$u(x,t) = u_0(x,t) + \int_0^t \int_{\mathbb{R}} k(r,x,y) f(u(x-y, t-r))\,\mathrm{d}y\,\mathrm{d}r \tag{3.50}$$

with

$$k(r,x,y) = \eta \int_0^r P(\,\mathrm{d}a) \mathcal{F}(a) e^{-\nu(r-a)}\,\Gamma\left(\tilde{D}(r-a) + \theta(a), y\right) S_0(x-y). \tag{3.51}$$

If we consider fixed incubation period τ, then P is the Dirac measure concentrated at τ,

$$k(r,x,y) = \begin{cases} 0, & 0 \le r < \tau \\ \eta\,\mathcal{F}(\tau) e^{-\nu(r-\tau)}\,\Gamma\left(\theta(\tau) + \tilde{D}(r-\tau), y\right) S_0(x-y). & r \ge \tau \end{cases} \tag{3.52}$$

If we further let $S_0(x)$ be constant, (3.52) becomes the same integration kernel as in (3.24). Then, similar to (3.23), equation (3.50) is in a form that can be analyzed for asymptotic spreading speeds and traveling wave solutions by theories developed in (Thieme, 1979; Thieme and Zhao, 2003).

3.3 Asymptotic spread speeds

We have assumed constant $S_0(x)$ and fixed incubation period τ in both models (3.2) and (3.25). We arrive at identical integral equations in (3.23) and (3.50), i.e.

$$u(x,t) = u_0(x,t) + \int_0^t \int_{\mathbb{R}} k(s, |y|) f(u(x-y, t-s))\,\mathrm{d}s\,\mathrm{d}y \tag{3.53}$$

with $k(s,|y|)$ and $f(u)$ defined in (3.24) and (3.19) respectively. This equation can be readily analyzed for asymptotic spread speed and traveling wave solutions using theories developed in (Thieme, 1979; Thieme and Zhao, 2003).

We first state a few definitions and results from Thieme (1979) and Thieme and Zhao (2003).

We consider nonlinear integral equation

$$u(x,t) = u_0(x,t) + \int_0^t \int_{\mathbb{R}^n} F\left(u(x-y,t-s),s,y\right)\,\mathrm{d}y\,\mathrm{d}s, \tag{3.54}$$

where $F : \mathbb{R}_+^2 \times \mathbb{R}^n \to \mathbb{R}$ is continuous in u and Borel measurable in (s,y), and $u_0 : \mathbb{R}^n \times \mathbb{R}_+ \to \mathbb{R}_+$ is Borel measurable and bounded. n is the dimension. In (3.23) and (3.50) we consider $n = 1$. The following assumptions are imposed on F:

(A) There exists a function $k : \mathbb{R}_+ \times \mathbb{R}^n \to \mathbb{R}_+$ such that

$(A1)$ $k^* := \int_0^\infty \int_{\mathbb{R}^n} k(s,x)\,\mathrm{d}x\,\mathrm{d}s < \infty$.

$(A2)$ $0 \le F(u,s,x) \le uk(s,x), \forall u,s \ge 0, x \in \mathbb{R}^n$.

$(A3)$ For every compact interval I in $(0,\infty)$, there exists some $\epsilon > 0$ such that

$$F(u,s,x) \ge \epsilon k(s,x), \quad \forall u \in I, s \ge 0, x \in \mathbb{R}^n.$$

$(A4)$ For every $\epsilon > 0$, there exists some $\delta > 0$ such that

$$F(u,s,x) \ge (1-\epsilon)uk(s,x), \quad \forall u \in [0,\delta], s \ge 0, x \in \mathbb{R}^n.$$

$(A5)$ For every $w > 0$, there exists some $\Lambda > 0$ such that

$$|F(u,s,x) - F(v,s,x)| \le \Lambda\,|u-v|\,k(s,x), \forall u,v \in [0,w], s \ge 0, x \in \mathbb{R}^n.$$

Proposition 3.1 (Proposition 2.1 in Thieme and Zhao (2003)) *Let (A) hold. Then for every Borel measurable, nonnegative and bounded function $u_0(x,t)$, there exists a unique*

Borel measurable solution $u : \mathbb{R}^n \times \mathbb{R}_+ \to \mathbb{R}_+$ *of (3.54), and* u *is bounded on* $[0, r] \times \mathbb{R}^n$ *for every* $r > 0$.

Let $c > 0$ and $u : \mathbb{R}^n \times [0, \infty) \to \mathbb{R}$. We define

$$\liminf_{t\to\infty, |x|\le ct} u(x,t) = \sup_{t\ge 0} \inf\{u(x,s) : \ s \ge t, |x| \le cs\}$$

and

$$\limsup_{t\to\infty, |x|\le ct} u(x,t) = \inf_{t\ge 0} \sup\{u(x,s) : \ s \ge t, |x| \le cs\}.$$

We say that

$$\lim_{t\to\infty, |x|\le ct} u(x,t) = u^*$$

if and only if

$$u^* = \limsup_{t\to\infty, |x|\le ct} u(x,t) = \liminf_{t\to\infty, |x|\le ct} u(x,t)$$

Definition (Definition 2.1 **in Thieme and Zhao (2003))** A number $c^* > 0$ is called the asymptotic speed of spread for a function $u : \mathbb{R}^n \times \mathbb{R}_+ \to \mathbb{R}_+$ if $\lim_{t\to\infty, |x|\le ct} u(x,t) = 0$ for every $c > c^*$, and if there exists some $\epsilon > 0$ such that $\liminf_{t\to\infty, |x|\le ct} u(x,t) \ge \epsilon$ for every $c \in (0, c^*)$.

Recall that a function $\Phi : \mathbb{R}^n \to \mathbb{R}$ is said to be isotropic if $\Phi(x) = \Phi(y)$ whenever $|x| = |y|$. A function $k : [0, \infty) \times \mathbb{R}^n \to \mathbb{R}$ is said to be isotropic if $k(s, \cdot)$ is isotropic for almost all $s > 0$. We make the following assumptions on $k : \mathbb{R}_+ \times \mathbb{R}^n \to \mathbb{R}_+$

(B) k is a Borel measurable function such that

$(B1)$ $k^* > 1$ where k^* is defined in $(A1)$.

$(B2)$ There exists some $\lambda_0 > 0$ such that

$$\int_0^\infty \int_{\mathbb{R}^n} e^{\lambda_0 y_1} k(s,y)\, \mathrm{d}y\, \mathrm{d}s < \infty$$

where y_1 is the first component of y.

($B3$) There exist numbers $\sigma_2 > \sigma_1 > 0, \rho > 0$ such that

$$k(s,x) > 0, \qquad \forall s \in (\sigma_1, \sigma_2), |x| \in [0, \rho).$$

($B4$) k is isotropic.

Let

$$\mathscr{K}(c,\lambda) = \int_0^\infty \int_{\mathbb{R}^n} e^{-\lambda(cs+y_1)}\, k(s,y)\, \mathrm{d}y\, \mathrm{d}s \tag{3.55}$$

with y_1 the first coordinate of y.

Lemma 3.2 (Lemma 2.1 **in Thieme and Zhao (2003))** *Let (B) hold. Then for every $c > 0$ there exists $\bar{\lambda}(c) \in (0, \infty]$ such that $\mathscr{K}(c,\lambda) < \infty$ for $\lambda \in [0,\ \bar{\lambda}(c)\ )$ and $\mathscr{K}(c,\lambda) = \infty$ for $\lambda \in (\bar{\lambda}(c),\ \infty)$. Note that the last interval is possibly empty.*

We define

$$c^* := \inf\{c \geq 0 :\ \mathscr{K}(c,\lambda) < 1 \text{ for some } \lambda > 0\}. \tag{3.56}$$

Lemma 3.3 *c^* is monotone increasing with respect to $\mathscr{K}$.*

Proof Let $\tilde{\mathscr{K}}(c,\lambda) \leq \mathscr{K}(c,\lambda)$ for all $c, \lambda \geq 0$. Also suppose

$$\tilde{c^*} = \inf\{c \geq 0 :\ \tilde{\mathscr{K}}(c,\lambda) < 1 \text{ for some } \lambda > 0\}$$

Now let $c_0, \lambda_0 > 0$ be arbitrary such that $\mathscr{K}(c_0,\lambda_0) < 1$. Then $c^* \leq c_0$. Note that since $\tilde{\mathscr{K}}(c,\lambda) \leq \mathscr{K}(c,\lambda)$ for all $c, \lambda > 0$, it also implies

$$\tilde{\mathscr{K}}(c_0,\lambda_0) \leq \mathscr{K}(c_0,\lambda_0) < 1.$$

Hence we find

$$\{c \geq 0 :\ \mathscr{K}(c,\lambda) < 1 \text{ for some } \lambda > 0\} \subseteq \{c \geq 0 :\ \tilde{\mathscr{K}}(c,\lambda) < 1 \text{ for some } \lambda > 0\}.$$

It follows from the definition of infimum that $\tilde{c^*} \leq c^*$.

Proposition 3.4 (Proposition 2.3 **in Thieme and Zhao (2003))** *Let* (B) *hold and assume that*

$$\liminf_{\lambda \nearrow \bar{\lambda}(c)} \mathscr{K}(c,\lambda) \geq k^*$$

for every $c > 0$*. Then there exists a unique* $\lambda^* \in (0,\ \bar{\lambda}(c^*)\,)$ *such that* $\mathscr{K}(c^*,\lambda^*) = 1$ *and* $\mathscr{K}(c^*,\lambda) > 1$ *for* $\lambda \neq \lambda^*$*. Moreover,* c^* *and* λ^* *are uniquely determined as the solutions of the system*

$$\mathscr{K}(c,\lambda) = 1, \qquad \textit{and} \qquad \frac{\mathrm{d}}{\mathrm{d}\lambda}\mathscr{K}(c,\lambda) = 0.$$

Note that

$$\liminf_{\lambda \nearrow \bar{\lambda}(c)} \mathscr{K}(c,\lambda) = \lim_{\lambda \to \bar{\lambda}(c)^-} \inf\{\mathscr{K}(c,y) :\ y \in (\lambda, \bar{\lambda}(c))\}.$$

We define the admissibility of $u_0(x,t)$

Definition (Admissible $u_0(x,t)$**)** We say $u_0(x,t)$ is admissible if for every $c, \lambda > 0$ with $\mathscr{K}(c,\lambda) < 1$, there exists some $\gamma > 0$ such that

$$u_0(x,t) \leq \gamma\, e^{\lambda(ct - |x|)}, \qquad \forall t \geq 0,\ x \in \mathbb{R}^n. \tag{3.57}$$

Theorem 3.5 (Theorem 2.1 **in Thieme and Zhao (2003))** *Let* (A) *and* (B) *hold. Then for every admissible* $u_0(x,t)$*, the unique solution* $u(x,t)$ *of (3.54) satisfies* $\lim_{t\to\infty, |x|\geq ct} u(x,t) = 0$ *for each* $c > c^*$*.*

Theorem 3.5 does not guarantee that c^* is the asymptotic speed of spread for $u(x,t)$. However, if the integrand is a special case, i.e. $F(u,s,x) = k(s,x)f(u)$, and $f(u)$ satisfies the following assumptions, we can ensure that c^* is the asymptotic speed of spread.

(C) $f : \mathbb{R}_+ \to \mathbb{R}_+$ is a Lipschitz continuous function such that

$(C1)$ $f(0) = 0$ and $f(u) > 0, \forall u > 0$;

($C2$) f is differentiable at $u = 0$, $f'(0) = 1$ and $f(u) \leq u$, $\forall u > 0$;

($C3$) $\lim_{u\to\infty} \dfrac{f(u)}{u} = 0$;

($C4$) there exists a positive solution u^* of

$$u = k^* f(u) \tag{3.58}$$

such that $k^* f(u) > u$, $\forall u \in (0, u^*)$, and $k^* f(u) < u$, $\forall u > u^*$.

Theorem 3.6 (Theorem 2.2 in Thieme and Zhao (2003)) *Let $F(u, s, x) = f(u)k(s, x)$. Assume that (B) and (C) hold, and f is monotone increasing. Then for any Borel measurable function $u_0 : \mathbb{R}^n \times \mathbb{R}_+ \to \mathbb{R}_+$ with the property that $u_0(x, t) \geq \eta > 0$, $\forall t \in (t_1, t_2), |x| \leq \eta$, for appropriate $t_2 > t_1 \geq 0$, $\eta > 0$, there holds*

$$\liminf_{t\to\infty, |x|\leq ct} u(x, t) \geq u^*, \qquad \forall c \in (0, c^*)$$

where u^* is defined in (3.58).

For special case of $F(u, s, x) = f(u)k(s, x)$, theorems 3.5 and 3.6 together imply that c^* is the asymptotic spread speed for the unique solution $u(x, t)$ in (3.54).

Moreover for the limiting equation of (3.54)

$$u(x, t) = \int_0^t \int_{\mathbb{R}} F(u(x - y, t - s), s, y)\, \mathrm{d}y\, \mathrm{d}s \tag{3.59}$$

Thieme and Zhao (2003) established the existence of traveling wave solutions $u(x, t) = v(x + ct)$ for $c \geq c^*$ and the non-existence of traveling wave solutions when $c < c^*$.

Theorem 3.7 (Theorems 3.3, 3.4 in Thieme and Zhao (2003)) *Let $(A2)$ and (B) with $n = 1$ hold. Assume $F(\cdot, s, x)$ is increasing on $[0, u^*]$ for each $(s, x) \in \mathbb{R}_+ \times \mathbb{R}$, and $F(u, s, x) \geq (u - bu^\sigma)k(s, x)$, $\forall u \in [0, \delta]$, $(s, x) \in \mathbb{R}_+ \times \mathbb{R}$ for appropriate $\delta \in (0, u^*]$, $\sigma > 1$ and $b > 0$. Also $k(s, \cdot)$ is continuous on $\mathbb{R}$ for all $s \geq 0$. Then for each $c \geq c^*$, there exists a monotone traveling wave solution of (3.59) with speed c and connecting 0 and u^*.*

Theorem 3.8 (Theorem 3.5 in Thieme and Zhao (2003)) *Let $(A), (B)$ hold. Then for each $c \in (0, c^*)$, there exists no traveling wave solution $u(x,t) = v(x+ct)$ of (3.59) with wave speed c such that $v(\cdot)$ is positive and bounded on $\mathbb{R}$ and $\lim_{\xi \to -\infty} v(\xi) = 0$.*

Note that in the following sections, because of the special form of $F(u,s,x) = f(u)k(s,x)$ where $f(u) = 1 - e^{-u}$, the satisfaction of conditions $(A), (B), (c)$ implies that conditions for Theorems 3.7 and 3.8 hold. Theorefore, it is important to note here that by Theorems-the 3.7 and 3.8 asymptotic speeds of spread c^* calculated in the following sections are also minimum traveling wave speeds for their corresponding limiting integral equations.

3.3.1 Asymptotic spread speed for a fixed delay

Now we are ready to find the asymptotic speed of spread for both (3.23) and (3.50). We observe that the integrands in both equations satisfy $F(u,s,y) = k(s,y)f(u)$, with $k(s,y), f(u)$ defined respectively in (3.24) and (3.19). In other words

$$u(x,t) = u_0(x,t) + \int_0^t \int_{\mathbb{R}} k(s,|y|) f(u(x-y, t-s))\, \mathrm{d}y\, \mathrm{d}s$$

with

$$k(s,|y|) = \begin{cases} 0 & 0 \le s < \tau \\ \eta\, \mathcal{F}(\tau) e^{-\nu(s-\tau)}\, \Gamma\left(\theta(\tau) + \tilde{D}(s-\tau), y\right) S_0, & s \ge \tau \end{cases}$$

and

$$f(u) = 1 - e^{-u}.$$

Note that $\Gamma(t,x)$ is the Gaussian kernel, or the fundamental solution associated with the partial differential operator $\partial_t - \Delta_x$.

First we verify assumptions (A) for $k(s,|y|)$

(A1)

$$k^* = \int_0^\infty \int_{\mathbb{R}} k(s,|y|)\,\mathrm{d}y\,\mathrm{d}s$$
$$= \eta\mathcal{F}(\tau)S_0 \int_\tau^\infty \int_{\mathbb{R}} e^{-\nu(s-\tau)} \frac{1}{\sqrt{4\pi[\theta(\tau)+\tilde{D}(s-\tau)]}} e^{-\frac{y^2}{4[\theta(\tau)+\tilde{D}(s-\tau)]}}\,\mathrm{d}y\,\mathrm{d}s$$

We make a change of variables and let

$$A = \theta(\tau) + \tilde{D}(s-\tau).$$

Then

$$k^* = \frac{\eta}{\tilde{D}}\mathcal{F}(\tau)\,S_0 \int_{\theta(\tau)}^\infty \int_{\mathbb{R}} e^{-\nu\frac{A-\theta(\tau)}{\tilde{D}}} \frac{e^{-\frac{y^2}{4A}}}{\sqrt{4\pi A}}\,\mathrm{d}y\,\mathrm{d}A$$
$$= \frac{\eta}{\tilde{D}}\mathcal{F}(\tau)\,S_0 \int_{\theta(\tau)}^\infty e^{-\nu\frac{A-\theta(\tau)}{\tilde{D}}} \left(\int_{\mathbb{R}} \frac{e^{-\frac{y^2}{4A}}}{\sqrt{4\pi A}}\,\mathrm{d}y\right)\mathrm{d}A$$
$$= \frac{\eta}{\tilde{D}}\mathcal{F}(\tau)\,S_0 \int_{\theta(\tau)}^\infty e^{-\nu\frac{A-\theta(\tau)}{\tilde{D}}}\,\mathrm{d}A$$
$$= \frac{\eta}{\nu}\mathcal{F}(\tau)\,S_0$$

So

$$k^* = \frac{\eta}{\nu}\mathcal{F}(\tau)\,S_0 < \infty \tag{3.60}$$

because $\eta, \nu, \mathcal{F}(\tau), S_0$ are all constant.

(A2) Since $f(0) = 0$, f is differentiable and $f'(u) = e^{-u}$, $f(u) = f(u) - f(0) = f'(v)u \leq u$ by mean value theorem and the fact that $f'(v) = e^{-v} \leq 1$. Accordingly $0 \leq k(s,x)f(u) \leq k(s,x)u$, $\forall u, s \geq 0, x \in \mathbb{R}$.

(A3) Since $f(u) = 1 - e^{-u} \geq 0$ is continuous for $u \geq 0$, and only at $u = 0$ $f(u) = 0$, for every compact interval I in $(0,\infty)$ $f(u)$ has a minimum, i.e. there exists some $\epsilon > 0$ such that $f(u) \geq \epsilon$. Hence $k(s,x)f(u) \geq \epsilon k(s,x)$, $\forall u \in I, s \geq 0, x \in \mathbb{R}$.

(A4) The case for $\epsilon \geq 1$ is trivial. So next we assume $0 < \epsilon < 1$.

For an arbitrary $\epsilon > 0$, we can choose $\delta > 0$ such that $\delta < -\ln(1-\epsilon)$. Then for every $u \in [0, \delta]$, $f'(u) = e^{-u} \geq e^{-\delta} > e^{\ln(1-\epsilon)} = 1 - \epsilon$.

So for all $\epsilon > 0$ there exists $\delta > 0$ we have $k(s,x)f(u) \geq (1-\epsilon)uk(s,x)$, $\forall u \in [0,\delta]$, $s \geq 0, x \in \mathbb{R}$.

(A5) Since $0 < f'(u) = e^{-u} \leq 1$, for every $w > 0$ and $\forall u, v \in [0, w]$, by mean value theorem $|f(u) - f(v)| = |f'(p)(u-v)| \leq |u - v|$. So there exists $\Lambda = 1$ such that

$$|k(s,x)f(u) - k(s,x)f(v)| \leq \Lambda\,|u-v|k(s,x), \qquad \forall u, v \in [0,w], s \geq 0, x \in \mathbb{R}.$$

Now we check assumptions (B) for $k(s,x)$.

(B1) We compute in (3.60) that $k^* < \infty$. Here to satisfy $(B1)$ we assume that

$$k^* = \frac{\eta}{\nu}\,\mathcal{F}(\tau)\,S_0 > 1. \tag{3.61}$$

(B2) We verify for $k(a,|y|)$ that there is some $\lambda_0 > 0$ such that

$$\bar{k}(\lambda_0) = \int_0^\infty \int_{\mathbb{R}} e^{\lambda_0 y} k(s,|y|)\,\mathrm{d}y\,\mathrm{d}s < \infty \tag{3.62}$$

with $k(s,|y|)$ defined in (3.24).

With a change of variables

$$A = \theta(\tau) + \tilde{D}(s - \tau)$$

we find that

$$\begin{aligned}\bar{k}(\lambda_0) &= \int_\tau^\infty \int_{\mathbb{R}} e^{\lambda_0 y}\,\eta\,\mathcal{F}(\tau) e^{-\nu(a-\tau)}\,\Gamma\left(\theta(\tau) + \tilde{D}(a-\tau), y\right) S_0\,\mathrm{d}y\,\mathrm{d}a \\ &= \frac{\eta}{\tilde{D}}\,\mathcal{F}(\tau)\,S_0 \int_{\theta(\tau)}^\infty e^{-\nu\,\frac{A-\theta(\tau)}{\tilde{D}}} \left(\int_{\mathbb{R}} e^{\lambda_0 y}\,\Gamma(A,y)\,\mathrm{d}y\right)\mathrm{d}A\end{aligned}$$

By proposition 2.3 and the fact that Γ is isotropic

$$\begin{aligned}\bar{k}(\lambda_0) &= \frac{\eta}{\tilde{D}}\,\mathcal{F}(\tau)\,S_0\int_{\theta(\tau)}^{\infty} e^{-\nu\frac{A-\theta(\tau)}{\tilde{D}}}\,e^{\lambda_0^2 A}\,\mathrm{d}A \\ &= \frac{\eta}{\tilde{D}}\,\mathcal{F}(\tau)\,S_0\,e^{\frac{\nu}{\tilde{D}}\theta(\tau)}\int_{\theta(\tau)}^{\infty} e^{\left(\lambda_0^2-\frac{\nu}{\tilde{D}}\right)A}\,\mathrm{d}A\end{aligned}$$

The above integral converges if

$$\lambda_0 < \sqrt{\frac{\nu}{\tilde{D}}}. \tag{3.63}$$

Now if we choose a $\lambda_0 > 0$ such that (3.63) holds, we have

$$\bar{k}(\lambda_0) = \frac{\eta}{\nu - \tilde{D}\lambda_0^2}\,\mathcal{F}(\tau)\,S_0\,e^{\frac{\nu}{\tilde{D}}\theta(\tau)} < \infty. \tag{3.64}$$

(B3) If we choose $\sigma_2 > \sigma_1 > \tau > 0$ and any $\rho > 0$, by (3.24) $k(s,x) > 0$ for $s \in (\sigma_1, \sigma_2)$ and $|x| \in [0, \rho)$.

(B4) k is isotropic, by definition of the Gaussian kernel.

We then verify assumptions (C) for f.

(C1) $f(0) = 1 - e^0 = 0$, and $f(u) = 1 - e^{-u} > 0$, $\forall u > 0$ since $e^{-u} < 1\ \forall u > 0$.

(C2) $f(u) = 1 - e^{-u}$ so f is differentiable at $u = 0$, with $f'(u) = e^{-u}$, so $f'(0) = 1$; then by mean value theorem $f(u) - f(0) = f'(v)u$ with $v \in [0, u]$, we have $f(u) - f(0) = f(u) \leq u$ since $f'(v) = e^{-v} \leq 1$ for $v \in [0, u]$.

(C3) Since $f(u) = 1 - e^{-u} \to 0$ as $u \to \infty$, we find $\lim\limits_{u\to\infty} \dfrac{f(u)}{u} = 0$.

(C4) From $(B1)$ we have $k^* > 1$. Define function

$$g(u) = k^* f(u) - u.$$

Observe that $g'(u) = k^* e^{-u} - 1$. Since $k^* > 1$ and $e^{-u} \leq 1$ is decreasing for $u \geq 0$, $g(u)$ is increasing for $u \in (0, \ln(k^*))$ but decreasing for $u > \ln(k^*)$. Also notice that $g(0) = 0$ and $g(u) \to -\infty$ as $u \to \infty$, so we can find a unique u^* such that

$$g(u) = k^* f(u) - u > 0, \ \forall u \in (0, u^*) \qquad \text{and} \qquad g(u) = k^* f(u) - u < 0, \ \forall u > u^*.$$

In summary we have verified assumptions (A), (B) and (C) for k, f, provided (3.61) holds. Now by lemma 3.2 for every $c > 0$ there exists some $\bar{\lambda}(c) \in (0, \infty]$ such that

$$\mathscr{K}(c, \lambda) < \infty, \ \forall \lambda \in [0, \bar{\lambda}(c)\,) \quad \text{and} \quad \mathscr{K}(c, \lambda) = \infty, \ \forall \lambda \in (\bar{\lambda}(c), \infty)$$

where $\mathscr{K}(c, \lambda)$ is defined in (3.55).

Now we compute $\mathscr{K}(c, \lambda)$

$$\begin{aligned}\mathscr{K}(c, \lambda) &= \int_0^\infty \int_{\mathbb{R}} e^{-\lambda(cs+y)}\, k(s, |y|)\, \mathrm{d}y\, \mathrm{d}s \\ &= \eta\, \mathcal{F}(\tau) S_0 \int_\tau^\infty \int_{\mathbb{R}} e^{-\lambda c s}\, e^{-\lambda y}\, e^{-\nu(s-\tau)}\, \Gamma\left(\theta(\tau) + \tilde{D}(s-\tau), y\right) \mathrm{d}y\, \mathrm{d}s\end{aligned}$$

We make a change of variable and let $A = \theta(\tau) + \tilde{D}(s - \tau)$,

$$\mathscr{K}(c, \lambda) = \frac{\eta}{\tilde{D}}\, \mathcal{F}(\tau) S_0\, e^{\nu\tau} \int_{\theta(\tau)}^\infty e^{-(\lambda c + \nu)\left(\tau + \left(\frac{A - \theta(\tau)}{\tilde{D}}\right)\right)} \left(\int_{\mathbb{R}} e^{-\lambda y}\, \Gamma\,(A, y)\ \mathrm{d}y \right) \mathrm{d}A$$

By proposition 2.3,

$$\begin{aligned}\mathscr{K}(c, \lambda) &= \frac{\eta}{\tilde{D}}\, \mathcal{F}(\tau) S_0\, e^{(\lambda c + \nu)\left(\frac{\theta(\tau)}{\tilde{D}} - \tau\right)}\, e^{\nu\tau} \int_{\theta(\tau)}^\infty e^{\left(\lambda^2 - \frac{c}{\tilde{D}}\lambda - \frac{\nu}{\tilde{D}}\right)A}\, \mathrm{d}A \\ &= \frac{\eta}{\tilde{D}} S_0\, e^{(\lambda c + \nu)\left(\frac{\theta(\tau)}{\tilde{D}} - \tau\right)}\, e^{\nu\tau - \int_0^\tau \mu(s)\, \mathrm{d}s} \int_{\theta(\tau)}^\infty e^{\left(\lambda^2 - \frac{c}{\tilde{D}}\lambda - \frac{\nu}{\tilde{D}}\right)A}\, \mathrm{d}A. \qquad (3.65)\end{aligned}$$

We make the general assumptions that

$$\mu(\tau) \geq \nu \qquad \text{and} \qquad D(\tau) \leq \tilde{D}. \qquad (3.66)$$

Then from (3.65) it is readily seen that $\mathscr{K}$ is monotone decreasing in τ because

$$\frac{\mathrm{d}}{\mathrm{d}\tau}\left(\frac{\theta(\tau)}{\tilde{D}} - \tau\right) = \frac{D(\tau)}{\tilde{D}} - 1 \leq 0, \quad \frac{\mathrm{d}}{\mathrm{d}\tau}\left(\nu\tau - \int_0^\tau \mu(s)\, \mathrm{d}s\right) = \nu - \mu(\tau) \leq 0$$

and the lower bound of the integral in (3.65) is increasing in τ.

In (3.65) let

$$g(\lambda) = \lambda^2 - \frac{c}{\tilde{D}}\lambda - \frac{\nu}{\tilde{D}}.$$

Since $c > 0$ and $\nu, \tilde{D} > 0$ are constant, $g(\lambda)$ is a quadratic function that has a negative root and positive root $\bar{\lambda}(c)$. If $\lambda \in [0, \bar{\lambda}(c)\,)$, $g(\lambda) < 0$ and the integral in (3.65) converges; if $\lambda \geq \bar{\lambda}(c)$ the integral diverges and $\mathscr{K}(c, \lambda) = \infty$.

We find that

$$\bar{\lambda}(c) = \frac{c + \sqrt{c^2 + 4\nu\tilde{D}}}{2\tilde{D}}. \tag{3.67}$$

If $\lambda \in [0, \bar{\lambda}(c)\,)$,

$$\mathscr{K}(c, \lambda) = \eta\, \mathcal{F}(\tau) S_0 \frac{e^{\theta(\tau)\lambda^2 - \tau c\lambda}}{\nu + c\lambda - \tilde{D}\lambda^2}. \tag{3.68}$$

It is readily seen from (3.68) that $\mathscr{K}$ is monotone increasing in $\eta, S_0, \tilde{D}$ and monotone decreasing in ν. However, if we impose the assumption that the diffusion of exposed individuals is negligible, i.e.

$$\theta(\tau) = \int_0^\tau D(s)\,\mathrm{d}s \ll 1 \tag{3.69}$$

then with a change of variable $c = \sqrt{\tilde{D}}\,\bar{c}$ and $\lambda = \frac{\bar{\lambda}}{\sqrt{\tilde{D}}}$,

$$\mathscr{K}(c, \lambda) = \mathscr{K}(\bar{c}, \bar{\lambda}) \approx \eta\, \mathcal{F}(\tau) S_0 \frac{e^{-\tau\bar{c}\bar{\lambda}}}{\nu + \bar{c}\bar{\lambda} - \bar{\lambda}^2}.$$

The above formula is independent of $\tilde{D}$. It follows from the definition of c^* and lemma 3.3 that if (3.69) is satisfied then c^* is increasing in and proportional to $\sqrt{\tilde{D}}$. For the case of fixed delay, the results of dependencies of c^* on parameter values are summarized in the following proposition.

Proposition 3.9 *Suppose the delay $\tau > 0$ is a fixed constant. The asymptotic spread speed c^* is an increasing function of $\eta, S_0, \tilde{D}$ and a decreasing function of ν. Additionally, if (3.66) holds, c^* is monotone decreasing in τ. If (3.69) holds, then c^* is proportional to $\sqrt{\tilde{D}}$.*

Since in (3.68)

$$e^{\theta(\tau)\lambda^2-\tau c\lambda} \geq e^{-\frac{\tau^2 c^2}{4\theta(\tau)}}$$

and

$$\nu + c\lambda - \tilde{D}\lambda^2 \to 0^+ \qquad \text{as } \lambda \to \bar{\lambda}(c)^-$$

it follows that $\mathscr{K}(c,\lambda) \to \infty$ as $\lambda \to \bar{\lambda}(c)^-$, and

$$\liminf_{\lambda \nearrow \bar{\lambda}(c)} \mathscr{K}(c,\lambda) \geq k^*$$

for every $c > 0$.

It then follows from proposition 3.4 that c^*, as defined in (3.56), together with a unique $\lambda^* \in (0, \bar{\lambda}(c^*)\,)$, are uniquely determined as solutions of the system

$$\mathscr{K}(c,\lambda) = 1, \qquad \frac{\mathrm{d}}{\mathrm{d}\lambda}\mathscr{K}(c,\lambda) = 0.$$

More precisely c^* and λ^* are unique positive solutions of

$$\begin{aligned} &\eta\,\mathcal{F}(\tau) S_0\, e^{\theta(\tau)\lambda^2-\tau c\lambda} = \nu + c\lambda - \tilde{D}\lambda^2 \\ &c - 2\tilde{D}\lambda = (\nu + c\lambda - \tilde{D}\lambda^2)(2\theta(\tau)\lambda - \tau c). \end{aligned} \tag{3.70}$$

If additionally $u_0(x,t)$ satisfies the admissibility conditions in (3.57), by theorems 3.5 and 3.6 we can conclude that $c^* > 0$ obtained above is the asymptotic speed of spread for the solution $u(x,t)$ from (3.53).

Before starting any asymptotic analysis, we can perform numerical experiments on solutions of system (3.70). In order to compare the solutions to (3.70) with those we obtained in Chapter 2 in the delayed SI model, we use the set of parameter values in Table 2.1 for foxes. Additionally, for convenience we make simpifying assumptions about $\mathcal{F}(\tau)$ and $\theta(\tau)$. We suppose that during the incubation period with fixed length τ, animals die at a constant rate $\mu > 0$ and diffuse at a constant rate $D_i > 0$. Thus we have

$$\mathcal{F}(\tau) = e^{-\mu\tau} \qquad \text{and} \qquad \theta(\tau) = D_i\tau.$$

Using Newton method and appropriate initial conditions, we obtain in Figure 3.1 the relationships between asymptotic spread speed c^* with respect to parameters $S_0, \tau, D_i, \tilde{D}$. In particular, compared with Figure 2.3, c^* shows similar monotone relationship with respect to both diffusion rates, and is nonlinear decreasing in τ. Also c^* depends on S_0 in the same way minimum wave speed v_c depends on carrying capacity K in Figure 2.3.

In fact, for this special case of $\mathcal{F}(\tau)$ and $\theta(\tau)$, the equations in (3.70) are identical to those in (2.32) for the simple time-delayed SI model in chapter 2, if we consider $\eta = \beta, S_0 = K, \nu = \mu$. Therefore we expect the same results and the simple delayed SI model in (2.6) is a special case with a fixed delay for both the alternative model with general infection-age-dependent parameters in (3.2) and the alternative model with distributed delay in (3.25).

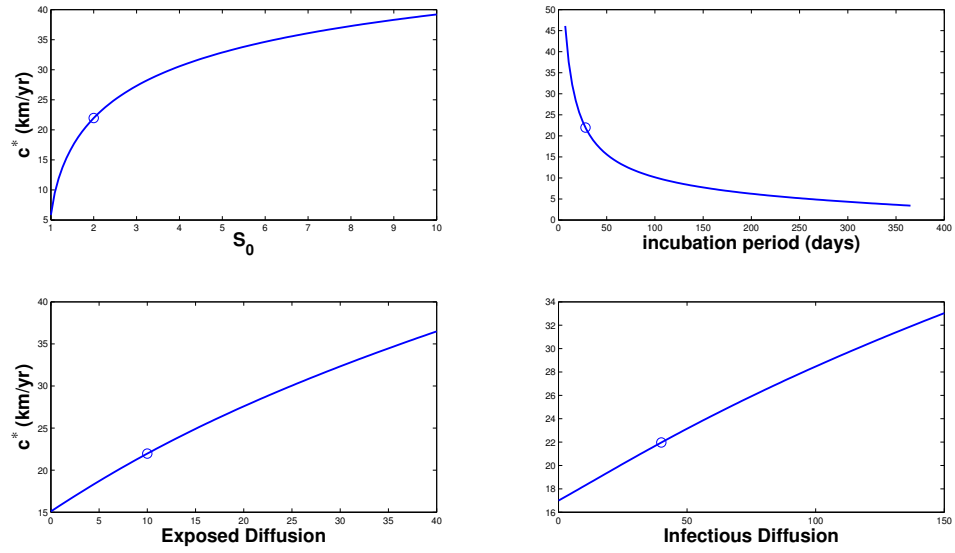

Figure 3.1: We use simplifying assumptions for $\mathcal{F}(\tau)$ and $\theta(\tau)$. Parameter values are from Table 2.1. In particular, circles in the graph are obtained by setting $D_i = 10, \tilde{D} = 40, S_0 = 2, \tau = 28/365$ (yr).

3.3.2 Asymptotic spread speed for model (3.25)

When we discuss the integral equation (3.23) for the model (3.25) with a general dependence of parameters on incubation period, we can still apply the theory established by Thieme (1979) and Thieme and Zhao (2003) as in section 3.3.1.

First note that the kernel now is

$$k(a,y) = \eta(a)\mathcal{F}(a)\Gamma(\theta(a),y)S_0$$

and the integral equation

$$u(x,t) = u_0(x,t) + \int_0^t \int_{\mathbb{R}} k(a,y) f(u(x-y,t-a))\,\mathrm{d}y\,\mathrm{d}a$$

where we get rid of the absolute value sign around y due to the fact that k and the Gaussian kernel Γ are isotropic.

We impose the following assumptions on $\eta(a), D(a)$ and $\mu(a)$

(Q) $\eta, D, \mu : [0,\infty) \to [0,\infty)$ are continuous functions such that

$(Q1)$ $\theta(a) \le \bar{D}a$ for all $a \ge 0$, and there exist $\hat{\mu} > 0$ such that $\mu \ge \hat{\mu}$ for all $a \ge 0$.

$(Q2)$ There exist $\sigma_2 > \sigma_1 > 0$ such that $\eta(a) > 0$ for $a \in (\sigma_1, \sigma_2)$.

$(Q3)$ $\eta(a)\mathcal{F}(a)e^{\xi a}$ is bounded on $a \in [0,\infty)$ for any $\xi > 0$, $\int_0^\infty \eta(a)\,\mathrm{d}a < \infty$.

We verify the assumptions (A) for $k(a,y)$.

(A1)

$$\begin{aligned}
k^* &= \int_0^\infty \int_{\mathbb{R}} \eta(a)\mathcal{F}(a)\Gamma\left(\theta(a),y\right) S_0\,\mathrm{d}y\,\mathrm{d}a \\
&= S_0 \int_0^\infty \eta(a)\mathcal{F}(a) \left(\int_{\mathbb{R}} \Gamma\left(\theta(a),y\right)\,\mathrm{d}y \right) \mathrm{d}a \\
&= S_0 \int_0^\infty \eta(a)\mathcal{F}(a)\,\mathrm{d}a \qquad \text{by property of Gaussian kernel} \\
&\le S_0 \int_0^\infty \eta(a)\,\mathrm{d}a < \infty \qquad \text{by } (Q3).
\end{aligned}$$

$(A2)$ through $(A5)$ are verified similarly as in section 3.3.1.

Now we check assumptions (B) for $k(a, y)$.

(B1) In addition to $k^* < \infty$, we also assume that

$$k^* = \int_0^\infty \eta(a)\mathcal{F}(a)S_0 \,\mathrm{d}a > 1. \tag{3.71}$$

(B2) We find that

$$\begin{aligned}
\bar{k}(\lambda) &= \int_0^\infty \int_{\mathbb{R}} e^{\lambda y}\eta(a)\mathcal{F}(a)\Gamma\left(\theta(a), y\right) S_0 \,\mathrm{d}y \,\mathrm{d}a \\
&= S_0 \int_0^\infty \eta(a)\mathcal{F}(a) \left(\int_{\mathbb{R}} e^{\lambda y}\Gamma\left(\theta(a), y\right) \,\mathrm{d}y \right) \mathrm{d}a \\
&= S_0 \int_0^\infty \eta(a)\mathcal{F}(a) e^{\lambda^2\theta(a)} \,\mathrm{d}a \qquad \text{by proposition 2.3} \\
&\leq S_0 \int_0^\infty \eta(a) e^{\lambda^2 \bar{D}a - \hat{\mu}a} \,\mathrm{d}a \qquad \text{by } (Q1)
\end{aligned}$$

Then if $\lambda < \sqrt{\hat{\mu}/\bar{D}}$ the above integral converges and we find

$$\bar{k}(\lambda) \leq S_0 \int_0^\infty \eta(a) \,\mathrm{d}a < \infty \qquad \text{by } (Q3).$$

(B3) This is an direct result of assumption $(Q2)$.

(B4) $k(a, y)$ is isotropic by properties of the Gaussian kernel $\Gamma(t, x)$.

$(C1)$ through $(C4)$ conditions can be checked in the same manner as in section 3.3.1.

Now we can compute the $\mathscr{K}(c, \lambda)$ defined in (3.55).

$$\begin{aligned}
\mathscr{K}(c, \lambda) &= \int_0^\infty \int_{\mathbb{R}} e^{-\lambda(ca+y)}\eta(a)\mathcal{F}(a)\Gamma\left(\theta(a), y\right) S_0 \,\mathrm{d}y \,\mathrm{d}a \\
&= S_0 \int_0^\infty e^{-\lambda ca}\eta(a)\mathcal{F}(a) \left(\int_{\mathbb{R}} e^{-\lambda y}\Gamma\left(\theta(a), y\right) \,\mathrm{d}y \right) \mathrm{d}a \\
&= S_0 \int_0^\infty \eta(a)\mathcal{F}(a) e^{\lambda^2\theta(a) - \lambda ca} \,\mathrm{d}a \qquad \text{by proposition 2.3} \qquad (3.72) \\
&\leq S_0 \int_0^\infty \eta(a)\mathcal{F}(a) e^{\lambda^2 \bar{D}a} e^{-\lambda ca} \,\mathrm{d}a \qquad \text{by } (Q1) \qquad (3.73)
\end{aligned}$$

We have verified that (B) hold for kernel $k(a, y)$. Then by lemma 3.2, for every $c > 0$ there exists $\bar{\lambda}(c) \in (0, \infty]$ such that $\mathscr{K}(c, \lambda) < \infty$ for $\lambda \in [0,\ \bar{\lambda}(c)\,)$ and $\mathscr{K}(c, \lambda) = \infty$ for $\lambda \in (\bar{\lambda}(c),\ \infty)$. Note that the last interval is possibly empty.

Note that in (3.73) there is a constant $\gamma > 0$ such that $\eta(a)\mathcal{F}(a)e^{\lambda^2 \bar{D}a} \leq \gamma$ for all $a \geq 0$ by $(Q3)$. Then

$$\mathscr{K}(c, \lambda) \leq S_0\gamma \int_0^\infty e^{-\lambda ca}\,\mathrm{d}a = \frac{S_0\gamma}{\lambda c} < \infty$$

for any $\lambda, c > 0$. However, by $(Q2)$ and (3.72) we have

$$\mathscr{K}(c, \lambda) \geq S_0 e^{\lambda^2\theta(\sigma_1) - \lambda c\sigma_2} \int_{\sigma_1}^{\sigma_2} \eta(a)\mathcal{F}(a)\,\mathrm{d}a \to \infty$$

as $\lambda \to \infty$.

Therefore $\bar{\lambda}(c) = \infty$ and $\mathscr{K}(c, \lambda) < \infty$ for all $c > 0$ and $\lambda \in [0, \infty)$, but $\mathscr{K}(c, \lambda) \to \infty$ as $\lambda \to \infty$. As a result, as λapproaches $\bar{\lambda}(c) = \infty$ from below, we have $\liminf\limits_{\lambda \nearrow \bar{\lambda}(c)} \mathscr{K}(c, \lambda) \geq k^*$.

By proposition 3.4, the asymptotic spread speed for the general model (3.25) can be calculated from the integral equation (3.23) by setting

$$\mathscr{K}(c, \lambda) = 1 \qquad \text{and} \qquad \frac{\partial}{\partial\lambda}\mathscr{K}(c, \lambda) = 0$$

and solve the unique positive pair (c^*, λ^*).

Therefore, for the asymptotic spread speed for the general model (3.2), we have

$$\begin{aligned} &S_0 \int_0^\infty \eta(a)\mathcal{F}(a)e^{\lambda^2\theta(a) - \lambda ca}\,\mathrm{d}a = 1 \\ &S_0 \int_0^\infty \eta(a)\mathcal{F}(a)e^{\lambda^2\theta(a) - \lambda ca}(2\lambda\theta(a) - ca)\,\mathrm{d}a = 0 \end{aligned} \tag{3.74}$$

If additionally $u_0(x, t)$ satisfies the admissibility conditions in (3.57), by theorems 3.5 and 3.6 we can conclude that $c^* > 0$ obtained above is the asymptotic speed of spread for the solution $u(x, t)$ from (3.23).

3.3.3 Asymptotic spread speed for (3.50) with exponential probability measure $P(\,\mathrm{d}a)$

We have discussed the case where $P(\,\mathrm{d}a)$ is Dirac probability measure in (3.50), which leads to asymptotic spread speed in the case of a fixed delay in section 3.3.1. In this section we consider the case where $P(\,\mathrm{d}a)$ is an exponentially distributed probability measure. The probability density function becomes

$$P(a) = \sigma e^{-\sigma a}$$

where, consistent with discussions in chapter 2, we use σ as the rate of conversion from exposed to infectious class. Note that the mean of this exponential probability distribution is $1/\sigma$, which is the average incubation period.

Now suppose that the initial susceptible density is constant S_0. The kernel $k(r, y)$ defined in (3.51) can be further written as

$$k(r, y) = \eta \int_0^r \sigma e^{-\sigma a} \mathcal{F}(a) e^{-\nu(r-a)} \Gamma \left(\tilde{D}(r-a) + \theta(a), y \right) S_0 \,\mathrm{d}a.$$

The value $\eta > 0$ in model (3.25) is defined as the infectivity of infectious individuals. Similar to last section we assume that

(R) $D, \mu : [0, \infty) \to [0, \infty)$ are continuous functions such that

$(R1)$ $\theta(a) \leq \bar{D}a$ for all $a \geq 0$, and there exists $\hat{\mu} > 0$ such that $\mu \geq \hat{\mu}$ for all $a \geq 0$;

$(R2)$ $\mathcal{F}(a)e^{\xi a}$ remains bounded for all $a \geq 0, \xi > 0$.

To apply theories developed by Thieme (1979) and Thieme and Zhao (2003), we check a list of conditions. First we check assumptions (A).

$(A1)$

$$
\begin{aligned}
k^* &= \int_0^\infty \int_{\mathbb{R}} k(r,y)\,\mathrm{d}y\,\mathrm{d}r \\
&= \eta\sigma S_0 \int_0^\infty \left(\int_0^r e^{-\sigma a}\mathcal{F}(a) e^{-\nu(r-a)} \left(\int_{\mathbb{R}} \Gamma\left(\tilde{D}(r-a)+\theta(a), y\right) \mathrm{d}y \right) \mathrm{d}a \right) \mathrm{d}r \\
&= \eta\sigma S_0 \int_0^\infty \left(\int_0^r e^{-\sigma a}\mathcal{F}(a) e^{-\nu(r-a)}\,\mathrm{d}a \right) \mathrm{d}r \qquad \text{by properties of } \Gamma(t,x) \\
&= \eta\sigma S_0 \int_0^\infty e^{-\sigma a}\mathcal{F}(a) e^{\nu a} \left(\int_a^\infty e^{-\nu r}\,\mathrm{d}r \right) \mathrm{d}a \\
&= \frac{\eta\sigma S_0}{\nu} \int_0^\infty e^{-\sigma a}\mathcal{F}(a)\,\mathrm{d}a \\
&\leq \frac{\eta\sigma S_0}{\nu} \int_0^\infty e^{-\sigma a}\,\mathrm{d}a = \frac{\eta S_0}{\nu} < \infty \qquad \text{note } \mathcal{F}(a) \leq 1.
\end{aligned}
$$

Items $(A2)$ through $(A5)$ are checked by similar arguments as in section 3.3.1.

For assumptions (B), we find

$(B1)$ In addition to $k^* < \infty$, we require that

$$k^* = \eta\sigma S_0 \int_0^\infty e^{-\sigma a}\mathcal{F}(a)\,\mathrm{d}a > 1. \tag{3.75}$$

$(B2)$ Note that

$$\bar{k}(\lambda) = \int_0^\infty \int_{\mathbb{R}} e^{\lambda y} k(r,y)\,\mathrm{d}y\,\mathrm{d}r.$$

Hence

$$
\begin{aligned}
&\bar{k}(\lambda) = \\
&\eta\sigma S_0 \int_0^\infty \left(\int_0^r e^{-\sigma a}\mathcal{F}(a) e^{-\nu(r-a)} \left(\int_{\mathbb{R}} e^{\lambda y}\Gamma\left(\tilde{D}(r-a)+\theta(a), y\right) \mathrm{d}y \right) \mathrm{d}a \right) \mathrm{d}r \\
&= \eta\sigma S_0 \int_0^\infty \left(\int_0^r e^{-\sigma a}\mathcal{F}(a) e^{-\nu(r-a)} e^{\lambda^2(\tilde{D}(r-a)+\theta(a))}\,\mathrm{d}a \right) \mathrm{d}r \\
&= \eta\sigma S_0 \int_0^\infty e^{-\sigma a}\mathcal{F}(a) e^{\nu a} e^{\lambda^2(-\tilde{D}a+\theta(a))} \left(\int_a^\infty e^{(\lambda^2\tilde{D}-\nu)r}\,\mathrm{d}r \right) \mathrm{d}a.
\end{aligned}
$$

Then it is clear that if

$$\lambda < \sqrt{\frac{\nu}{\tilde{\bar{D}}}}$$

we have

$$\begin{aligned}
\bar{k}(\lambda) &= \frac{\eta\sigma S_0}{\nu - \lambda^2\tilde{D}} \int_0^\infty e^{-\sigma a}\mathcal{F}(a)e^{\lambda^2\theta(a)}\,\mathrm{d}a \\
&\leq \frac{\eta\sigma S_0}{\nu - \lambda^2\tilde{D}} \int_0^\infty e^{-\sigma a}\mathcal{F}(a)e^{\lambda^2\bar{D}a}\,\mathrm{d}a \qquad \text{by } (R1) \\
&\leq \frac{\eta\sigma S_0}{(\nu - \lambda^2\tilde{D})(\sigma - \lambda^2\bar{D})} < \infty \qquad \text{if } \lambda < \sqrt{\frac{\sigma}{\bar{D}}} \text{ and note } \mathcal{F}(a) \leq 1.
\end{aligned}$$

Therefore if we have $\lambda < \min\{\sqrt{\nu/\tilde{D}}, \sqrt{\sigma/\bar{D}}\}$ then $\bar{k}(\lambda) < \infty$.

Conditions $(B3)$ and $(B4)$ are verified similarly as in section 3.3.1.

Assumptions $(C1)$ through $(C4)$ are all true by arguments in section 3.3.1 since the function $f(u) = 1 - e^{-u}$ is the same.

Now by definition in (3.55)

$$\begin{aligned}
&\mathscr{K}(c,\lambda) = \\
&\eta\sigma S_0 \int_0^\infty e^{-\lambda cr}\left(\int_0^r e^{-\sigma a}\mathcal{F}(a)e^{-\nu(r-a)}\left(\int_{\mathbb{R}} e^{-\lambda y}\Gamma\left(\tilde{D}(r-a)+\theta(a), y\right)\,\mathrm{d}y\right)\,\mathrm{d}a\right)\,\mathrm{d}r \\
&= \eta\sigma S_0 \int_0^\infty e^{-\lambda cr}\left(\int_0^r e^{-\sigma a}\mathcal{F}(a)e^{-\nu(r-a)}e^{\lambda^2(\tilde{D}(r-a)+\theta(a))}\,\mathrm{d}a\right)\,\mathrm{d}r \\
&= \eta\sigma S_0 \int_0^\infty e^{-\sigma a}\mathcal{F}(a)e^{\nu a}e^{\lambda^2(-\tilde{D}a+\theta(a))}\left(\int_a^\infty e^{(\lambda^2\tilde{D}-\lambda c-\nu)r}\,\mathrm{d}r\right)\,\mathrm{d}a. \qquad (3.76)
\end{aligned}$$

Then if $\lambda^2\tilde{D} - \lambda c - \nu < 0$, the inner integral converges. Let

$$\lambda_0 = \frac{c + \sqrt{c^2 + 4\tilde{D}\nu}}{2\tilde{D}}.$$

If $\lambda \in [0, \lambda_0)$ we have

$$\begin{aligned}\mathscr{K}(c,\lambda) &= \frac{\eta\sigma S_0}{\nu + \lambda c - \lambda^2 \tilde{D}} \int_0^\infty \mathcal{F}(a) e^{\lambda^2 \theta(a) - \lambda c a - \sigma a} \, \mathrm{d}a \\ &\leq \frac{\eta\sigma S_0}{\nu + \lambda c - \lambda^2 \tilde{D}} \int_0^\infty \mathcal{F}(a) e^{\lambda^2 \bar{D} a} e^{-(\lambda c + \sigma)a} \, \mathrm{d}a \qquad \text{by } (R1).\end{aligned}$$

By $(R2)$ we have $\mathcal{F}(a)e^{\xi a}$ is bounded for all $a \geq 0, \xi > 0$. Then for any $\lambda \in [0, \lambda_0)$

$$\begin{aligned}\mathscr{K}(c,\lambda) &\leq \frac{\eta\sigma S_0 \gamma}{\nu + \lambda c - \lambda^2 \tilde{D}} \int_0^\infty e^{-(\lambda c + \sigma)a} \, \mathrm{d}a \\ &= \frac{\eta\sigma S_0 \gamma}{(\nu + \lambda c - \lambda^2 \tilde{D})(\lambda c + \sigma)} < \infty.\end{aligned}$$

So $\bar{\lambda}(c) = \lambda_0$ and for $\lambda \in [0, \lambda_0)$ we have $\mathscr{K}(c,\lambda) < \infty$, but since when $\lambda \geq \lambda_0$ the inner integral in (3.76) diverges we have $\mathscr{K}(c,\lambda) = \infty$, from which it follows naturally that $\liminf_{\lambda \nearrow \bar{\lambda}(c)} \mathscr{K}(c,\lambda) \geq k^*$.

By proposition 3.4 the asymptotic spread speed c^* can be obtained by solving for the unique positive pair (c^*, λ^*) in

$$\mathscr{K}(c,\lambda) = 1 \qquad \text{and} \qquad \frac{\partial}{\partial \lambda} \mathscr{K}(c,\lambda) = 0.$$

Observe that conditions in $(A), (B), (C)$ are verified at most using assumption $(R1)$. Next we consider a special case where

$$D(a) = \bar{D} \qquad \text{and} \qquad \mu(a) = \hat{\mu}$$

with $\bar{D}, \hat{\mu} > 0$ constant. In this case $(R1)$ holds and conditions $(A), (B), (C)$ are all verified as true or assumed to be true already. To verify conditions on $\mathscr{K}(c,\lambda)$, note that for $\lambda \in [0, \lambda_0)$,

$$\begin{aligned}\mathscr{K}(c,\lambda) &= \frac{\eta\sigma S_0}{\nu + \lambda c - \lambda^2 \tilde{D}} \int_0^\infty \mathcal{F}(a) e^{\lambda^2 \theta(a) - \lambda c a - \sigma a} \, \mathrm{d}a \\ &= \frac{\eta\sigma S_0}{\nu + \lambda c - \lambda^2 \tilde{D}} \int_0^\infty e^{(\lambda^2 \bar{D} - \lambda c - \sigma - \hat{\mu})a} \, \mathrm{d}a \\ &= \frac{\eta\sigma S_0}{(\nu + \lambda c - \lambda^2 \tilde{D})(\sigma + \hat{\mu} + \lambda c - \bar{D}\lambda^2)}\end{aligned}$$

where the last equality holds only if $\lambda \in [0, \lambda_1)$ with

$$\lambda_1 = \frac{c + \sqrt{c^2 + 4\bar{D}(\sigma + \hat{\mu})}}{2\bar{D}}.$$

Now let $\bar{\lambda}(c) = \min\{\lambda_0, \lambda_1\}$. It is readily seen that $\mathscr{K}(c, \lambda) < \infty$ for $\lambda \in [0, \bar{\lambda}(c))$ while $\mathscr{K}(c, \lambda) = \infty$ with $\lambda \geq \bar{\lambda}(c)$, which implies $\liminf_{\lambda \nearrow \bar{\lambda}(c)} \mathscr{K}(c, \lambda) \geq k^*$.

By proposition 3.4 the asymptotic speed of spread c^* is obtained by solving for the unique pair of positive c, λ such that

$$\begin{aligned} &(\tilde{D}\lambda^2 - c\lambda - \nu)(\bar{D}\lambda^2 - c\lambda - \sigma - \hat{\mu}) = \eta\sigma S_0 \\ &(2\tilde{D}\lambda - c)(\bar{D}\lambda^2 - c\lambda - \hat{\mu} - \sigma) + (2\bar{D}\lambda - c)(\tilde{D}\lambda^2 - c\lambda - \nu) = 0. \end{aligned} \tag{3.77}$$

In fact, if we introduce rescalings similar to chapter 2 for the SEI diffusive model

$$\begin{aligned} &\nu' = \frac{\nu}{\eta S_0},\ \sigma' = \frac{\sigma}{\eta S_0},\ \hat{\mu}' = \frac{\hat{\mu}}{\eta S_0} \\ &\lambda' = \sqrt{\frac{\tilde{D}}{\eta S_0}}\lambda,\ c' = \frac{c}{\sqrt{\tilde{D}\eta S_0}},\ \epsilon = \frac{\bar{D}}{\tilde{D}}, \end{aligned}$$

we can obtain that the first equation in (3.77), on removing the primes, is the same as

$$(\lambda^2 - c\lambda - \nu)(\lambda^2 - \frac{c}{\epsilon}\lambda - \frac{\sigma + \hat{\mu}}{\epsilon}) = \frac{\sigma}{\epsilon}. \tag{3.78}$$

Compare with the function $f(\lambda), g(\lambda)$ in (2.17) and (2.18), if we consider $c = v, \nu = \mu, \hat{\mu} = b, \eta = \beta, S_0 = K$ where in each equation we have notations from (3.77) on the left hand side and those from (2.17), (2.18) on the right hand side, we can notice that they are identical. Therefore, it is worth noticing that the minimum wave speed and traveling wave solutions of the SEI diffusion model (2.1) is a special case of the alternative model with distributed delay in (3.25) with the incubation period is exponentially distributed.

3.3.4 Admissible u_0

First for the model with a general dependency of parameters on the incubation period (3.2) we show a sufficient condition for admissible u_0. Then we prove a sufficient condition in the special case of fixed constant incubation period for both models (3.2) and (3.25).

In model (3.2) with parameters generally dependent on the incubation period, we arrive at the formula of $\mathscr{K}(c,\lambda)$ in (3.72)

$$\mathscr{K}(c,\lambda) = S_0 \int_0^\infty \eta(a)\mathcal{F}(a)e^{\lambda^2\theta(a)-\lambda ca}\,\mathrm{d}a.$$

In the formula for u_0 from (3.21) we make a change of variable $z = x - y$. Then

$$u_0(x,t) = \int_0^t \mathrm{d}s \int_0^\infty \eta(a+s)\frac{\mathcal{F}(a+s)}{\mathcal{F}(a)}\,\mathrm{d}a \int_{\mathbb{R}} \Gamma\left(\theta(a+s)-\theta(a),z\right) I_0(x-z,a)\,\mathrm{d}z.$$

Let $c,\lambda > 0$ be arbitrary so that $\mathscr{K}(c,\lambda) < 1$. We assume that there exists some $\gamma > 0$ such that

$$I_0(x,a) \le \gamma e^{-\lambda ca}e^{-\lambda|x|}\mathcal{F}(a), \quad \text{for all } x \in \mathbb{R},\ a \ge 0. \tag{3.79}$$

The sufficient condition in (3.79) assumes that there is sufficiently fast decrease in both x, a for I_0 and I_0 is bounded by $\gamma\mathcal{F}(a)$ where $\gamma > 0$ is a constant and $\mathcal{F}(a)$ can be seen as survivability function.

Then we claim that the u_0 defined in (3.21) with the initial condition I_0 given in (3.79) is admissible.

Proposition 3.10 *In the general model (3.2) I_0 satisfies (3.79). Then the u_0 defined in (3.21) is admissible.*

Proof By assumption (3.79) and note that $|x| - |x-z| \le |z|$,

$$\begin{aligned}
&u_0(x,t)\\
&\quad\le \gamma \int_0^t \mathrm{d}s \int_0^\infty \eta(a+s)\frac{\mathcal{F}(a+s)}{\mathcal{F}(a)}\,\mathrm{d}a \int_{\mathbb{R}} \Gamma\left(\theta(a+s)-\theta(a),z\right) e^{-\lambda ca}e^{-\lambda|x-z|}\mathcal{F}(a)\,\mathrm{d}z\\
&\quad\le \gamma e^{-\lambda|x|} \int_0^t \mathrm{d}s \int_0^\infty e^{-\lambda ca}\eta(a+s)\mathcal{F}(a+s)\,\mathrm{d}a \int_{\mathbb{R}} \Gamma\left(\theta(a+s)-\theta(a),z\right) e^{\lambda|z|}\,\mathrm{d}z\\
&\quad= 2\gamma e^{-\lambda|x|} \int_0^t \mathrm{d}s \int_0^\infty e^{-\lambda ca}\eta(a+s)\mathcal{F}(a+s)\,\mathrm{d}a \int_{-\infty}^0 \Gamma\left(\theta(a+s)-\theta(a),z\right) e^{-\lambda z}\,\mathrm{d}z\\
&\quad\le 2\gamma e^{-\lambda|x|} \int_0^t \mathrm{d}s \int_0^\infty e^{-\lambda ca}\eta(a+s)\mathcal{F}(a+s)\,\mathrm{d}a \int_{\mathbb{R}} \Gamma\left(\theta(a+s)-\theta(a),z\right) e^{-\lambda z}\,\mathrm{d}z.
\end{aligned}$$

Then by proposition 2.3

$$u_0(x,t) \leq 2\gamma e^{-\lambda|x|} \int_0^t \mathrm{d}s \int_0^\infty e^{-\lambda ca}\eta(a+s)\mathcal{F}(a+s)e^{\lambda^2(\theta(a+s)-\theta(a))}\,\mathrm{d}a.$$

Now we let $r = a + s$,

$$\begin{aligned}
u_0(x,t) &\leq 2\gamma e^{-\lambda|x|} \int_0^t \mathrm{d}s \int_s^\infty e^{-\lambda c(r-s)}\eta(r)\mathcal{F}(r)e^{\lambda^2(\theta(r)-\theta(r-s))}\,\mathrm{d}r \\
&\leq 2\gamma e^{-\lambda|x|} \int_0^t e^{\lambda cs}\,\mathrm{d}s \int_s^\infty e^{-\lambda cr}\eta(r)\mathcal{F}(r)e^{\lambda^2\theta(r)}\,\mathrm{d}r \\
&\leq 2\gamma e^{-\lambda|x|} \int_0^t e^{\lambda cs}\,\mathrm{d}s \int_0^\infty e^{-\lambda cr}\eta(r)\mathcal{F}(r)e^{\lambda^2\theta(r)}\,\mathrm{d}r \\
&= \frac{2\gamma e^{-\lambda|x|}}{S_0}\mathscr{K}(c,\lambda)\int_0^t e^{\lambda cs}\,\mathrm{d}s \qquad \text{by (3.72)} \\
&< \frac{2\gamma e^{-\lambda|x|}}{S_0}\int_0^t e^{\lambda cs}\,\mathrm{d}s \qquad \text{by assumption } \mathscr{K}(c,\lambda) < 1 \\
&= \frac{2\gamma e^{-\lambda|x|}}{c\lambda S_0}\left(e^{\lambda ct}-1\right) < \frac{2\gamma}{c\lambda S_0}e^{\lambda(ct-|x|)}.
\end{aligned}$$

By definition this implies that u_0 is admissible.

In both models (3.2) and (3.25) we arrive at equations (3.23) and (3.50) respectively. In what follows we give idealized initial conditions that produce admissible u_0 defined in (3.57) for both cases. For the first model we assign the idealized initial condition for $I_0(x,a)$, the initial profile of infected animals, by setting

$$I_0(x,a) = I^\circ\,\delta(x)\delta(a) \tag{3.80}$$

where $I^\circ > 0$ and δ here represents the Dirac delta distribution concentrated at 0.

Proposition 3.11 *In (3.23), if $I_0(x,a)$ satisfies (3.80), then $u_0(x,t)$ defined in (3.21) is admissible.*

Proof Let $I_0(x,a)$ be as defined in (3.80). Then

$$u_0(x,t) = I^\circ \int_0^t \eta(s)e^{-\int_0^s \mu(r)\,\mathrm{d}r}\frac{1}{\sqrt{4\pi\theta(s)}}e^{-\frac{x^2}{4\theta(s)}}\,\mathrm{d}s. \tag{3.81}$$

Note first that if $t < \tau$, $u_0(x,t) = 0$ since we consider fixed incubation length τ.

Now let $t \geq \tau$. Then from (3.81), for every $\lambda, c > 0$ with $\mathscr{K}(\lambda, c) < 1$, since $\eta(s) = 0$ for all $0 \leq s < \tau$,

$$\begin{aligned} u_0\, e^{\lambda|x|-\lambda ct} &= I^\circ \int_\tau^t \eta(s) e^{-\int_0^s \mu(r)\,\mathrm{d}r} \frac{1}{\sqrt{4\pi\theta(s)}} e^{-\frac{x^2}{4\theta(s)}} e^{\lambda|x|-\lambda ct}\,\mathrm{d}s \\ &= I^\circ \int_\tau^t \eta(s) e^{-\int_0^s \mu(r)\,\mathrm{d}r} \frac{1}{\sqrt{4\pi\theta(s)}} e^{-\frac{(|x|-2\lambda\theta(s))^2}{4\theta(s)}} e^{\lambda^2\theta(s)-\lambda ct}\,\mathrm{d}s \quad \text{completing squares} \\ &= I^\circ \int_\tau^t \eta(s) e^{-\int_0^s \mu(r)\,\mathrm{d}r} \frac{1}{\sqrt{4\pi\theta(s)}} e^{-\frac{(|x|-2\lambda\theta(s))^2}{4\theta(s)}} e^{\lambda^2\theta(\tau)-\lambda c\tau} e^{\lambda^2\tilde{D}(s-\tau)} e^{-\lambda c(t-\tau)}\,\mathrm{d}s \end{aligned}$$

where the last equality is by $\theta(s) = \theta(\tau) + \tilde{D}(t-\tau)$ and $t = (t-\tau) + \tau$.

Now by $\mathscr{K}(c,\lambda) < 1$ and (3.68)

$$\begin{aligned} u_0\, e^{\lambda|x|-\lambda ct} < \frac{\nu + c\lambda - \tilde{D}\lambda^2}{\eta\mathcal{F}(\tau)S_0} I^\circ \int_\tau^t \eta(s) e^{-\int_0^s \mu(r)\,\mathrm{d}r} \frac{1}{\sqrt{4\pi\theta(s)}} e^{-\frac{(|x|-2\lambda\theta(s))^2}{4\theta(s)}} \\ e^{(\lambda^2\tilde{D}-\lambda c)(s-\tau)} e^{-\lambda c(t-s)}\,\mathrm{d}s \end{aligned}$$

where we use $t - \tau = (t-s) + (s-\tau)$.

From the formula for $\mathscr{K}(c,\lambda) > 0$ in (3.68), we have $\lambda^2\tilde{D} - \lambda c < \nu$. So

$$\begin{aligned} u_0\, e^{\lambda|x|-\lambda ct} < \frac{\nu + c\lambda - \tilde{D}\lambda^2}{\eta\mathcal{F}(\tau)S_0} I^\circ \int_\tau^t \eta\mathcal{F}(\tau) e^{-\nu(s-\tau)} \frac{1}{\sqrt{4\pi\theta(s)}} \\ e^{-\frac{(|x|-2\lambda\theta(s))^2}{4\theta(s)}} e^{\nu(s-\tau)} e^{-\lambda c(t-s)}\,\mathrm{d}s \end{aligned}$$

where we use the fact that for $s \in [\tau, t]$ $\eta(s) = \eta$ and

$$\mathcal{F}(s) = e^{-\int_0^s \mu(r)\,\mathrm{d}r} = e^{-\int_0^\tau \mu(r)\,\mathrm{d}r - \nu(s-\tau)} = \mathcal{F}(\tau) e^{-\nu(s-\tau)}.$$

Hence

$$\begin{aligned} u_0\, e^{\lambda|x|-\lambda ct} &< \frac{\nu + c\lambda - \tilde{D}\lambda^2}{S_0} I^\circ \int_\tau^t \frac{1}{\sqrt{4\pi\theta(s)}} e^{-\frac{(|x|-2\lambda\theta(s))^2}{4\theta(s)}} e^{-\lambda c(t-s)}\,\mathrm{d}s \\ &\leq \frac{\nu + c\lambda - \tilde{D}\lambda^2}{S_0\sqrt{4\pi\theta(\tau)}} I^\circ \int_\tau^t e^{-\lambda c(t-s)}\,\mathrm{d}s \qquad \text{since } \theta(s) \geq \theta(\tau) \\ &\leq \frac{\nu + c\lambda - \tilde{D}\lambda^2}{c\lambda S_0\sqrt{4\pi\theta(\tau)}} I^\circ =: \gamma. \end{aligned}$$

Hence for every $\lambda, c > 0$ with $\mathscr{K}(\lambda, c) < 1$, there exists γ as defined above such that

$$u_0 < \gamma\, e^{\lambda(ct-|x|)}.$$

Therefore u_0 is admissible.

Note that the idealized sufficient condition in (3.80) is a special case that satisfies the general sufficient condition in (3.79), but the initial condition (3.80) can be related to the particular situation of dropping infected individuals into a susceptible population.

For the second model (3.25), $I_0(x, a)$ refers to initial profile of incubating animals and $J^\circ(x)$ represents the initial density of infective animals. Hence $u_0(x, t)$ is defined differently in (3.39), (3.42) and (3.48).

We provide an admissible $u_0(x, t)$ by considering similarly the idealized situation where there are initially no infective animals

$$J^\circ(x) = 0. \tag{3.82}$$

We use the same initial condition for incubating animals $I_0(x, a)$ as for infected animals in (3.80). But in light of (3.33), to treat incubating animals $I(x, t, a)$ as if there were no loss terms, we use the following initial condition

$$G(a)I_0(x, a) = G(a)I^\circ\delta(x)\delta(a)$$

with

$$G(a) = \exp\left(\int_0^a \beta(r)\,\mathrm{d}r\right)$$

for the computation of $h_0(x, t)$ in (3.39).

For $t > \tau$, it is obvious that $h_0(x, t) = 0$.

Let $t \leq \tau$. Then

$$h_0(x,t) = \int_t^\infty P(\,\mathrm{d}a)\frac{\mathcal{F}(a)}{\mathcal{F}(a-t)} \int_{\mathbb{R}} \Gamma\left(\theta(a) - \theta(a-t), x-y\right) I_0(y, a-t)\,\mathrm{d}y$$

$$= \frac{\mathcal{F}(\tau)}{\mathcal{F}(\tau-t)} \int_{\mathbb{R}} \Gamma\left(\theta(\tau) - \theta(\tau-t), x-y\right) I_0(y, \tau-t)\,\mathrm{d}y$$

$$= \frac{\mathcal{F}(\tau)}{\mathcal{F}(\tau-t)}\, \Gamma\left(\theta(\tau) - \theta(\tau-t), x\right) G(\tau-t) I^\circ \delta(\tau-t)$$

Substitute $h_0(x,t)$ in (3.42), (3.48)

$$J_0(x,t) = \int_0^t \int_{\mathbb{R}} \Gamma\left(\tilde{D}(t-s), x-z\right) e^{-\nu(t-s)} h_0(z,s)\,\mathrm{d}z\,\mathrm{d}s$$

$$= \int_0^t \int_{\mathbb{R}} e^{-\nu(t-s)} \frac{\mathcal{F}(\tau)}{\mathcal{F}(\tau-s)}\, G(\tau-s) I^\circ \delta(\tau-s)$$

$$\Gamma\left(\tilde{D}(t-s), x-z\right) \Gamma\left(\theta(\tau) - \theta(\tau-s), z\right)\,\mathrm{d}z\,\mathrm{d}s.$$

By Chapman-Komolgorov equation for Γ

$$\int_{\mathbb{R}} \Gamma\left(\tilde{D}(t-s), x-z\right) \Gamma\left(\theta(\tau) - \theta(\tau-s), z\right)\,\mathrm{d}z = \Gamma\left(\tilde{D}(t-s) + \theta(\tau) - \theta(\tau-s), x\right).$$

Hence if $t < \tau$ $J_0(x,t) = 0$. If $t \geq \tau$

$$J_0(x,t) = \int_0^t e^{-\nu(t-s)} \frac{\mathcal{F}(\tau)}{\mathcal{F}(\tau-s)}\, G(\tau-s) I^\circ \delta(\tau-s) \Gamma\left(\tilde{D}(t-s) + \theta(\tau) - \theta(\tau-s), x\right)\,\mathrm{d}s$$

$$= I^\circ\, e^{-\nu(t-\tau)} \mathcal{F}(\tau) \Gamma\left(\tilde{D}(t-\tau) + \theta(\tau), x\right). \tag{3.83}$$

Now according to (3.48) $u(x,t) = 0$ for $t < \tau$. For $t \geq \tau$

$$u_0(x,t) = \eta\, I^\circ\, \mathcal{F}(\tau) \int_\tau^t e^{-\nu(s-\tau)}\, \Gamma\left(\tilde{D}(s-\tau) + \theta(\tau), x\right)\,\mathrm{d}s$$

Proposition 3.12 *In (3.50) if $I_0(x,t)$ satisfies (3.80) and $J_0(x,t)$ satisfies (3.82), then $u_0(x,t)$ defined in (3.48) is admissible.*

Proof Proof is similar to proposition 3.11.

Next we show that in the first model, initial condition for $I_0(x,a)$ in (3.80) not only ensures admissibility of $u_0(x,t)$, it also implies that c^* computed from (3.70) is the asymptotic speed of spread for (3.23).

Theorem 3.13 *In (3.23), let (A), (B) and (C) hold. If $I_0(x,t)$ satisfies (3.80), then the unique real positive c^* computed from (3.70) is the asymptotic speed of spread for $u(x,t)$.*

Proof Notice that with $I_0(x,t)$ defined in (3.80) $u_0(x,t)$ is given by (3.81).

Since $\eta(a)$ is only defined for $a \geq \tau$, so $u_0(x,t) = 0$ for $t < \tau$.

$$\begin{aligned} u_0(x,t) &\geq I^\circ \eta \mathcal{F}(\tau) \frac{e^{-\nu(t-\tau)}}{\sqrt{4\pi\theta(t)}} \int_\tau^t e^{-\frac{x^2}{4(\theta(\tau)+\tilde{D}(s-\tau))}} \, \mathrm{d}s \\ &\geq I^\circ \eta \mathcal{F}(\tau) \frac{e^{-\nu(t-\tau)}}{\sqrt{4\pi\theta(t)}} \int_\tau^t e^{-\frac{x^2}{4\theta(\tau)}} \, \mathrm{d}s \\ &= I^\circ \eta \mathcal{F}(\tau) \, e^{-\frac{x^2}{4\theta(\tau)}} \, g(t-\tau) \end{aligned}$$

where

$$g(z) = \frac{z e^{-\nu z}}{\sqrt{4\pi\theta(\tau) + 4\pi\tilde{D}z}}.$$

Note that derivative of g is

$$g'(z) = 4\pi e^{-\nu z} \frac{-\tilde{D}\nu z^2 + \left(\frac{\tilde{D}}{2} - \theta(\tau)\nu\right) z + \theta(\tau)}{\left(4\pi\theta(\tau) + 4\pi\tilde{D}z\right)^{3/2}}.$$

Hence

$$g'(0) = \frac{1}{\sqrt{4\pi\theta(\tau)}} > 0$$

and there exists $z_0 > 0$ such that $g'(z) = 0$ and $g'(z) < 0$ and is decreasing for $z > z_0$.

Setting $g'(z) = 0$ and solve for positive root we obtain

$$z^* = \frac{\frac{\tilde{D}}{2} - \theta(\tau)\nu + \sqrt{\left(\theta(\tau)\nu - \frac{\tilde{D}}{2}\right)^2 + 4\nu\tilde{D}\theta(\tau)}}{2\nu\tilde{D}}$$

Let $\phi > 0$ be arbitrary such that $|x| \geq \phi$. Note that

$$u_0(x,t) \geq I^\circ \eta \mathcal{F}(\tau)\, e^{-\frac{\phi^2}{4\theta(\tau)}}\, g(t-\tau).$$

We can choose $z^* + \tau > t_2 > t_1 > \tau$. Then $\forall t \in (t_1, t_2)$ $g(t-\tau)$ is increasing with respect to t. We can pick sufficiently small $\phi > 0$ such that

$$u_0(x,t) \geq I^\circ \eta \mathcal{F}(\tau)\, e^{-\frac{\phi^2}{4\theta(\tau)}}\, g(t-\tau) \geq I^\circ \eta \mathcal{F}(\tau)\, e^{-\frac{\phi^2}{4\theta(\tau)}}\, g(t_1-\tau) \geq \phi$$

since $e^{-\frac{\phi^2}{4\theta(\tau)}}$ is a decreasing function of ϕ but ϕ is an increasing function.

Note that by proposition 3.11 $u_0(x,t)$ is admissible. We showed that for appropriate $t_2 > t_1 \geq \tau$, $\phi > 0$ we have $u_0(t,x) \geq \phi$ for every $t \in (t_1, t_2)$, $|x| \leq \phi$. Note that also (A), (B) and (C) hold, so by Theorem 3.5 and 3.6, by definition the unique positive c^* computed from (3.70) is the asymptotic speed of spread for (3.23).

For the second model in (3.50) we have

Theorem 3.14 *In (3.50), let (A), (B) and (C) hold. If $I_0(x,t)$ satisfies (3.80) and $J_0(x,t)$ satisfies (3.82), then the unique real positive c^* computed from (3.70) is the asymptotic speed of spread for $u(x,t)$.*

Proof Proof is similar to Theorem 3.13

3.3.5 Estimation of c^*

Let $\sigma = \eta \mathcal{F}(\tau) S_0$. Then by (3.61) we have $\sigma > \nu$. In this subsection we estimate c^* when the dispersal of incubating animals is negligible. So we consider

$$\theta(\tau) = \int_0^\tau D(s)\, \mathrm{d}s \ll 1. \tag{3.84}$$

which is the same as the assumption (3.69).

Now we set $\epsilon = \theta(\tau)$ and

$$\lambda^* = \lambda_0 + \epsilon\lambda_1 + \epsilon^2\lambda_2 + \cdots \tag{3.85}$$

$$c^* = c_0 + \epsilon c_1 + \epsilon^2 c_2 + \cdots . \tag{3.86}$$

Consider $g(\epsilon) = e^{\epsilon(\lambda^*)^2 - \tau c^* \lambda^*}$.

Plugging in expansions of λ^* and c^*, to first order in ϵ we see that

$$g(\epsilon) = g(0) + \epsilon g'(0) \tag{3.87}$$

where

$$g(0) = e^{-\tau c_0 \lambda_0}$$

and

$$g'(0) = e^{-\tau c_0 \lambda_0} \left(\lambda_0^2 - \tau c_1 \lambda_0 - \tau c_0 \lambda_1\right).$$

Hence (3.70) becomes

$$\begin{aligned}
\sigma \left(e^{-\tau c_0 \lambda_0} + \epsilon\, e^{-\tau c_0 \lambda_0} \left(\lambda_0^2 - \tau c_1 \lambda_0 - \tau c_0 \lambda_1\right)\right) &= \nu + (c_0 + \epsilon c_1 + \cdots)(\lambda_0 + \epsilon\lambda_1 + \cdots) \\
&\quad - \tilde{D} \left(\lambda_0^2 + 2\lambda_0\lambda_1\epsilon + \cdots\right) \\
(c_0 + \epsilon c_1 + \cdots) - 2\tilde{D} \left(\lambda_0 + \epsilon\lambda_1 + \cdots\right) &= \Big[\nu + (c_0 + \epsilon c_1 + \cdots)\left(\lambda_0 + \epsilon\lambda_1 + \cdots\right) \\
&\quad - \tilde{D} \left(\lambda_0^2 + 2\lambda_0\lambda_1\epsilon + \cdots\right)\Big] \Big[2\epsilon\Big(\lambda_0 + \epsilon\lambda_1 + \cdots\Big) - \tau \left(c_0 + \epsilon c_1 + \cdots\right)\Big].
\end{aligned} \tag{3.88}$$

In (3.88) first we consider the order $O(1)$

$$\begin{aligned}
\sigma\, e^{-\tau c_0 \lambda_0} &= \nu + c_0\lambda_0 - \tilde{D}\lambda_0^2 \\
c_0 - 2\tilde{D}\lambda_0 &= \left(\nu + \lambda_0 c_0 - \tilde{D}\lambda_0^2\right)(-\tau c_0).
\end{aligned} \tag{3.89}$$

Hence,

$$\begin{aligned}
(-\tau c_0 \lambda_0)\, \sigma\, e^{-\tau c_0 \lambda_0} &= c_0\lambda_0 - 2\tilde{D}\lambda_0^2 \\
&= c_0\lambda_0 - 2\left(\nu + c_0\lambda_0 - \sigma\, e^{-\tau c_0 \lambda_0}\right) \\
&= -c_0\lambda_0 - 2\nu + 2\sigma\, e^{-\tau c_0 \lambda_0}.
\end{aligned}$$

Therefore if we set $y = c_0\lambda_0$

$$y + 2\nu - \sigma\tau e^{-\tau y}\left(y + \frac{2}{\tau}\right) = 0. \tag{3.90}$$

The roots of equation (3.90) can be analyzed using the following proposition.

Consider

$$F(z) = z^n + az^{n-1} + \cdots - Ke^{i\theta}e^{-\tau z}\left(z^m + bz^{m-1} + \cdots\right) = 0$$

where $\tau > 0, K \geq 0$ and $\theta \geq 0$ are real constants and a, b are complex constants.

Proposition 3.15 (Theorem I from Krall (1964)) *If $n = m$: when $K \neq 0$ $F(z)$ has an infinite number of zeros given by*

$$(1/\tau)\left(\ln K + i\left(\theta + 2k\pi\right)\right) + o(1)$$

as $k = 0, \pm 1, \pm 2, \cdots$, and only a finite number of other zeros. If $K < 1$, $F(z)$ has only a finite number of zeros with positive real part. If $K > 1$, $F(z)$ has only a finite number of zeros with negative real part.

In the case of (3.90) we consider $F(y)$ for $n = m = 1$, $\theta = 0$, $a = 2\nu, b = \frac{2}{\tau}$ and $K = \sigma\tau$. Therefore, by proposition 3.15 the only real solution is

$$c_0\lambda_0 = \frac{1}{\tau}\ln\left(\sigma\tau\right) + \delta \tag{3.91}$$

where $\delta \sim o(1)$ or equivalently $\delta \ll 1$.

Hence

$$\tilde{D}\lambda_0^2 = \nu + c_0\lambda_0 - \sigma e^{-\tau c_0\lambda_0} = \nu + \frac{1}{\tau}\ln\left(\sigma\tau\right) + \delta - \frac{1}{\tau}e^{-\delta\tau}.$$

Since $c_0 = c_0\lambda_0/\sqrt{\lambda_0^2}$, expand c_0 up to the first order of δ

$$c_0 = \frac{\frac{1}{\tau}\ln\left(\sigma\tau\right)}{\left[\frac{1}{\tilde{D}}\left(\nu - \frac{1}{\tau} + \frac{1}{\tau}\ln\left(\sigma\tau\right)\right)\right]^{1/2}} + \frac{\frac{1}{\tilde{D}}\left(\nu - \frac{1}{\tau}\right)}{\left[\frac{1}{\tilde{D}}\left(\nu - \frac{1}{\tau} + \frac{1}{\tau}\ln\left(\sigma\tau\right)\right)\right]^{3/2}}\delta. \tag{3.92}$$

Observe that τ is the length of incubation period and $\frac{1}{\nu}$ is the average time from onset of rabid symptoms to death. Usually we have $\tau > \frac{1}{\nu}$. Once the rabid symptoms appear, usually it is about one week before the infected animal dies, but it can take up to 150 days for incubation of rabies. So we have

$$\tau > \frac{1}{\nu} \qquad \text{or} \qquad \nu > \frac{1}{\tau} \qquad \text{or} \qquad \nu\tau > 1.$$

Note that by (3.61)

$$\sigma > \nu.$$

Hence

$$\ln(\sigma\tau) > \ln(\nu\tau) > 0.$$

From here we can expand λ_0 up to the first order in δ

$$\lambda_0 = \left[\frac{1}{\tilde{D}}\left(\nu - \frac{1}{\tau} + \frac{1}{\tau}\ln(\sigma\tau)\right)\right]^{1/2} + \left[\frac{1}{\tilde{D}}\left(\nu - \frac{1}{\tau} + \frac{1}{\tau}\ln(\sigma\tau)\right)\right]^{-1/2}\delta. \tag{3.93}$$

We can go on to compute c_1, λ_1 using c_0, λ_0 from (3.92), (3.93). However, since $\epsilon \ll 1$, obtaining c_1, λ_1 does not serve any purposes other than adding another term of order $o(1)$ to (3.92), (3.93). Therefore we stop at order $O(1)$ to conclude from (3.92)

$$c^* = \frac{\frac{1}{\tau}\ln(\eta\mathcal{F}(\tau)S_0\tau)}{\left[\frac{1}{\tilde{D}}\left(\nu - \frac{1}{\tau} + \frac{1}{\tau}\ln(\eta\mathcal{F}(\tau)S_0\tau)\right)\right]^{1/2}} + o(1). \tag{3.94}$$

Consequently, when the dispersal from incubating animals is negligible, we obtain an esimate of c^* in (3.94). The asymptotic speed of spread is an increasing function in and proportional to $\sqrt{\tilde{D}}$ and decreasing function of ν. This result is already summarized and predicted in proposition 3.9.

Taking the derivative of c^* with respect to τ, and noting the fact that $\mu(\tau) = \nu$, i.e. the

death rate at the end of incubation is the same as death rate for infective animals, we have

$$\frac{\partial c^*}{\partial \tau} = \left[-\frac{1}{2\tilde{D}\tau^2} \ln\left(\eta \mathcal{F}(\tau) S_0 \tau\right) \left(2\left(\nu - \frac{1}{\tau}\right) + \nu + \frac{\ln\left(\eta \mathcal{F}(\tau) S_0 \tau\right)}{\tau} \right) - \frac{(1-\nu\tau)^2}{\tilde{D}\tau^3} \right] \cdot$$

$$\left[\frac{1}{\tilde{D}} \left(\nu - \frac{1}{\tau} + \frac{1}{\tau} \ln\left(\eta \mathcal{F}(\tau) S_0 \tau\right) \right) \right]^{3/2} + o(1) < 0$$

since $\nu > \frac{1}{\tau}$. So, when the dispersal from incubating animals is negligible, c^* is a decreasing function with respect to incubation period τ.

The estimation of c^* in (3.94) is difficult to analyze when we consider $\tau \to 0$. Hence we want to find better estimation for c^* than (3.94). The following arguments are similar to those used in Jones *et al.* (2013).

Equation (3.90) can be rewritten as

$$y + 2\nu - \sigma e^{-\tau y}(\tau y + 2) := F(\tau, y) = 0 \tag{3.95}$$

Also from the second equation of (3.89) it is readily obtained that

$$\lambda_0^2 = y \frac{\tau(\nu + y) + 1}{\tilde{D}(2 + \tau y)}. \tag{3.96}$$

Once y is found from (3.95) we have

$$c_0^2 = \frac{y^2}{\lambda_0^2} = \frac{\tilde{D} y (2 + \tau y)}{\tau(\nu + y) + 1}. \tag{3.97}$$

At least two special cases of τ lead to easy solution of y from (3.95).

$$\tau = 0 \Rightarrow y = 2(\sigma - \nu),\ c_0^2 = 4\tilde{D}(\sigma - \nu)$$

$$\tau = \frac{1}{\nu} \Rightarrow y = \nu \ln\left(\frac{\sigma}{\nu}\right),\ c_0^2 = \tilde{D}\nu \ln\left(\frac{\sigma}{\nu}\right)$$

Consider the function $F(\tau, y)$ defined in (3.95). F is a strictly increasing function of both

τ and y, given that $c_0, \lambda_0 > 0$ and $\tau \geq 0$. In fact

$$\frac{\partial F}{\partial \tau} = \mu(\tau)\sigma e^{-\tau y}(\tau y + 2) - \sigma e^{-\tau y}(-y)(\tau y + 2) - \sigma e^{-\tau y} y$$

$$= \sigma e^{-\tau y}(\tau y^2 + \tau \nu y + y + 2\nu) > 0$$

$$\frac{\partial F}{\partial y} = 1 + \tau\sigma e^{-\tau y}(\tau y + 1) > 0$$

since σ is a function of τ and we assume that $\mu(\tau) = \nu$.

It follows that there exists a unique $y > 0$ such that y is strictly decreasing function of τ. As a result

$$y \leq 2(\sigma - \nu). \tag{3.98}$$

It follows from implicit function theorem that y is differentiable with respect to τ.

Let $z = \tau y$. Then from (3.95) we have

$$y + 2\nu - \sigma e^{-z}(z + 2) := G(z, y) = 0. \tag{3.99}$$

It is easily verified that G is strictly increasing with respect to both z and y. Therefore z must be strictly decreasing function of y, hence strictly increasing with respect to τ.

Since $y > 0$ is bounded and decreasing function of τ, it must have a limit as $\tau \to \infty$. Suppose $y \to y_\infty \in (0, 2(\sigma - \nu))$. Then from (3.95)

$$y_\infty + 2\nu = 0$$

which is a contradiction. So we must have $y \to 0$ as $\tau \to \infty$, and $z \to z_\infty$ as $\tau \to \infty$ where z_∞ is given by

$$\sigma e^{-z_\infty}(z_\infty + 2) = 2\nu.$$

Therefore from (3.97)

$$(c_0\tau)^2 = \frac{\tilde{D}z(z+2)}{(y+\nu) + 1/\tau} \to \frac{\tilde{D}z_\infty(z_\infty + 2)}{\nu} \quad \text{as } \tau \to \infty. \tag{3.100}$$

So when the incubation period τ is big and incubating animals rarely disperse, the first order of asymptotic spread speed is proportional to $\frac{1}{\tau}$.

Next we consider the function

$$\theta(z) = e^{-z}(z+2)$$

from the function $G(z, y)$ in (3.99). Since

$$\theta(0) = 2,\ \theta'(z) = -e^{-z}(z+1),\ \theta''(z) = e^{-z}z$$

we find the Taylor expansion of θ

$$\theta(z) = 2 - z + \frac{1}{2}z^2 e^{-\tilde{z}}\tilde{z}$$

where $\tilde{z} \in (0, z)$. From this Taylor expansion

$$2 - z \leq \theta(z) \leq 2 - z + \frac{1}{2}z^3.$$

Using equation of G in (3.99)

$$\sigma(2 - \tau y) \leq y + 2\nu \leq \sigma(2 - \tau y + \frac{1}{2}\tau^3 y^3)$$

$$\Leftrightarrow 2(\sigma - \nu) \leq (1 + \sigma\tau)y \leq 2(\sigma - \nu) + \frac{1}{2}\sigma\tau^3 y^3$$

$$\Leftrightarrow \frac{2(\sigma - \nu)}{1 + \sigma\tau} \leq y \leq \frac{2(\sigma - \nu)}{1 + \sigma\tau} + \frac{\frac{1}{2}\sigma\tau^3 y^3}{1 + \sigma\tau}.$$

Since $y \leq 2(\sigma - \nu)$ from (3.98), plugging this in above equation

$$\frac{2(\sigma - \nu)}{1 + \sigma\tau} \leq y \leq \frac{2(\sigma - \nu)[1 + 2\sigma\tau^3(\sigma - \nu)^3]}{1 + \sigma\tau} \tag{3.101}$$

which remains a good approximation of y when τ or $\sigma - \nu$ is small.

We can use (3.101) to find a good approximation for c_0 when τ is small. Since c_0^2 is increasing in y from (3.97)

$$c_0^2 = \frac{\tilde{D}y(2 + \tau y)}{\tau(\nu + y) + 1} \geq \frac{4\tilde{D}(\sigma - \nu)}{1 + \sigma\tau} \cdot \frac{(1 + \sigma\tau) + \tau(\sigma - \nu)}{(1 + \sigma\tau)(1 + \tau\nu) + 2\tau(\sigma - \nu)}.$$

Let $\epsilon = \sigma - \nu$. We find

$$\begin{aligned} c_0^2 &\geq \frac{4\tilde{D}(\sigma-\nu)}{1+\sigma\tau} \cdot \frac{(1+\sigma\tau)+\tau\epsilon}{(1+\sigma\tau)(1+(\sigma-\epsilon)\tau)+2\tau\epsilon} \\ &= \frac{4\tilde{D}(\sigma-\nu)}{1+\sigma\tau} \cdot \frac{(1+\sigma\tau)+\tau\epsilon}{(1+\sigma\tau)^2-\epsilon\sigma\tau^2+\epsilon\tau} \\ &\geq \frac{4\tilde{D}(\sigma-\nu)}{1+\sigma\tau} \cdot \frac{(1+\sigma\tau)+\tau\epsilon}{(1+\sigma\tau)^2+\epsilon\tau(1+\sigma\tau)} \\ &= \frac{4\tilde{D}(\sigma-\nu)}{(1+\sigma\tau)^2}. \end{aligned}$$

Therefore when τ or $\sigma - \nu$ is small,

$$c_0 \approx \frac{2\sqrt{\tilde{D}(\sigma-\nu)}}{1+\sigma\tau} \tag{3.102}$$

is a good approximation. Next we consider how approximation of c_0 depends on large σ. By assumption $\sigma = \eta\mathcal{F}(\tau)S_0 > \nu$, large σ can be obtained from large infection rate η, large initial susceptible individuals S_0 and small death rate μ during incubation stage. These situations can occur naturally when a large group of susceptible animals are first introduced with rabies infection.

In (3.95) we let $F(\tau, y) = 0$ then

$$e^{\tau y} = \frac{\sigma(\tau y+2)}{y+2\nu} = \frac{\sigma}{\nu}\frac{1+\tau(y/2)}{1+(1/\nu)(y/2)}.$$

Taking natural logarithms

$$\tau y = \ln\left(\frac{\sigma}{\nu}\right) + \ln\left(1+\tau(y/2)\right) - \ln\left(1+(1/\nu)(y/2)\right). \tag{3.103}$$

It is easily seen from Taylor expansion of e^x that

$$\ln\left(1+\tau(y/2)\right) \leq \tau(y/2).$$

Hence substituting this in (3.103) we have

$$\tau y \leq 2\ln\left(\frac{\sigma}{\nu}\right).$$

Hence the τy satisfies

$$\tau y \leq \ln\left(\frac{\sigma}{\nu}\right) + \ln\left(1 + \ln\left(\frac{\sigma}{\nu}\right)\right). \tag{3.104}$$

Although the incubation period τ is usually greater than the mean life span of infectious individuals $1/\nu$, for example in the case of foxes, we still need to consider situations where this is not true.

(i) $\tau > \nu$. Incubation period is large. Then from (3.103) $\tau y \geq \ln\left(\frac{\sigma}{\nu}\right)$. Then further we find

$$\frac{\tau y}{\ln\left(\frac{\sigma}{\nu}\right)} \to 1 \quad \text{as } \frac{\sigma}{\nu} \to \infty$$

since

$$\frac{\ln\left(1 + \ln\left(\frac{\sigma}{\nu}\right)\right)}{\ln\left(\frac{\sigma}{\nu}\right)} \to 0 \quad \text{as } \frac{\sigma}{\nu} \to \infty.$$

(ii) $\tau \leq 1/\nu$. Incubation period is small. Then $\tau y \leq \ln\left(\frac{\sigma}{\nu}\right)$. and

$$\ln\left(\frac{\sigma}{\nu}\right) - \ln\left(1 + \frac{1}{2\tau\nu}\ln\left(\frac{\sigma}{\nu}\right)\right) \leq \tau y \leq \ln\left(\frac{\sigma}{\nu}\right).$$

Hence we still have

$$\frac{\tau y}{\ln\left(\frac{\sigma}{\nu}\right)} \to 1 \quad \text{as } \frac{\sigma}{\nu} \to \infty.$$

Note from (3.97) that $c_0^2/y \to 1$ as $y \to \infty$. So

$$\frac{c_0^2}{\ln\left(\frac{\sigma}{\nu}\right)} \to \frac{1}{\tau} \quad \text{as } \frac{\sigma}{\nu} \to \infty. \tag{3.105}$$

Therefore when σ is large from (3.105) c_0 is approximately proportional to $1/\sqrt{\tau}$.

In Figure 3.2 we compare the various approximation formulas for c^* above with the exact value of c^* from (3.70) with small diffusion from exposed individuals and varying incubation period τ. Like all previous calculations, we use parameter values consistent with Table 2.1. In the numerical experiment, we set the diffusion constant for exposed individuals as 1, which is negligible compared with the diffusion constant of infectious

animals 40. We find that when τ is very large or very small, $1/\tau$ is a good approximation of exact c^*. Additionally (3.102) remains consistently smaller than and almost proportional to the exact c^* throughout all values of τ. If we ignore $\theta(\tau)$, the system of equations (3.89) is resulted and produces an approximate c^* that is a very good approximation to the exact c^* when τ is small. The approximate $O(1)$ term obtained using perturbation analysis in (3.94) remains an uppber bound for the exact c^*, but when τ is small, (3.94) is also a good approximation to the exact c^*. In this figure, $1/\sqrt{\tau}$ is a poor approximation to the exact c^* since our σ is not set very large.

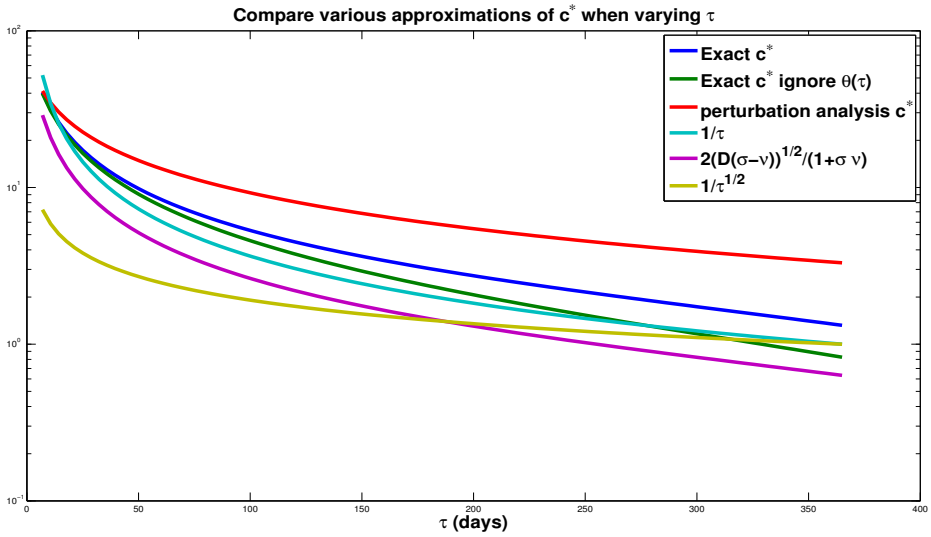

Figure 3.2: Based on Table 2.1. We let $\eta = 80$, $S_0 = 2$, $\nu = 365/5$, $\tilde{D} = 40$. And in particular the diffusion constant for exposed individuals is set as 1.

3.4 Conclusion and Discussion

This chapter is devoted to the construction and asymptotic speed of spread for a Kermack and McKendrick's model where infectivity, death rate and diffusion rate can depend on the age of infection. We consider a population of animals divided into susceptible and infected classes. Here we assume that the total population is closed and homogeneous over

a one-dimensional space, which means we do not take into account natural birth or death. Here the main feature for this chapter is the introduction of the age of infection. The age of infection was used in epidemic models to model the period of latency necessary for infected individuals to become clinically infectious (see Thieme and Castillo-Chavez (1989, 1993) and references therein). In particular it allows us to track the history of infected individuals during incubation period.

The modeling is non-trivial and from two approaches we arrive at the same integral equations for a special case of fixed incubation period that can be analyzed for the asymptotic speed of spread using theories developed in Thieme (1979) and Thieme and Zhao (2003). Then we are able to obtain an estimation for the asymptotic speed of spread c^* when the dispersal of incubating individuals is negligible, where we also show that to the first order in the integral $\theta(\tau)$ from (3.84) c^* can asymptotically be approximated by $1/\tau$ when τ is large and small or $\sigma - \nu$ is small, and by $1/\sqrt{\tau}$ when σ is large.

The asymptotic speed of spread here is used on the cumulated force of infection $u(x,t)$ given by (3.12). And the sufficient condition given by (3.61)

$$k^* = \frac{\eta}{\nu}\mathcal{F}(\tau)S_0 > 1$$

also depends on the initial susceptible population size S_0. However it still can be understood in the normal sense of reproduction number R_0. Since $1/\nu$ is the mean life span of infectious individuals, η is the infectivity of infectious animals, and $\mathcal{F}(\tau)$ can be understood as the probability of surviving the incubation period, k^* can be seen as the expected number of infections resulted from introduction of a single infectious individual in a completely susceptible population S_0.

Both the alternative model with infection-age-dependent parameters and the alternative model with distributed delay result in integral equations (3.23) and (3.50) that can be analyzed for asymptotic speed of spread using theories developed in Thieme (1979)

and Thieme and Zhao (2003). It is important to note that in the limiting equation for both integral equations, as seen in Theorems 3.7 and 3.8, Thieme and Zhao (2003) showed that traveling wave solutions exist and the asymptotic speed of spread is in fact the minimum traveling wave speed. Therefore it is no coincidence that if we use a fixed delay in both alternative models, then asymptotic spread speed c^* can be calculated by the same equations (3.70) as that used for the minimum traveling wave speed (2.32) in the delayed SI model (2.6), and if we use an exponentially distributed incubation period in the alternative model with distributed delay, with some rescalings and simplifying assumptions on death and diffusion rates for exposed individuals, the asymptotic speed of spread c^* is obtained by the same equations (3.78) as equations (2.17) and (2.19) for the minimum traveling wave speed for the SEI diffusive model (2.1). Therefore it is reasonable to conclude that both the SEI and delayed SI diffusive models from chapter 2 are special cases of the alternative models in this chapter. Although both SEI diffusive (2.1) and delayed SI models (2.6) in chapter 2 incorporate population turnover, which both alternative models (3.2) and (3.25) do not, it is noteworthy that the role of K, the carrying capacity, in both models with population turnover, is played by S_0, the initial population density of susceptible animals, in the alternative models without population turnover. Also the estimation of c^* when dispersal of incubating animals is not negligible can be studied in the future.

Chapter 4

SPATIAL SPREAD OF RABIES – INCORPORATE A REALISTIC LANDSCAPE

We proposed in Borchering *et al.* (2012) a rabies model for skunk and bat interaction in northeastern Texas, and used homogeneous diffusion on structured grids to model spatial movement of animals. Though the model and simulations suggested the possibility of interspecies interactions between rabid bats and susceptible skunks, they only considered homogeneous environment and landscape, reflected by constant diffusion coefficients. In this chapter, we aim to describe the spread of rabies infection over a real two-dimensional square $(300km)^2$ region Ω with some realistic geographic features. To do that, instead of finite difference schemes in space, we resort to unstructured discretizations based on finite element methods in space. This approach is not novel, and there are studies on numerical simulations of age-structured models over one-dimensional domains (Ayati and Dupont, 2002; Cusulin and Gerardo-Giorda, 2010) and works that provide theoretic convergence and stability results for the scheme (Kim and Park, 1998); however, studies that focus on numerical simulations over a two-dimensional realistic domain in the context of epidemiological models are rare.

4.1 Functional spaces

Let $\Omega \subset \mathbf{R}^2$ be an open two-dimensional domain of interest with coordinates x, y. Let the boundary of Ω be $\Gamma = \partial\,\Omega$. Each function here is a function of location (x, y) and/or time $t \in [0, T]$ with $T > 0$. We first define properly the underlying functional spaces.

Let $L^2(\Omega)$ be the space of all functions f that satisfy

$$\|f\|_{L^2}^2 = \int_\Omega f^2(x, y)\,\mathrm{d}x\,\mathrm{d}y < \infty.$$

Of course, f is in Sobolev space $H^1(\Omega)$, if in addition to $f \in L^2(\Omega)$ we have

$$\|f\|_{H^1}^2 = \int_\Omega \left(f^2 + (\partial_x f)^2 + (\partial_y f)^2\right) \,\mathrm{d}x\,\mathrm{d}y < \infty.$$

In the meantime the seminorm in $H^1(\Omega)$ is defined as

$$|f|_{H^1} = \left(\int_\Omega (\partial_x f)^2 + (\partial_y f)^2\right) \,\mathrm{d}x\,\mathrm{d}y)^{1/2}.$$

In our case, $\|f\|_{H^1}$ can also be a function of time. If, in addition,

$$\int_0^T \|f\|_{H^1}^2(t)\,\mathrm{d}t < \infty$$

we denote that $f \in L^2\left(0, T; H^1(\Omega)\right)$.

For implementations of the finite element method, in our case since we employ Neumann boundary conditions we mainly focus on the weak formulation of our problem

$$\text{find } u \text{ in } L^2(0,T;H^1(\Omega)) \text{ such that } a(u,v) = l_u(v) \quad \forall v \in H^1(\Omega),$$

where

$$a(u,v) = \frac{\mathrm{d}}{\mathrm{d}t}\int_\Omega uv\,\mathrm{d}x\,\mathrm{d}y + \int_\Omega (\Phi\nabla u)\cdot\nabla v\,\mathrm{d}x\,\mathrm{d}y$$

and

$$l_u(v) = \int_\Omega f(u)v\,\mathrm{d}x\,\mathrm{d}y.$$

with Φ a diffusion tensor that varies spatially.

In order to find a finite element approximation to the above problem, we also need to define a finite-dimensional subspace of $H^1(\Omega)$. Here we mainly consider the subspace $\mathscr{P}_1$ of continuous piecewise linear polynomial functions over a triangulation $\mathscr{T}$ of the computational domain Ω.

By a triangulation $\mathscr{T}$ of the computational domain Ω, we refer to a finite collection of two-dimensional triangles $\{K_i\}$ such that

(a) $K_i \cap K_j = \emptyset$ if $i \neq j$, and

(b) $\bigcup_i \bar{K}_i = \bar{\Omega}$.

We denote $\mathscr{P}_1$ to have dimension N if the triangulation $\mathscr{T}$ involves N vertices $\{(x_i, y_i)\}_{i=1}^N$, and therefore $\mathscr{P}_1$ over $\mathscr{T}$ is N-dimensional with a set of basis functions $\{\phi_i\}_{i=1}^N$ such that

$$\phi_i(x_j, y_j) = \begin{cases} 1 & i = j \\ 0 & i \neq j \end{cases}$$

In particular, every function in $\mathscr{P}_1$ is a piecewise continuous linear polynomial in two variables x, y. So over each $K_i \in \mathscr{T}$

$$f \in \mathscr{P}_1 \Leftrightarrow f = a_1 x + a_2 y + a_3$$

where a_1, a_2, a_3 are constant.

4.2 Rabies model for skunk and rabies interactions

Unlike previous studies on rabies infection that also used SEIR models on a single species (Dimitrov *et al.*, 2007; George *et al.*, 2011), the interspecies rabies infection between bat and skunk populations here can be modeled by a coupled system of nonlinear ordinary (ODE) and partial (PDE) differential equations. The infected bats come into contact with both susceptible bats and susceptible skunks. In Fig. 4.1, the dotted line represents infection between compartments. The small arrows represent departure from one compartment into another compartment. We assume logistic growth of the populations. The bat system includes a recovered compartment. Unlike skunks, some bats survive rabies infection.

The skunk population is modeled by the following coupled set of nonlinear ODEs/PDEs:

$$\begin{aligned} \frac{\partial S_s}{\partial t} &= r_s S_s \left(1 - \frac{N_s}{K_s}\right) - \beta_s S_s I_s - \gamma S_s I_b + d_{ss} \nabla^2 S_s \\ \frac{\partial E_s}{\partial t} &= \beta_s S_s I_s - (\sigma_s + m_s) E_s + \gamma S_s I_b + d_{es} \nabla^2 E_s \\ \frac{\partial I_s}{\partial t} &= \sigma_s E_s - m_{rs} I_s + d_{is} \nabla^2 I_s \end{aligned} \tag{4.1}$$

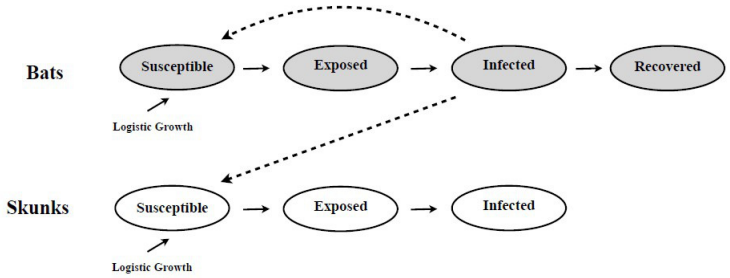

Figure 4.1: Coupled SEIR system.

while the bat population is modeled by a similar set of coupled nonlinear ODEs/PDEs:

$$\begin{aligned}
\frac{\partial S_b}{\partial t} &= r_b S_b \left(1 - \frac{N_b}{K_b}\right) - \beta_b S_b I_b \\
\frac{\partial E_b}{\partial t} &= \beta_b S_b I_b - (\sigma_b + m_b) E_b \\
\frac{\partial I_b}{\partial t} &= \sigma_b E_b - m_{rb} I_b - \rho_b I_b + d_b \nabla^2 I_b \\
\frac{\partial R_b}{\partial t} &= \rho_b I_b - m_{wb} R_b
\end{aligned} \tag{4.2}$$

where S_s = susceptible skunks, E_s = exposed skunks, I_s = infected skunks, and the total number of skunks is $N_s = S_s + E_s + I_s$; and S_b = susceptible bats, E_b = exposed bats, I_b = infected bats, R_b = recovered bats, and the total number of bats is $N_b = S_b + E_b + I_b + R_b$. Logistic growth is represented in each susceptible compartment with the appropriate birth rates (r_s and r_b) and carrying capacities (K_s and K_b).

Infection and Incubation. Skunks are susceptible to infection from skunks and bats. The term $\beta_s S_s I_s$ represents infected skunks produced per year resulting from contact between infected and susceptible skunks at a transmission rate β_s. Susceptible skunks progress into the exposed class after being inoculated with rabies virus due to contact with infected skunks. The transmission function $\gamma S_s I_b$ represents skunk infection resulting from contact with infected bats. The term $\beta_b S_b I_b$ represents the infection of susceptible bats by infected bats at a bat transmission rate β_b. After an average incubation period of $1/\sigma_b$, exposed

individuals move into the infected compartment. The incubation period for skunks is σ_s^{-1}.

Fertility. We assume that only susceptible animals are capable of reproduction and the total population production follows logistic growth equation.

Mortality. In the exposed compartments, individuals die from background mortality (terms $m_s E_s$ and $m_b E_b$). In the infected compartments, individuals die at a much higher rate that accounts for disease related mortality (terms $m_{rs} I_s$ and $m_{rb} I_b$). Recovered bat mortality is expressed by $m_{wb} R_b$.

Diffusion and Recovery. Diffusion terms ($d_{is}\nabla^2 I_s$ and $d_b \nabla^2 I_b$) have been added to the infected compartments. Although symptoms of (furious) rabies include disregard for territorial boundaries and a general increase in movement, diffusion rates d_{ss} and d_{es} for susceptible and exposed skunks were assumed to be the same as d_{is}, as results of field study suggest practically no difference between characteristics of dispersal and home ranges between members of healthy and rabid skunk populations (Greenwood, 1997). Some bats survive rabies infection. These bats are accounted for by the advancement of ρI_b from the infected bat compartment into the recovered bat compartment.

The skunk and bat parameters are described in Tables 4.1 and 4.2.

4.3 Simulation results with homogeneous and isotropic diffusion

The systems (4.1) and (4.2) are equipped with simple homogeneous and isotropic diffusion. Generally in 2D, the diffusion is accounted for by the term

$$\nabla \cdot (\Phi \nabla u)$$

where Φ in our case is a 2×2 symmetric and positive definite diffusion tensor matrix, and u is a twice continuously differentiable function over a two-dimensional domain. From this term and by Fick's law the flux vector is defined as

$$\mathbf{j} = -\Phi \nabla u.$$

Table 4.1: Skunk parameter set.

Name	Value	Information	Reference
K_s	20	0.7–18.5 individuals per km^2	Wade-Smith and Verts (1982)
β_s	2.5	unknown	ad hoc
r_s	4	litter size 3–9	Schmidly (1994)
m_s^{-1}	2.5	lifespan 2–3 years	Pybus (1988)
m_{rs}^{-1}	0.0274	yrs (10 days)	Chalton *et al.* (1987)
σ^{-1}	0.164	yrs (60 days), 21–117 days	Chalton *et al.* (1987)
d_{ss}	10	km^2 per year	Greenwood (1997)
d_{es}	10	km^2 per year	Greenwood (1997)
d_{is}	10	km^2 per year	Greenwood (1997)

For the diffusion to be isotropic, the direction of **j** and concentration gradient ∇u have to be parallel. Also, for the diffusion to be homogeneous, the matrix Φ needs to be constant throughout the whole domain Ω. As a result, for our systems (4.1) and (4.2), the diffusion is homogeneous and isotropic.

Simulations of this coupled ODE/PDE models were carried out over a two-dimensional $(300 \text{ km})^2$ geographic area in northeast Texas (see Figure 4.2). This area is principally located in the Texan biotic province (Blair, 1950), a geographic area with forests to the east and semiarid grasslands to the west. Rabid skunks, in most cases striped skunks (*Mephitis mephitis*), in Texas have been observed to be prevalent chiefly in the Texan biotic province (Pool and Hacker, 1982), due to frequent occurrences in this area of agricultural lands used for pasturage, row crops, wooded acreage. On the other hand, most cases of bat rabies in the $(300 \text{ km})^2$ area have been distributed with a focus in Dallas, and the dominant bat species is eastern red bat (*Lasiurus borealis*). This area has been observed (Pool and Hacker, 1982)

Table 4.2: Bat parameter set.

Name	Value	Information	Reference
K_b	250	per km^2, 1 red bat per acre	Schwartz and Schwartz (2002)
β_b	0.12	estimated by Dimitrov et. al.	Dimitrov and King (2008)
r_b	0.4	per year, litter size 1–4	Schwartz and Schwartz (2002)
m_b^{-1}	10	years, up to 12 years	Saunders (1988)
m_{rb}^{-1}	0.0384	years (14 days)	Constantine and Woodball (1966)
m_{wb}^{-1}	10	years, same as m_b^{-1}	ad hoc
σ_b^{-1}	0.0384	years (14 days)	Constantine and Woodball (1966)
ρ_b^{-1}	0.5	years	Turmelle *et al.* (2010)
γ	0.05	much smaller than β_s	ad hoc
d_b	300	km^2 per year	Mager and Nelson (2000)

to be free of rabies cases in other major mammalian reservoir species, in particular foxes.

We applied Gaussian distributions to initial values for each compartment. The result is infected individuals spreading out from the center, with following smaller periodic waves of infections. We used MATLAB to solve the partial differential equation system with an adaptive Runge-Kutta 4/5 order solver. Homogeneous Neumann boundary conditions were considered on the boundaries. Biologically, homogeneous Neumann boundary conditions imply no-flux across boundaries, or no flow of individuals in or out of the boundaries, so the system is a closed one.

We used confirmed case data from the region of interest in Texas to initialize the infected individuals in the model. Distributions of exposed and recovered skunks(bats) were initialized as proportional to that of infected skunks(bats). And susceptible skunks(bats) were initialized as the difference between carrying capacity for skunks(bats) and the sum

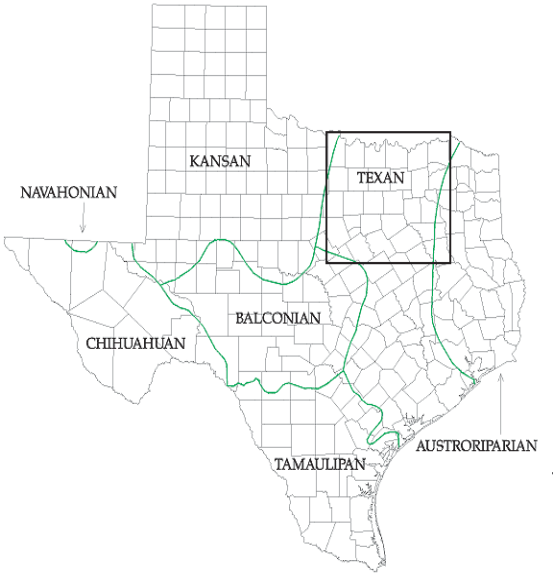

Figure 4.2: Region of study and biotic provinces in Texas.

of other classes of skunks(bats). We then perform simulations with and without infection of skunks from rabid bats in order to see the resulting changes in distribution of infected animals. And we compare the simulation results to the confirmed case data map (see Figure 4.3). Our simulation results qualitatively describes the changes over time of infected skunks and bats.

There are two glaring limitations from the simulation results. As we can see from Figure 4.3, the actual distribution of infected skunks is confined outside a blank region, which is geographically located at and around the major city Dallas. The simulations with homogeneous and isotropic diffusions did not generate such a pattern. Moreover individuals from the simulations spread out evenly in every direction, which might be true in a strictly homogeneous and local environment but is quite unrealistic when considering a larger region, as seen in Figure 4.2. So, to produce a closer fit to the confirmed case data map, we are modifying the system (4.1) and (4.2) by incorporating heterogeneous and anisotropic

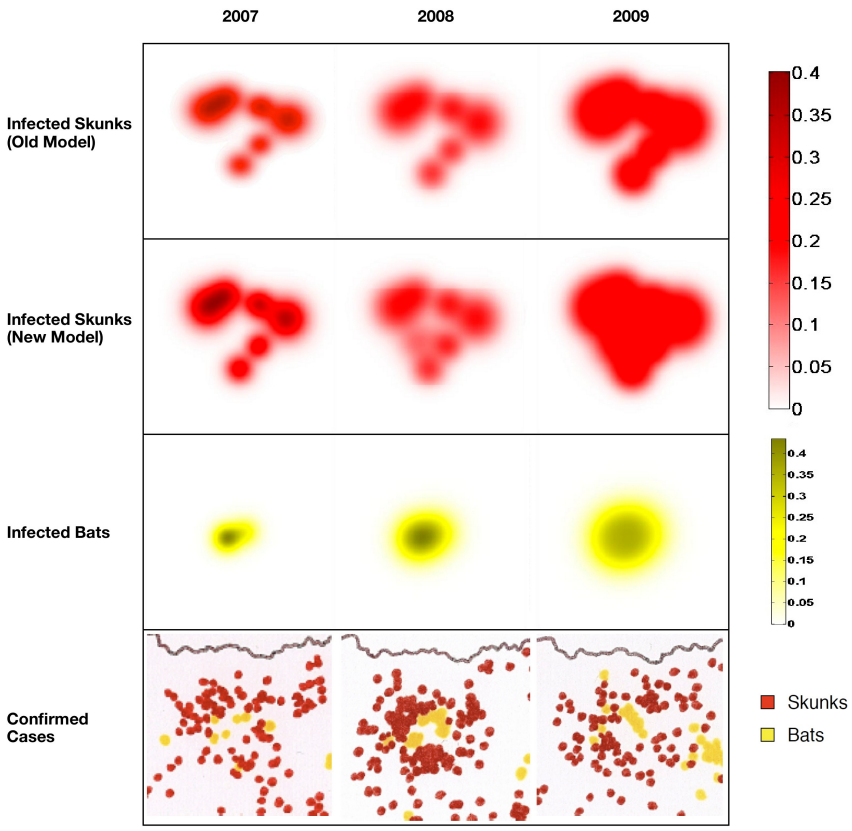

Figure 4.3: Simulations and confirmed case data.

diffusions, which in turn reflect changes in landscape features.

4.4 Variational formulation

The application of finite element method is dependent on the variational formulation of the problem. First we can reorganize each diffusion term as

$$\nabla \cdot (\Phi_u \nabla u)$$

where Φ_u are 2×2 diffusion tensor matrices, and $u = S_s, E_s, I_s, S_b, E_b, I_b, R_b$. The tensors are designed to model the spatial heterogeneities of the landscape. As a result, each tensor

is a function of location $(x, y) \in \Omega$. Similarly, original diffusion tensors can be written as

$$\Phi_u = \begin{pmatrix} d_u & 0 \\ 0 & d_u \end{pmatrix}$$

where $u = S_s, E_s, I_s, S_b, E_b, I_b, R_b$ and for our simulations we considered $d_u = 0$ for $u = S_b, E_b, R_b$.

With these new notations we can write our rabies model for skunk and bat interactions as

$$\begin{aligned}
\partial_t S_s - \nabla\cdot(\Phi_{S_s}\nabla S_s) &= r_s S_s\left(1 - \frac{N_s}{K_s}\right) - \beta_s S_s I_s - \gamma S_s I_b \\
\partial_t E_s - \nabla\cdot(\Phi_{E_s}\nabla E_s) &= \beta_s S_s I_s - (\sigma_s + m_s)E_s + \gamma S_s I_b \\
\partial_t I_s - \nabla\cdot(\Phi_{I_s}\nabla I_s) &= \sigma_s E_s - m_{rs} I_s \\
\partial_t S_b - \nabla\cdot(\Phi_{S_b}\nabla S_b) &= r_b S_b\left(1 - \frac{N_b}{K_b}\right) - \beta_b S_b I_b \\
\partial_t E_b - \nabla\cdot(\Phi_{E_b}\nabla E_b) &= \beta_b S_b I_b - (\sigma_b + m_b)E_b \\
\partial_t I_b - \nabla\cdot(\Phi_{I_b}\nabla I_b) &= \sigma_b E_b - m_{rb} I_b - \rho_b I_b \\
\partial_t R_b - \nabla\cdot(\Phi_{R_b}\nabla R_b) &= \rho_b I_b - m_{wb} R_b
\end{aligned} \tag{4.3}$$

where now we assume that Φ_u's vary with spatial variables, and we inherit our previous assumptions that Φ_u are all zero 2×2 matrices, with $u = S_b, E_b, R_b$.

Let the vector

$$\mathbf{u} = [S_s\, E_s\, I_s\, S_b\, E_b\, I_b\, R_b]^T$$

denote the vector of solutions to (4.3). Then a compact representation of (4.3) is

$$\partial_t \mathbf{u} - \nabla\cdot\,(\Phi\nabla\mathbf{u}) = f(\mathbf{u}) \tag{4.4}$$

where $f(\mathbf{u}) = (A - B(\mathbf{u}))\mathbf{u}$ and

$$A = \begin{pmatrix} r & & & & & & & \\ & -(\sigma_s + m_s) & & & & & & \\ & \sigma_s & -m_{rs} & & & & & \\ & & & r_b & & & & \\ & & & & -(\sigma_b + m_b) & & & \\ & & & & \sigma_b & -m_{rb} - \rho_b & & \\ & & & & & \rho_b & -m_{wb} \end{pmatrix}$$

where unfilled entries are all zero, and

$$B(\mathbf{u}) = \begin{pmatrix} -\frac{r}{K_s} N_s & 0 & -\beta S_s & 0 & 0 & -\gamma S_s & 0 \\ \beta I_s & 0 & 0 & 0 & 0 & \gamma S_s & 0 \\ 0 & 0 & 0 & 0 & 0 & 0 & 0 \\ -\frac{r_b}{K_b} N_b & 0 & 0 & 0 & 0 & -\beta_b S_b & 0 \\ 0 & 0 & 0 & 0 & 0 & \beta_b S_b & 0 \\ 0 & 0 & 0 & 0 & 0 & 0 & 0 \\ 0 & 0 & 0 & 0 & 0 & 0 & 0 \end{pmatrix}$$

and

$$\Phi = \begin{pmatrix} \Phi_{S_s} & & & & & & \\ & \Phi_{E_s} & & & & & \\ & & \Phi_{I_s} & & & & \\ & & & \Phi_{S_b} & & & \\ & & & & \Phi_{E_b} & & \\ & & & & & \Phi_{I_b} & \\ & & & & & & \Phi_{R_b} \end{pmatrix}$$

The compact representation (4.4) indicates that the system of concern is a vector general-

ization of the one-dimensional Fisher's equation

$$\partial_t u - \partial_{xx} u = (1-u)u.$$

Analysis of this equation and traveling wave solutions taking the form

$$u(x,t) = g(x - ct)$$

for some constant c and appropriate function g are well studied.

The problem (4.4) is well-defined and complete with appropriate initial conditions

$$\mathbf{u}(0,x,y) = \mathbf{u}_0 \geq 0 \in H^1(\Omega) \tag{4.5}$$

and homogeneous Neumann boundary conditions

$$\mathbf{n} \cdot \nabla \mathbf{u} = 0 \tag{4.6}$$

with $(t,x,y) \in [0,T] \times \Gamma$ and $\mathbf{n}$ the normal vector pointing outward at Γ.

Now we are ready to give the variational formulation of (4.4), (4.5) and (4.6). Let v be an arbitrary function in $H^1(\Omega)$. Let $u \in L^2(0,T;H^1(\Omega))$ be $S_s, E_s, I_s, S_b, E_b, I_b, R_b$, and $f^u(\mathbf{u})$ be the component of $f(\mathbf{u})$ corresponding to u. Then from (4.4) we have

$$\partial_t u - \nabla \cdot (\Phi_u \nabla u) = f^u(\mathbf{u}). \tag{4.7}$$

Multiply equation (4.7) by v and integrate over Ω we obtain that

$$\int_\Omega \left(\partial_t u\, v - \nabla \cdot (\Phi_u \nabla u) v\right) \,\mathrm{d}x\,\mathrm{d}y = \int_\Omega f^u(\mathbf{u}) v \,\mathrm{d}x\,\mathrm{d}y.$$

Now applying divergence theorem and homogeneous Neumann boundary conditions (4.6), we arrive at

$$\frac{\mathrm{d}}{\mathrm{d}t}\int_\Omega uv \,\mathrm{d}x\,\mathrm{d}y + \int_\Omega (\Phi_u \nabla u) \cdot \nabla v \,\mathrm{d}x\,\mathrm{d}y = \int_\Omega f^u(\mathbf{u}) v \,\mathrm{d}x\,\mathrm{d}y \tag{4.8}$$

for every $v \in H^1(\Omega)$ with $u = S_s, E_s, I_s, S_b, E_b, I_b, R_b$.

Consequently our problem is reformulated as:

find a seven-component vector $\mathbf{u}(t, x, y)$ with each component in $L^2(0, T; H^1(\Omega))$, such that Equation (4.8) is satisfied for each $v \in H^1(\Omega)$ for the initial condition (4.5) and boundary condition (4.6).

Note that to ensure every integral in (4.8) is well-defined, we need to have Lipschitz continuous boundary for Ω, then by Sobolev embedding theorem, last term of (4.8) is well-defined since the integrand is the product of two $H^1(\Omega)$ functions hence it's in $L^2(\Omega)$.

4.5 Incorporating landscape features

In our previous simulations from Borchering *et al.* (2012), the diffusion coefficients were constant for the whole study area. In other words, we did not consider heterogeneities in diffusion coefficients caused by different landscape features. This leads to an evenly spreading, ring-like diffusion pattern that doesn't agree well qualitatively with real rabies cases data. As a result, in this chapter, we incorporate specific landscape features that can provide sufficient heterogeneities so that numerical simulation results could resemble patterns observed from real case data maps.

Two types of landscape features are incorporated here

(1) localized heterogeneities: here we choose major waterways to model and examine their effects;

(2) large-scale heterogeneities: lakes for example, but here we use human-populated cities, and assume that dispersals for terrestrial animals, in particular skunks, are restricted to be outside city limits.

4.5.1 Localized heterogeneities

By localized heterogeneities, we refer to certain landscape features that can cause local changes in diffusivity of terrestrial animals, in our case skunks. For example, in areas

covered with thick plants or other obstacles, we expect the movement of animals to be significantly reduced, i.e. diffusion constant is reduced. We can model these localized effects by incorporating the dependence of diffusion tensor matrices Ω_u on the spatial coordinates x, y.

We only consider rivers here that generate localized changes in diffusivity. Although rivers have width, it is relatively small compared with the dimensions of area of study. So we choose to model rivers as one-dimensional lines or curves, which also reduces computational burdens. For each point (x, y) on a river, we associate with it a pair of perpendicular unit directions, $e^{\perp}$ that is normal to the river and the other $e^{||}$ tangent to it. Diffusivity along the direction $e^{\perp}$ between the river and any point $(\bar{x}, \bar{y})$ that is within certain distance ϵ of the river is reduced according to the following function

$$h(D) = d_{low} + (d_{high} - d_{low}) \exp\left(\frac{D - \epsilon}{D}\right)$$

where $D \in [0, \epsilon]$ is the distance along the local normal direction $e^{\perp}$ from $(\bar{x}, \bar{y})$ to the river, and $d_{high},\ d_{low}$ are regular non-river diffusivity and low diffusivity value at the river.

Consequently, in coordinates spanned by unit directions $(e^{||}, e^{\perp})$ we obtain that, diffusivity tensor of any point within ϵ distance of the rivers is given by

$$\tilde{\Phi}_u = \begin{pmatrix} d_{high} & 0 \\ 0 & h(D) \end{pmatrix}$$

The above tensor is then converted back into Cartesian coordinates by rotation matrix R, ie

$$\Phi_u = R\, \tilde{\Phi}_u\, R^T$$

where $u = S_s, E_s, I_s, I_b$ and

$$R = \begin{pmatrix} \cos(\theta) & -\sin(\theta) \\ \sin(\theta) & \cos(\theta) \end{pmatrix}$$

with $\theta \in [-\frac{\pi}{2}, \frac{\pi}{2}]$ the angle between x direction and $e^{||}$.

4.5.2 *Large-scale heterogeneities*

City areas are human populated and usually very hostile to dispersing terrestrial animals. Densities of animals within city limits are extremely low and survivability is usually close to zero. As a result, after setting a two-dimensional city block within Ω, we can

(1) set birth rate of terrestrial animals (in this case skunks) to be low and death rate to be high;

(2) set diffusivity within city boundaries to be low.

Bats, on the other hand, usually don't have this restriction because of their airborne features.

4.6 Numerical scheme

We use finite element method to discretize spatial elements in numerical simulation to implement real landscape features, in particular waterways and city blocks. So far we have derived the variational formulation (4.8). To perform finite element approximation of solutions to (4.4) in the sense of (4.8), we still need to reformulate (4.8) in a finite element space, in our case, in a finite-dimensional piecewise continuous linear polynomial space $\mathscr{P}_1$ over a triangulation $\mathscr{T}_N$ that involves N vertices.

Consider a triangulation $\mathscr{T}_N$ of domain Ω. Assume also the mesh has N nodes. Suppose that the N-dimensional piecewise continuous linear polynomial space $\mathscr{P}_1$ has N basis functions $\{\phi_i\}_{i=1}^N$. Now each component u of solution $\mathbf{u}$ can be written as

$$u(t,x,y) = \sum_{j=1}^{N} u_j(t)\phi_j(x,y) \tag{4.9}$$

where $u = S_s, E_s, I_s, S_b, E_b, I_b, R_b$ is the name of corresponding class, and $\phi_j(x,y)$ are piecewise continuous linear polynomials that are equal to 1 on the j^{th} mesh node and 0 on the remaining nodes.

Now we can reformulate our problem as:

find a seven-component vector $\mathbf{u}(t, x, y)$ with each component in $L^2(0, T; \mathscr{P}_1)$, such that Equation (4.8) is satisfied for each $v \in \mathscr{P}_1$ for the initial condition (4.5) and boundary condition (4.6).

where it is understood that if $u \in L^2(0, T; \mathscr{P}_1)$ then

$$u(t) \in \mathscr{P}_1 \subset H^1(\Omega)$$

for each $t \in [0, T]$ and

$$\int_0^T \|u\|_{H^1}(t)\,\mathrm{d}t < \infty.$$

Now in (4.8), if we replace u by (4.9) and v by any basis function $\phi_k \in \mathscr{P}_1$, with $k = 1, \cdots, N$, we obtain that

$$\begin{aligned}
\frac{\mathrm{d}}{\mathrm{d}t}\int_\Omega u\phi_k\,\mathrm{d}x\,\mathrm{d}y &= \frac{\mathrm{d}}{\mathrm{d}t}\int_\Omega \left(\sum_{j=1}^N u_j(t)\phi_j\right)\phi_k\,\mathrm{d}x\,\mathrm{d}y \\
&= \sum_{j=1}^N \left(\int_\Omega \phi_j\phi_k\,\mathrm{d}x\,\mathrm{d}y\right)\frac{\mathrm{d}u_j(t)}{\mathrm{d}t}. \\
\int_\Omega (\Phi_u\nabla u)\cdot\nabla\phi_k\,\mathrm{d}x\,\mathrm{d}y &= \int_\Omega \left(\Phi_u\sum_{j=1}^N u_j(t)\nabla\phi_j\right)\cdot\nabla\phi_k\,\mathrm{d}x\,\mathrm{d}y \\
&= \int_\Omega \sum_{j=1}^N u_j(t)\,(\Phi_u\nabla\phi_j)\cdot\nabla\phi_k\,\mathrm{d}x\,\mathrm{d}y \\
&= \sum_{j=1}^N \left(\int_\Omega (\Phi_u\nabla\phi_j)\cdot\nabla\phi_k\,\mathrm{d}x\,\mathrm{d}y\right)u_j(t).
\end{aligned}$$

Let M be an $N \times N$ mass matrix where

$$M_{jk} = \int_\Omega \phi_j\phi_k\,\mathrm{d}x\,\mathrm{d}y$$

and $H(u)$ be an $N \times N$ matrix where

$$H_{jk}(u) = \int_\Omega (\Phi_u\nabla\phi_j)\cdot\nabla\phi_k\,\mathrm{d}x\,\mathrm{d}y$$

and $G(u)$ be an $N \times 1$ matrix where

$$(G)_k(u) = \int_\Omega f^u(\mathbf{u})\phi_k \,\mathrm{d}x\,\mathrm{d}y.$$

with $j, k = 1, \cdots, N$ and $u = S_s, E_s, I_s, S_b, E_b, I_b, R_b$.

The matrices M and $H(u)$ are respectively mass matrix and stiffness matrix. Now, for each u we have an ODE

$$M\frac{\mathrm{d}\mathbf{v}_u}{\mathrm{d}t} + H(u)\mathbf{v}_u = G(u) \tag{4.10}$$

with $\mathbf{v}_u = [u_1(t) \cdots u_N(t)]^T$. The initial condition for (4.10) depends on the continuous piecewise linear polynomial representation of $\mathbf{u}_0$.

The computation of $G(u)$ in (4.10) usually involves complicated quadrature rules, but for simplicity we are adopting the linear interpolation for $f^u(\mathbf{u})$

$$f^u(\mathbf{u}) \approx \sum_{j=1}^{N} f_j^u(\mathbf{u})\phi_j$$

where $f_j^u(\mathbf{u}) = f^u(\mathbf{u}(t, x_j, y_j))$ with $\phi_j(x_j, y_j) = 1$ and $t \in [0, T]$. Hence we have

$$\begin{aligned} G(u) &\approx \int_\Omega \left(\sum_{j=1}^{N} f_j^u(\mathbf{u})\phi_j\right)\phi_k \,\mathrm{d}x\,\mathrm{d}y \\ &= \sum_{j=1}^{N}\left(\int_\Omega \phi_j\phi_k \,\mathrm{d}x\,\mathrm{d}y\right) f_j^u(\mathbf{u}) \end{aligned}$$

If we denote $\mathbf{f}^u = [f_1^u(\mathbf{u})\, f_2^u(\mathbf{u}) \cdots f_N^u(\mathbf{u})]^T$, we can write the approximation of $G(u)$ as

$$G(u) \approx M\mathbf{f}^u$$

with $u = S_s, E_s, I_s, S_b, E_b, I_b, R_b$. As a result, the equation (4.10) now has a more computable version

$$M\frac{\mathrm{d}\mathbf{v}_u}{\mathrm{d}t} + H(u)\mathbf{v}_u = M\mathbf{f}^u \tag{4.11}$$

We refer to the Appendix for details of time advancement scheme as well as assembling mass and stiffness matrices.

4.7 Mesh generation

To generate a triangulation mesh we use the third-party mesh generation software *Netgen* that is available for free online. There are also many two or three-dimensional mesh generation softwares or tools out there, including MATLAB's built-in function *delaunay*, but we choose *Netgen* mainly for the convenience of its GUI from which it is relatively easy to manipulate mesh generation processes. To generate a two-dimensional triangulation mesh using *Netgen*, we need to define a geometry file with a suffix "in2d" that describes the basic geometry, such as regions and curves, of region of concern.

Before creating the geometry file we still need to identify the region of interest, geographic features we want to model, and the xy-coordinates of those points that describe these features. The region of interest is described in Figure 4.2. Then over the Texas river and county map, we use the software *ImageJ* to handpick those pixels that reflect geographic features of concern (see Figure 4.4).

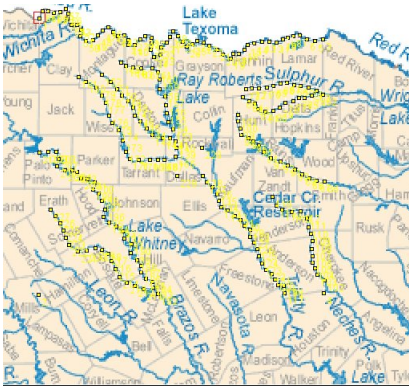

Figure 4.4: We selected major waterways and the city limits of Dallas (see the rectangular region in the center) as geographic features of concern. Selected pixels are highlighted in yellow.

We then specify in the geometry files the xy-coordinates of selected pixels and segments that mark important boundaries, i.e. waterways and city boundaries. With the help of

Netgen, we are able to draw the underlying geometry of the region to mesh, as seen from Figure 4.5.

Two subdomains, the city block in the center and the remaining region, are assigned in order to specify different parameter values for inside and outside the city. *Netgen* then generates a coarse triangulation that can be further refined, as seen in Figure 4.5.

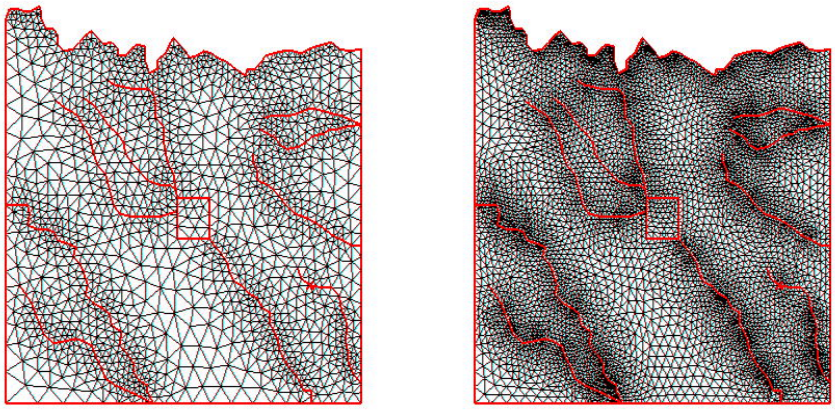

Figure 4.5: The bottom panels are snapshots of the coarse and refined triangulation meshes. The coarse mesh has 1616 vertices and 3072 triangular elements. The refined triangulation has 6303 vertices and 12288 triangular elements. Both meshes are overlapped with the underlying geometry in red lines.

4.8 Simulation results

We use the actual case data map to initialize the distribution of infectious skunks and bats. Gaussian distribution is used to initialize spatial distribution of infectious animals when regions with high population densities of infectious animals are highlighted. Density of exposed skunks is set as half as infectious skunk density. Susceptible, exposed and infectious skunk densities sum up to the carrying capacity of skunks. However since along rivers there are supposed to be no skunks, we initialize densities of every skunk classes as zero along rivers. Densities of exposed and recovered bats are set respectively as 1.5 and

0.5 of that of infectious bats. Susceptible bat density is initialized in ways similar to that of susceptible skunks, but there are no restrictions for bat densities with respect to rivers.

Initialization of infected skunks and infected bats can be viewed in Figures 4.6 and 4.7. Note that only great and moderate infection densities are indicated in the initialization.

We use a sufficiently refined triangulation mesh that has 24893 nodes and 49152 triangular elements. This mesh is generated from the refined mesh in Figure 4.5 using uniform refinement in *Netgen*.

Also to implement the effects of landscape features, we set the growth rate for susceptible skunks within city block as half the regular growth rate outside the city, and the death rate of exposed skunks to be twice the normal death rate outside the city. While modeling the effects of rivers on skunk diffusion, we set the threshold of distance from the river as 10 (km). In other words, if skunks are at locations within 10 (km) of any river we model here, their diffusion rate along the direction perpendicular to the river is reduced, the extent to which depends on the distance.

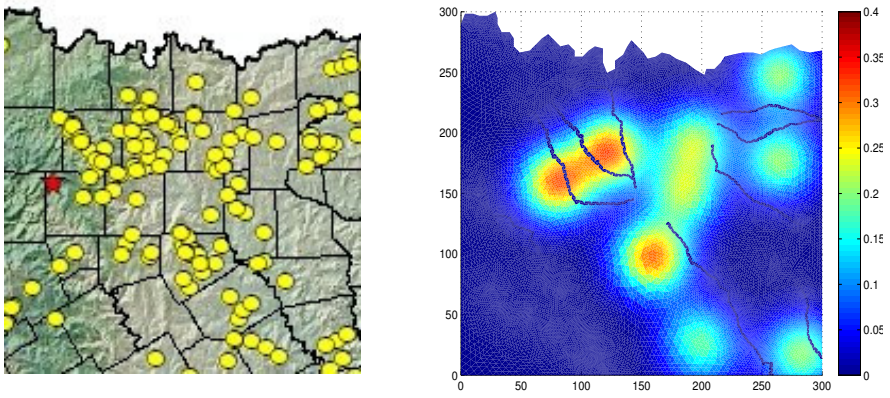

Figure 4.6: The left graph is the actual case map for infected skunks in 2007. Small yellow circles indicate one actual case of infected skunk. The right one is the initial condition for the finite element simulation and is the approximation of the left hand side graph. Notice the black curves in the right graph that correspond to rivers where there are no skunks.

We first run the simulation with the interaction between susceptible skunks and infected

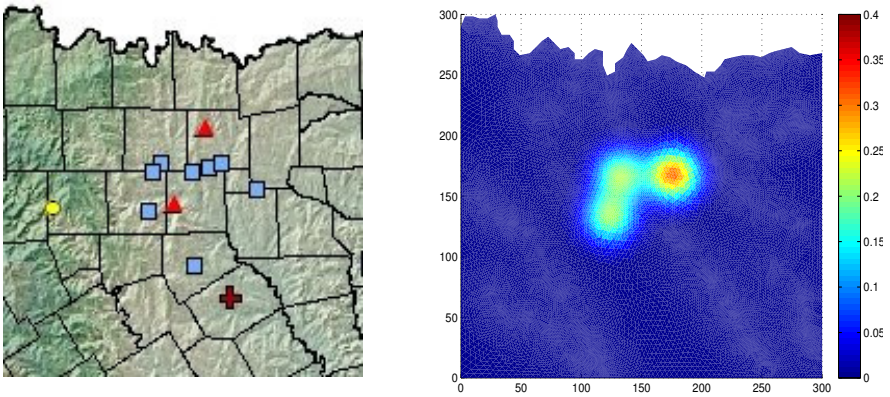

Figure 4.7: The left graph is the actual case map for infected bats in 2007. Small blue square means one actual case of infected bat. The right one is the initial condition for infected bats in the finite element simulation and is the approximation of the left hand side graph.

bats, which is represented by the infection term $\gamma S_s I_b$ with $\gamma \neq 0$. To see what effects this coupling term has on the spatial distribution of infectious skunks, we also run the simulation without interaction between susceptible skunks and infectious bats by setting $\gamma = 0$.

First we observe that both simulations with and without coupling term $\gamma S_s I_b$ generate distributions of infected skunks that roughly agree with the actual case maps, for both years 2008 and 2009. Compared with old simulation results in Figure 4.3, finite element approximation based on a triangulation mesh produces diffusion patterns that reflect natural effects of realistic landscape features, i.e. rivers and city blocks, unlike the evenly spreading diffusion pattern observed in previous simulation (Figure 4.3). Moreover, infectious skunk density within the city limit has been reduced thanks to increase in within-city skunk death rate and decrease in within-city skunk birth rate, while infectious skunks disperse mainly along rivers due to an implementation of diffusion .

Comparing the current simulation with and the one without interaction term, we can see that the simulation result for 2008 without interaction term produces a gap to the left of city block, which simulation with interaction term does a better job at covering. Compare

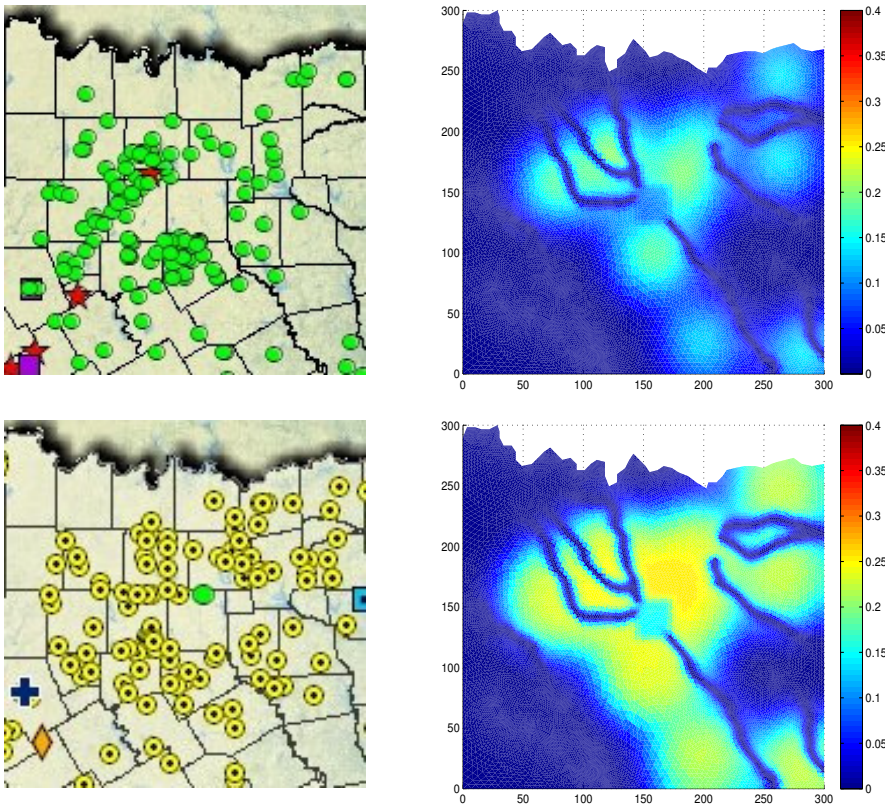

Figure 4.8: The graphs in the left panel are actual case maps for infected skunks in 2008 (small green circles) and 2009 (small yellow circles with center dots) from top to bottom. The graphs of the right panel reflect simulation results for densities of infected skunks in 2008 and 2009 (from top to bottom) with initial conditions specified as in Figure 4.6 and 4.7.

simulation results with the actual case map, qualitatively simulation with coupling term $\gamma S_s I_b$ is better than the one without the term.

4.9 Conclusion and Discussion

In this chapter, we use a simple spatial model that couples two rabies reservoir species with different manifestations of rabies infection, based on experimental evidence that bats, unlike skunks, are sometimes able to survive rabies infection (Turmelle *et al.*, 2010). Different from homogeneous spatial diffusion and constant parameters used in the system

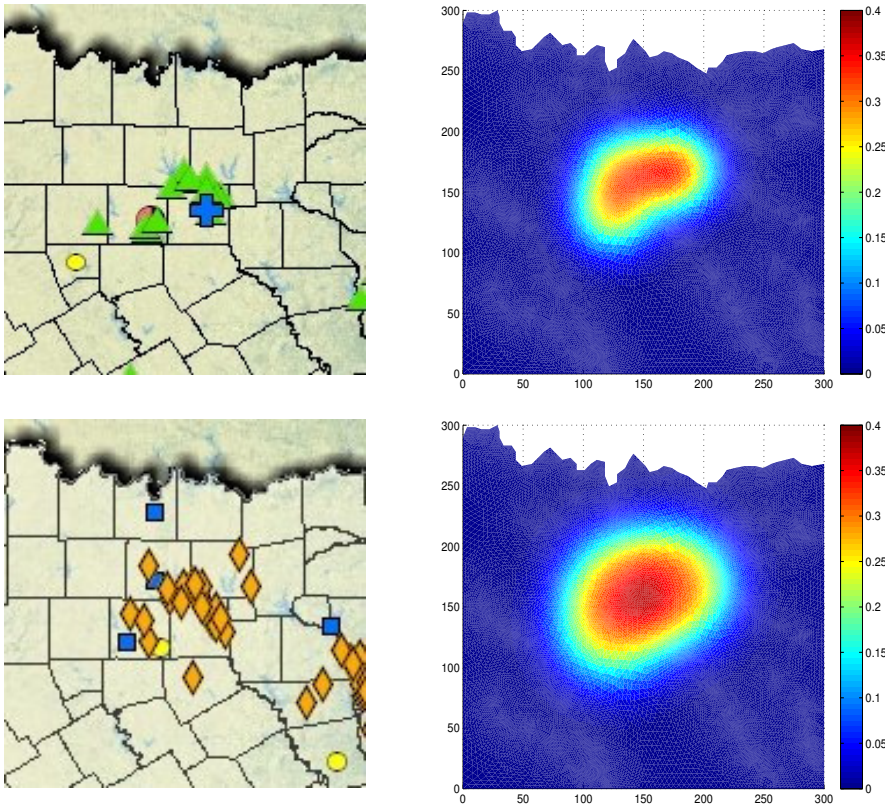

Figure 4.9: The graphs in the left panel are actual case maps for infected bats in 2008 (small green triangles) and 2009 (small yellow diamonds) from top to bottom. The graphs of the right panel reflect simulation results for density of infected bats in 2008 and 2009 (from top to bottom) with initial conditions specified as in Figure 4.6 and 4.7.

in Borchering *et al.* (2012), we implement in this chapter spatial heterogeneities by including rivers and city limits in finite element settings that enables the use of unstructured grids, which are more suited for representing complex geographical domain of interest. We demonstrate the effectiveness of such modeling method by illustrating a numerical simulation. This modeling approach proves to be more viable in reproducing, at least qualitatively, the skunk rabies case spatial spread in northeast Texas. This modeling tool has potential in terms of improvement in accuracy of prediction and description of landscape, so that public health resources such as rabies vaccines can be more accurately distributed.

Similar to Borchering *et al.* (2012), with finite element settings here, the coupled rabies

model for skunk here also produces better fit with the actual spatial distribution map for skunk rabies occurrences compared with the non-coupled version of the model. Hence the simulation results here also provide insights and support the possibility of spillover transmission of bat rabies virus to skunks. Although evidence exists that south central skunk rabies virus variant prevalent in Texas is strongly tied to bat rabies virus variant (Rupprecht *et al.*, 2011), admittedly little evidence corroborates the assumption of continuous dependence of skunk rabies enzootic cycles on those of bats (Pool and Hacker, 1982). Therefore, while we observe desired effects of the assumed weak continuous dependency, in effect it might still be weakened and instead be modeled by, for example, stochastic processes.

The surveillance, control and studies of zoonotic diseases are subject to the influence of sampling and reporting bias. In fact, the abundance of rabies case occurrences varies strongly with public awareness, human density and the availability of qualified reporting and processing infrastructures. In addition to our rabies model for skunk and bat interaction, other models cannot be ruled out that can produce qualitatively similar fit with the actual rabies case map for skunks. Also seasonality (Duke-Sylvester *et al.*, 2010) or other characteristics of bat and skunk ecology can potentially be important factors in spatial spread of rabies. In summary, although the finite element simulation of our model generates qualitatively good results, any suggestion or observations obtained should be considered preliminary.

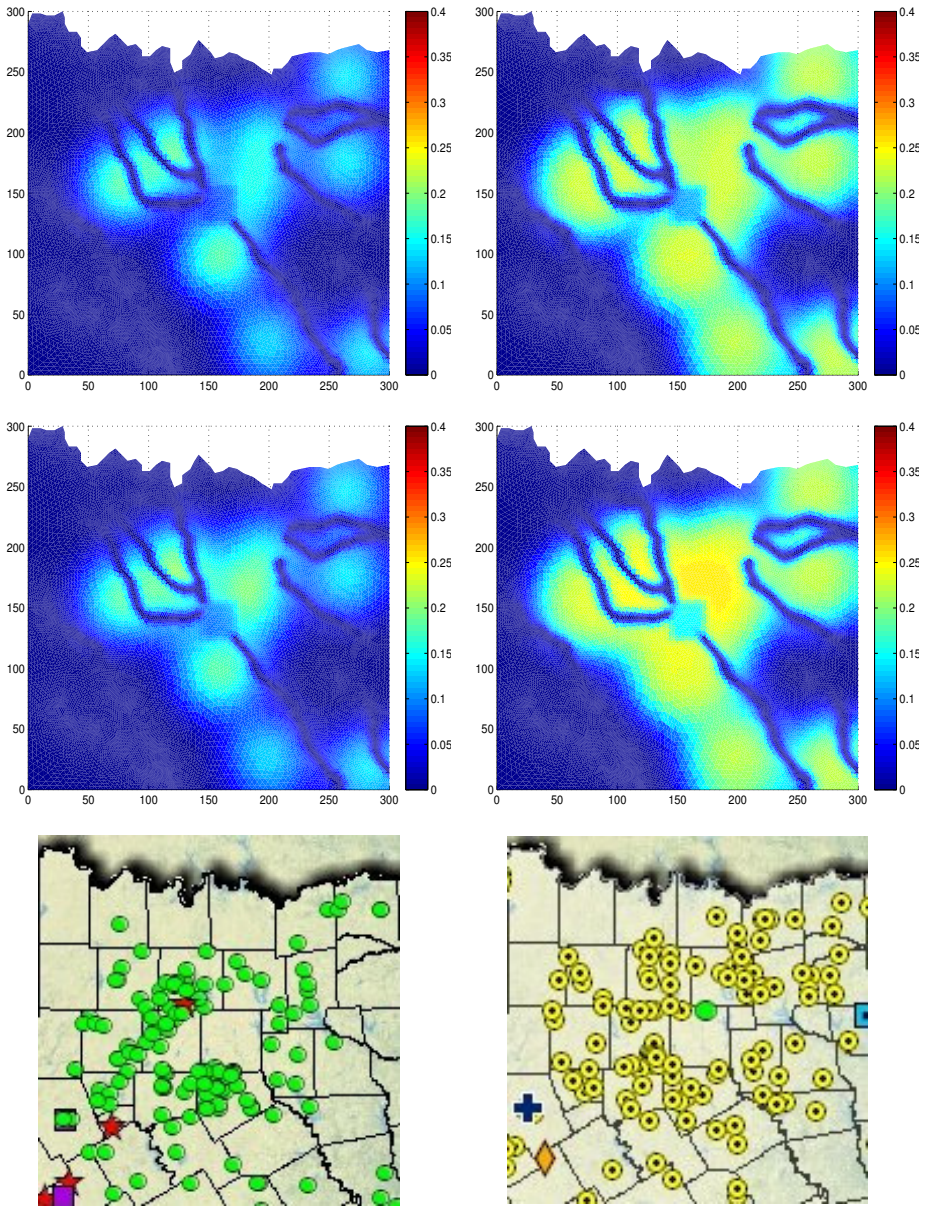

Figure 4.10: Panels on the left are for 2008 and those on the right side are for 2009. The first row corresponds to simulations without interaction between susceptible skunks and infected bats. The second row corresponds to simulations with interaction terms. All simulations have initial conditions specified as in Figure 4.6 and 4.7.

REFERENCES

(2011), URL `http://www.cdc.gov/rabies/`.

Allen, L., D. Flores, R. Ratnayake and J. Herbold, "Discrete-time deterministic and stochastic models for the spread of rabies", Applied Mathematics and Computation **132**, 271–292 (2002).

Anderson, R., H. Jackson, R. May and A. Smith, "Population dynamics of fox rabies in europe", Nature **289**, 765–771 (1981).

Anderson, R. and R. May, "Population biology of infectious diseases: Part 1", Nature **280**, 361–367 (1979).

Anderson, R. and R. May, "The population dynamics of microparasites and their invertebrate hosts", Philos. Trans. R. Soc. Lond. B Biol. Sci **291**, 451–524 (1981).

Andral, L., M. Artois, M. Aubert and J. Blancou, "Radio-tracking of rabid foxes", Comparative Immunology, Microbiology and Infectious Diseases **5**, 285–291 (1982).

Artois, M. and M. Aubert, "Structure des populations (age et sexe) de renards en zones indemné ou atteint de rage", Comparitive Immunology of Microbial Infectious Diseases **5**, 237–245 (1982).

Asano, E., L. Gross, S. Lenhart and L. Real, "Optimal control of vaccine distribution in a rabies metapopulation model", Mathematical Biosciences and Engineering **5**, 219 (2008).

Ayati, B. and T. Dupont, "Galerkin methods in age and space for a population model with nonlinear diffusion", SIAM J. Numer. Anal **40**, 3, 1064–1076 (2002).

Blair, W., "The biotic provinces of texas", Tex. J. Sci **2**, 97–117 (1950).

Borchering, R., H. Liu, M. Steinhaus, C. Gardner and Y. Kuang, "A simple spatiotemporal rabies model for skunk and bat interaction in northeast texas", Journal of Theoretical Biology **314**, 16–22 (2012).

Britton, M., "Spatial structures of periodic traveling waves in an integro-differential reaction-diffusion population model", SIAM J. Appl. Math **50**, 1663–1688 (1990).

Capasso, V., *Mathematical Structures of Epidemic Systems* (Springer, Verlag, 1991).

Chalton, K., G. Casey and J. Campbell, "Experimental rabies in skunks: immune response and salivary gland infection", Comparative Immunology, Microbiology and Infectious Diseases **10**, 3, 227–235 (1987).

Constantine, D. and D. Woodball, "Transmission experiments with bat rabies isolates: reactions of certain carnivora, opossum, rodents and bats to rabies virus of red bat origin when exposed by bat bite or by intramuscular inoculation.", Am. J. Vet. Res **27**, 116, 24–32 (1966).

Cusulin, C. and L. Gerardo-Giorda, "A numerical method for spatial diffusion in age-structured populations", Numer. Methods Partial Differential Equations **26**, 2, 253–273 (2010).

Diekmann, O., "Limiting behaviour in an epidemic model", Nonlinear Analysis **1**, 459–470 (1977).

Diekmann, O., "Threasholds and travelling waves for the geographical spread of infection", J. Math. Biol **6**, 109–130 (1978).

Dimitrov, D., T. Hallam, C. Rupprecht, A. Turmelle and G. McCracken, "Integrative models of bat rabies immunology, epizootiology and disease demography", Journal of Theoretical Biology **245**, 498–509 (2007).

Dimitrov, D. and A. King, "Modeling evolution and persistence of neurological viral diseases in wild populations", Mathematical Biosciences and Engineering **5**, 4, 729–741 (2008).

Ding, W., L. Gross, K. Langston, S. Lenhart and L. Real, "Rabies in raccoons: optimal control for a discrete time model on a spatial grid", Journal of Biological Dynamics **1**, 379–393 (2007).

Duke-Sylvester, S., L. Bolzoni and L. Real, *Strong seasonality produces spatial asynchrony in the outbreak of infectious diseases* (J. R. Soc. Interface, 2010).

Dunbar, S., "Traveling wave solutions of diffusive lotka-volterra equations: A heteroclinic connection in $\mathbb{R}^4$", American Mathematical Society **286**, 557–594 (1984).

Feng, Z. and H. Thieme, "Endemic models with arbitrarily distributed periods of infection i: Fundamental properties of the model", SIAM J. Appl. Math **61**, 803–833 (2000).

George, D., C. Webb, M. Farnsworth, T. O'Shea, R. Bowen, D. Smith, T. Stanley, L. Ellison and C. Rupprecht, "Host and viral ecology determine bat rabies seasonality and maintenance", Proceedings of the National Academy of Sciences USA **108**, 25, 10208–10213 (2011).

Gerardo-Giorda, L., "Balancing waveform relaxation for age-structured opulations in a multilayer environment", J. Numer. Math **16**, 281–306 (2008).

Gillespie, D., "Exact stochastic simulation of coupled chemical-reactions", J. Phys. Chem **81**, 2340–2361 (1977).

Gourley, S. and N. Britton, "A predator-prey reaction diffusion system with nonlocal effects", J. Math. Biol **34**, 297–333 (1996).

Gourley, S. and Y. Kuang, "A delay reaction-diffusion model of the spread of bacteriophage infection", SIAM. J. APPL. MATH **65**, 2, 550–566 (2005).

Gourley, S., R. Liu and J. Wu, "Spatiotemporal patterns of disease spread: Interaction of physiological structure, spatial movements, disease progression and human intervention", Strucutred Population Models in Biology and Epidemiology, Lecture Notes in Mathematics **1936**, 165–208 (2008).

Gourley, S., J. So and J. Wu, "Non-locality of reaction diffusion equations induced by delay: biological modeling and nonlinear dynamics", J. Math. Sci **124**, 5119–5153 (2004).

Gourley, S. and J. Wu, "Delayed nonlocal diffusive systems in biological invasion and disease spread", Nonlinear dynamics and evolution equations, Fields Instit. Commun **48**, 137–200 (2006).

Greenwood, R., "Population and movement characteristics of radio-controlled striped skunks in North Dakota during an epizootic of rabies", Journal of Wildlife Diseases **33**, 2, 226–241 (1997).

Gurtin, M. and R. MacCamy, "Non-linear age-dependent population dynamics", Arch. Rational Mech. Anal **54**, 281–300 (1974).

Gurtin, M. and R. MacCamy, *Population dynamics with age dependence* (Nonlinear Analysis and Mechanics: Heriot-Watt Symposium, Vol. III, : Pitman, London, 1979).

Hoppensteadt, F., "An age dependent epidemic model", J. Franklin Inst **297**, 325–333 (1974).

Jackiewicz, Z., H. Liu, B. Li and Y. Kuang, *Numerical simulations of traveling wave solutions in a drift paradox inspired diffusive delay population model* (Mathematics and Computers in Simulation, 2012).

Jackson, A., "Update on rabies", Research and Reports in Tropical Medicine **2**, 31–43 (2011).

Jackson, A. and W. Wunner, in "Rabies", (Academic Press, Chapter 1, 2002a).

Jackson, A. and W. Wunner, in "Rabies", pp. Chapter 4–5 (Academic Press, 2002b).

Jones, D., G. Röst, H. Smith and H. Thieme, "Spread of phage infection of bacteria in a petri dish", SIAM J. Applied Math **72**, 670–688 (2012).

Jones, D., H. Smith and H. Thieme, "Spread of viral infection of immobilized bacteria", Networks and Heterogeneous Media **8**, 327–342 (2013).

Kallen, A., P. Arcuri and J. Murray, "A simple model of spatial spread and control of rabies", J. Theor. Biol **116**, 377–393 (1985).

Kampen, N., *Stochastic processes in physics and chemistry* (Elsevier Science, Amsterdam, 2001).

Kaplan, C., "Rabies: A worldwide disease.", in "Population dynamics of rabies in wildlife", edited by P. Bacon (Academic Press, London, Orlando, 1985).

Keeling, M. and P. Rohani, *Moeling infectious disease in humans and animals* (U Press, Princeton, 2008).

Keller, J., L. Gerardo-Giorda and A. Veneziani, "Numerical simulation of a susceptible-exposed-infectious space-continuous model for the spread of rabies in raccoons across a realistic landscape", Journal of Biological Dynamics pp. 1–16 (2012).

Kermack, W. and A. McKendrick, "Contributions to the mathematical theory of epidemics. part i (1927)", Proc. Roy. Soc **115**, 271–288 (1927).

Kermack, W. and A. McKendrick, "Contributions to the mathematical theory of epidemics. part ii (1932)", Proc. Roy. Soc **138**, 55–85 (1932).

Kermack, W. and A. McKendrick, "Contributions to the mathematical theory of epidemics. part iii (1933)", Proc. Roy. Soc **141**, 94–122 (1933).

Kermack, W. and A. McKendrick, "Contributions to the mathematical theory of epidemics. part iv (1937)", J. Hyg., Camb. **37**, 172–187 (1937).

Kermack, W. and A. McKendrick, "Contributions to the mathematical theory of epidemics. part v (1939)", J. Hyg., Camb. **39**, 271–288 (1939).

Kim, M. and E. Park, "Characteristic finite element methods for diffusion epidemic models with age-structured populations", Comput. Math. Appl **97**, 55–70 (1998).

Krall, A., "On the real parts of zeros of exponential polynomials", Bulletin of the American Mathematical Society **70**, 291–292 (1964).

Lloyd, A., "Destabilization of epidemic models with the inclusion of realistic distributions of infectious periods", in "Proc. R. Soc. Lond. Series B: Biological Sciences", vol. 268, pp. 985–993 (2001a).

Lloyd, A., "Realistic distributions of infectious periods in epidemic models", Theor. Pop. Biol **60**, 59–71 (2001b).

Lyles, D. and C. Rupprecht, "Rhabdoviridae", in "Fields Virology", edited by M. Knipe and P. M. Howley, pp. 1364–1408 (Lippincott Williams and Wilkins, 5th ed, 2007).

MacDonald, D., *Rabies and wildlife: A biologisst's perspective* (Oxford University Press, 1980).

MacDonald, D., R. Bunce and P. Bacon, "Fox populations, habitat characterization and rabies control", J. Biogeogr **8**, 145–151 (1981).

MacInnes, C., R. Tinline, D. Voigt, L. Broekhoven and R. Rosatte, "Planning for rabies control in ontario", Rev. Infect. Dis **10**, 665–669 (1988).

Mager, K. and T. Nelson, "Roost-site selection by eastern red bats (Lasiurus borealis)", Am. Midl. Nat **145**, 120–126 (2000).

Metz, J. and O. Diekmann, in "The dynamics of physiologically structured populations", (Springer, New York, 1986).

Milner, F., "A numerical method for a model of population dynamics with spatial diffusion", Comp. Math. Appl **19**, 31, 31–43 (1990).

Mollison, D. and K. Kuulasmaa, "Spatial epidemic models: Theory and simulations", in "Population Dynamics of Rabies in Wildlife", pp. 291–309 (P. Bacon, ed, 1985).

Mollison, J., "The structure of epidemic models", Epidemic Models: their structure and relation to data pp. 17–33 (1995).

Murray, J., in "Mathematical Biology", (Springer-Verlag, New York Springer-Verlag, New York, 1989).

Murray, J., in "Mathematical Biology II: Spatial Models and Biomedical Applications", (Springer, Berlin, 2002).

Murray, J. and W. Seward, "On the spatial spread of rabies among foxes with immunity", Journal of Theoretical Biology **156**, 327–348 (1992).

Murray, J., E. Stanley and D. Brown, "On the spatial spread of rabies among foxes", Proceedings of the Royal society of London. Series B. Biological sciences **229**, 1255, 111–150 (1986).

Neilan, R. and S. Lenhart, "Optimal vaccine distribution in a spatiotemporal epidemic model with an application to rabies and raccoons", J. Math. Anal. Appl **378**, 603–619 (2011).

Ou, C. and J. Wu, "Spatial spread of rabies revisited: influence of age-dependent diffusion on nonlinear dynamics", SIAM J. Appl. Math **67**, 138–163 (2006).

Pool, G. and C. Hacker, "Geographic and seasonal distribution of rabies in skunks, foxes and bats in texas", Journal of Wildlife Diseases **18**, 4, 405–419 (1982).

Pozio, M., "Behavior of solutions of some abstract functional differential equations and application to predator-prey dynamics", Nonlinear Analysis **4**, 917–938 (1980).

Pozio, M., "Some conditions for global asymptotic stability of equilibra of integro-differential equations", J. Math. Anal. Appl **95**, 501–527 (1983).

Pybus, M., "Rabies and rabies control in striped skunks (Mephitis mephitis) in three prairie regions of Western North America", Journal of Wildlife Disease **24**, 3, 434–449 (1988).

Rass, L. and J. Radcliffe, "Math surverys monogr", in "Spatial Deterministic Epidemics", (American Mathematical Society, Providence, 2003).

Reddingius, J., "Notes on the mathematical theory of epidemics", Acta Biltheor **20**, 125–157 (1971).

Redlinger, R., "Existence theorems for semilinear parabolic systems with functionals", Nonlinear Anal **8**, 667–682 (1984).

Redlinger, R., "On volterra's population equation with diffusion", SIAM J. Math. Anal **16**, 135–142 (1985).

Ruan, S., "Spatial-temporal dynamics in nonlocal epidemiological models", in "Mathematics for Life Science and Medicine", edited by K. S. Y. Takeuchi and Y. Iwasa, pp. 97–122 (Springer, New York, 2007).

Rupprecht, C., J. Smith, M. Fekadu and J. Childs, "The ascension of wildlife rabies: a cause for public health concern or intervention?", Emerging Infectious Diseases **1**, 107–114 (1995).

Rupprecht, C., A. Turmelle and I. Kuzmin, "A perspective on lyssavirus emergence and perpetuation", Curr. Apin. Virol **1**, 662–670 (2011).

Russel, C., L. Real and D. Smith, "Spatial control of rabies on heterogeneous landscapes", PLoS ONE (2006).

Russel, C., D. Smith, L. Waller, J. Childs and L. Real, "A priori prediction of disease invasion dynamics in a novel environment", No. 1534, pp. 21–25 (The Royal Society, 2004).

Saunders, D., *Adirondack mammals* (Syracuse University Pr(Sd), 1988).

Schmidly, D., *The mammals of Texas* (University of Texas Press., Austin, TX, 1994), revised edn.

Schwartz, C. and E. Schwartz, in "The wildlife mammals of Missouri", pp. 90–91 (University of Missouri, 2002).

Shigesada, N. and K. Kawasaki, in "Biological Invasions: Theory and Practice", (Oxford University Press, Oxford, 1997).

Smith, D., B. Lucey, L. Waller, J. Childs and L. Real, "Predicting the spatial dynamics of rabies epidemics on heterogeneous landscapes", Proc. Natl. Acad. Sci. USA **99**, 6, 3668–3672 (2002).

Smith, D., L. Waller, C. Russell, J. Childs and L. Real, "Assessing the role of long-distance translocation and spatial heterogeneity in the raccoon rabies epidemic in connecticut", Prev. Vet. Med **71**, 225–240 (2005).

Smith, G. and S. Harris, "Rabies in urban foxes textitVulpes vulpes in britain: the use of a spatial stochastic simulation model to examine the pattern of spread and evaluate the efficacy of different control regimes", Vulpes vulpes pp. 450–479 (1991).

Smith, H., "Models of virulent phage growth with application to phage therapy", SIAM. J. Appl. Math **68**, 6, 1717–1737 (2008).

Smith, H. and H. Thieme, "Strongly order preserving semiflows generated by functional differential equations", J. Diff. Eqns **93**, 332–363 (1991).

So, J.-H., J. Wu and X. Zou, "A reaction-diffusion model for a single species with age structure, i. travelling wavefronts on unbounded domains", Proc. Roy. Soc. London Ser. A **457**, 1841–1853 (2001).

Stark, K., G. Regula, J. Hernandez, L. Knopf, K. Fuchs, R. Morris and P. Davies, "Concepts for risk-based surveillance in the field of veterinary medicine and veterinary public health:review of current approaches", BMC Health Services Research **6**, 1–8 (2006).

Sterner, R. and G. Smith, "Modeling wildlife rabies: Transmission, economics and conservation", Biological conservation **131**, 163–179 (2006).

Thieme, H., "A model for the spatial spread of an epidemic", J. Math. Biology **4**, 337–351 (1977).

Thieme, H., "Asymptotic estimates of the solutions of nonlinear integral equations and asymptotic speeds for the spread of populations", J. Reine Angew **306**, 94–121 (1979).

Thieme, H. and C. Castillo-Chavez, "On the role of variable infectivity in the dynamics of the human immunodeficiency virus epidemic", in "Mathematical and Statistical Approaches to AIDS Epidemiology, Lecture Notes in Biomath", edited by C. Castillo-Chavez, pp. 157–176 (Springer-Verlag, Berlin, Berlin, 1989).

Thieme, H. and C. Castillo-Chavez, "How many infection-age-dependent infectivity affect the dynamics of hiv/aids?", SIAM J. Appl. Math **53**, 5, 1447–1479 (1993).

Thieme, H. and X.-Q. Zhao, "A nonlocal and delayed predator-prey reaction-diffusion model", Nonlinear Analysis RWA **2**, 145–160 (2001).

Thieme, H. and X.-Q. Zhao, "Asymptotic speeds of spread and traveling waves for integral equations and delayed reaction-diffusion models", JDE **195**, 430–470 (2003).

Turmelle, A., F. Jackson, D. Green, G. McCracken and C. Rupprecht, "Host immunity to repeated rabies virus infection in big brown bats", Journal of Virology **91**, 2360–2366 (2010).

Voigt, D., R. Tinline and L. Broekhoven, "A spatial simulation model for rabies control", Popul. Dyn. Rabies Wildl pp. 311–349 (1985).

Volpert, A., V. Volpert and V. Volpert, *Traveling wave solutions of parabolic systems, Monographs* (AMS Providence, 1994).

Wade-Smith, J. and B. Verts, "Mephitis mephitis", Mammalian Species **173**, 1–7 (1982).

Webb, G., "An age-dependent epidemic model with spatial diffusion", Archive for Rational Mechanics and Analysis **75**, 91–102 (1980).

Webb, G., "Population models structured by age, size and spatial position", Lecture Notes in Mathematics **1936**, 1–49 (2008).

Wu, J. and X. Zou, "Travelling wave fronts of reaction-diffusion systems with delay", J. Dynam. Differential Equations **13**, 651–687 (2001).

Yamada, Y., "Asymptotic stability for some systems of semilinear voltera diffusion equations", J. Diff. Eqns **52**, 295–326 (1984).

APPENDIX A

NUMERICAL METHODS

A.1 Numerical methods for (2.38)

First we truncate $\mathbb{R}$ to $[-M, M]$ with $M > 0$ sufficiently large. Discretize this bounded domain with $L = 2N + 1$ points to get an equally spaced grid

$$-M = z_1 < z_2 < \cdots < z_{N+1} = 0 < z_{N+2} < \cdots < z_{2N} < z_{2N+1} = M$$

with the uniform step size

$$h = \frac{2M}{2N} = \frac{M}{N}.$$

Now we denote

$$S_j = S(z_j),\ E_j = E(z_j),\ I_j = I(z_j)$$

with $j = 1, \cdots, L$.

In our simulations we let $M = 100$ and $N = 1000$.

Using backward Euler in time and central difference in space, in other words this scheme being second order accurate both in time and space, the equations in (2.38) now becomes

$$S_1 - 1 = 0,\ S_L - S^* = 0,\ E_1 = 0,\ E_L - E^* = 0,\ I_1 = 0,\ I_L - I^* = 0$$

and for $j = 2, \cdots, L-1$

$$(-v + rh)\, S_j + vS_{j-1} - \frac{rh}{K} S_j^2 - \beta h S_j I_j = 0,$$

$$D_2 E_{j+1} - \left(2D_2 + vh + (b+\sigma)h^2\right) E_j + (D_2 + vh) E_{j-1} + \beta h^2 S_j I_j = 0$$

$$D_1 I_{j+1} - (2D_1 + vh + \mu h^2) I_j + (D_1 + vh) I_{j-1} + \sigma h^2 E_j = 0.$$

The above algebraic equations can be readily solved by MATLAB implementation of Newton method.

A.2 Numerical methods for (2.39)

We make a change of variable

$$\tilde{y} = y - x + z - vT.$$

Dropping tildes (2.39) becomes

$$\begin{aligned} vS' &= rS\left(1 - \frac{S}{K}\right) - \beta SI \\ vI' &= D_1\, I'' - \mu I + \beta e^{-bT} \int_{\mathbb{R}} S(y) I(y) \frac{e^{-\frac{(y-z+vT)^2}{4D_2 T}}}{2\sqrt{\pi D_2 T}}\, \mathrm{d}y \end{aligned} \tag{A.1}$$

equipped by asymptotic boundary conditions

$$S(-\infty) = K,\ I(-\infty) = 0,\ S(+\infty) = \hat{S},\ I(+\infty) = \hat{I}$$

where $\hat{S}, \hat{I}$ are defined in (2.27).

Now we can truncate the one-dimensional domain $(-\infty, \infty)$ to $[-M, M]$ with $M > 0$ sufficiently large. Notice that the integral contains the probability density function of a normal distribution. For simplicity we define

$$p(x, a_1, a_2) = \frac{1}{\sqrt{2\pi}a_2} e^{-\frac{(x-a_1)^2}{2a_2^2}} \tag{A.2}$$

to be the normal distribution probability density function with mean $a_1 > 0$ and standard deviation $a_2 > 0$ evaluated at x. This function is defined as a built-in routine normpdf in MATLAB.

The asymptotic boundary condition can be applied to the truncation so that

$$\int_{\mathbb{R}} S(y)I(y)\frac{e^{-\frac{(y-z+vT)^2}{4D_2T}}}{2\sqrt{\pi D_2 T}}\,\mathrm{d}y$$

$$= \int_{\mathbb{R}} S(y)I(y)p(y-z+vT, 0, \sqrt{2D_2T})\,\mathrm{d}y$$

$$\approx \int_{-M}^{M} S(y)I(y)p(y-z+vT, 0, \sqrt{2D_2T})\,\mathrm{d}y + \int_{M}^{\infty} S(y)I(y)p(y-z+vT, 0, \sqrt{2D_2T})\,\mathrm{d}y$$

$$\approx \underbrace{\int_{-M}^{M} S(y)I(y)p(y-z+vT, 0, \sqrt{2D_2T})\,\mathrm{d}y}_{H_1} + S(M)I(M)\underbrace{\int_{M}^{\infty} p(y-z+vT, 0, \sqrt{2D_2T})\,\mathrm{d}y}_{H_2}$$

because when M is sufficiently large $I = 0$.

Note that H_2 can be found using normcdf built-in function in MATLAB.

Discretize $[-M, M]$ with $L = 2N + 1$ equally spaced points so that

$$-M = z_1 < z_2 < \cdots < z_{N+1} = 0 < z_{N+2} < \cdots < z_{2N} < z_{2N+1} = M.$$

The uniform step size

$$h = \frac{2M}{2N} = \frac{M}{N}.$$

We also denote $S(z_j), I(z_j)$ as S_j, I_j with $j = 1, \cdots, L$. In our simulations we let $M = 200$ and $N = 2000$.

With the above discretization, we can obtain an approximation of H_2 using the composite Simpson's rule. Hence

$$H_1 \approx \frac{h}{3}\Bigg[S_1 I_1 p(z_1 - z + vT, 0, \sqrt{2D_2T}) + 4\sum_{k=1}^{N} S_{2k}I_{2k}p(z_{2k} - z + vT, 0, \sqrt{2D_2T})$$

$$+2\sum_{k=1}^{N-1} S_{2k+1}I_{2k+1}p(z_{2k+1} - z + vT, 0, \sqrt{2D_2T}) + S_{2N+1}I_{2N+1}p(z_{2N+1} - z + vT, 0, \sqrt{2D_2T})\Bigg]$$

For convenience we denote

$$P_{ij} = p(z_i - z_j + vT, 0, \sqrt{2D_2T}) \qquad g_j = \int_M^\infty p(y - z_j + vT, 0, \sqrt{2D_2T})\,\mathrm{d}y.$$

If we use backward Euler in time and central difference in space, i.e. second order accurate in both time and space, at each z_j, with $j = 2, \cdots, L-1$, then

$$v\frac{S_j - S_{j-1}}{h} = rS_j\left(1 - \frac{S_j}{K}\right) - \beta S_j I_j$$

$$v\frac{I_j - I_{j-1}}{h} = D_1\frac{I_{j+1} - 2I_j + I_{j-1}}{h^2}$$

$$+ \frac{\beta e^{-bT}h}{3}\left[S_1I_1P_{1j} + 4\sum_{k=1}^{N} S_{2k}I_{2k}P_{2k,j} + 2\sum_{k=1}^{N-1} S_{2k+1}I_{2k+1}P_{2k+1,j} + S_{2N+1}I_{2N+1}g_j\right]$$

Combined with the asymptotic boundary condition, we have the following equations

$$S_1 - K = 0, \quad S_L - \hat{S} = 0$$

$$(rh - v)S_j + vS_{j-1} - \frac{rh}{K}S_j^2 - \beta h S_j I_j = 0$$

$$I_1 = 0, \quad I_L - \hat{I} = 0$$

$$D_1I_{j+1} - (2D_1 + vh + \mu h^2)I_j + (D_1 + vh)I_{j-1}$$

$$+ \frac{\beta e^{-bT}h^3}{3}\left[S_1I_1P_{1j} + 4\sum_{k=1}^{N} S_{2k}I_{2k}P_{2k,j} + 2\sum_{k=1}^{N-1} S_{2k+1}I_{2k+1}P_{2k+1,j} + S_{2N+1}I_{2N+1}g_j\right]$$

with $j = 2, \cdots, L-1$.

Solving these algebraic equations give a numerical solution of (2.39) if $v > 0$ is provided.

Let

$$u = [S_1\ S_2 \cdots S_L\ I_1\ I_2 \cdots I_L]^T$$

where $u_j = S_j$ if $j = 1, \cdots, L$ and $u_j = I_{j-L}$ if $j = L+1, \cdots, 2L$.

Denote the above algebraic system as

$$F(u) = 0.$$

To solve this system of nonlinear algebraic system of equations, we use Newton method. The exact expression of the $2L \times 2L$ Jacobian matrix J is readily obtained. We attempt to solve the system with its solution close to the initial condition

$$S_j = K, I_j = 0 \quad j = 1, 2, \cdots, L$$

$$S_j = \hat{S}, I_j = \hat{I} \quad j = L+1, \cdots, 2L.$$

Classical Newton method results in

$$u_{k+1} = u_k - J_k^{-1} F(u_k)$$

for the k^{th} iteration, where J_k is the Jacobian matrix evaluated at u_k.

Simple implementation of classical Newton method quickly gives singular Jacobian matrices and increasing oscillations that both lead to blowup in numerical solutions. This is because the system

$$J_k \Delta_k = F(u_k)$$

where Δ_k is the Newton step, cannot produce accurate solutions when J_k is badly conditioned. However, we may modify this method using

$$(J_k^T J_k + \lambda_k I)\tilde{\Delta}_k = J_k^T F(u_k).$$

Although $J_k^T J_k$ is singular, the above system is non-singular provided $\lambda_k > 0$. Hence the Newton step $\tilde{\Delta}_k$ is always well defined if $\lambda_k > 0$ is appropriately chosen.

In our case, λ_k is chosen to be 1×10^{-6} uniformly for all k by trial and error.

A.3 Numerical methods for (2.1)

We truncate the one-dimensional spatial domain $(-\infty, \infty)$ to $[-M, M]$ with M sufficiently large. We discretize $[-M, M]$ into $L = 2N + 1$ equally spaced grid points. Let

$$-M = x_1 < x_2 < \cdots < x_{N+1} = 0 < x_{N+2} < \cdots < x_L = M.$$

For our simulations, we chose $M = 100, N = 1000$.

Let $S_j(t), E_j(t), I_j(t)$ be numerical approximations respectively for susceptible, incubating and infectious animal population densities at location x_j and time $t > 0$ with $j = 1, \cdots, L$.

With central difference for spatial derivatives, i.e. second order accurate in space, we arrive at discretized version of (2.1)

$$\begin{aligned}
S_j' &= rS_j\left(1 - \tfrac{S_j}{K}\right) - \beta S_j I_j \\
E_j' &= \beta S_j I_j - (b + \sigma)E_j + D_2 \tfrac{E_{j+1} - 2E_j + E_{j-1}}{h^2} \\
I_j' &= \sigma E_j - \mu I_j + D_1 \tfrac{I_{j+1} - 2I_j + I_{j-1}}{h^2}
\end{aligned}$$

with $j = 1, \cdots L$ and initial conditions

$$S_j(0) = S^\circ(x_j), \quad E_j(0) = E^\circ(x_j), \quad I^\circ(0) = I_0(x_j)$$

and, for convenience, homogeneous Neumann boundary conditions, which results in

$$S_0 = S_2,\ S_{L+1} = S_{L-1},\ E_0 = E_2,\ E_{L+1} = E_{L-1},\ I_0 = I_2,\ I_{L+1} = I_{L-1}$$

where variables with subscripts $0, L + 1$ are set up as "ghost points" to implement homogeneous boundary conditions.

To advance the discretized system in time, we use embedded pair of continuous Runge-Kutta method of order 4 and discrete Runge-Kutta method of order 3 which is used to estimate errors. See Jackiewicz *et al.* (2012) for an implementation example of this method in an epidemiological model.

For our model, we use the following initial conditions

$$\begin{aligned} &S^\circ(x_j) = K,\ E^\circ(x_j) = 0,\ I^\circ(x_j) = 0 \qquad j = 1, \cdots, N \\ &S^\circ(x_j) = S^*,\ E^\circ(x_j) = E^*,\ I^\circ(x_j) = I^*, \quad j = N+1, \cdots, L \end{aligned}$$

where $S^*,\ E^*,\ I^*$ are defined in (2.7).

A.4 Numerical methods for (2.6)

Notice that the derivation of (2.6) clearly indicates that we can rewrite it as the following system without non-local terms

$$\begin{aligned} &\frac{\partial S}{\partial t} = rS\left(1 - \frac{S}{K}\right) - \beta SI \\ &\frac{\partial I}{\partial t} = -\mu I + D_1 \frac{\partial^2 I}{\partial x^2} + p(x,t,T) \\ &\frac{\partial p}{\partial t} + \frac{\partial p}{\partial a} = D_2 \frac{\partial^2 p}{\partial x^2} - bp \\ &S(x,t) = S^\circ(x,t), \qquad t \in [-\tau, 0] \\ &I(x,t) = I^\circ(x,t), \qquad t \in [-\tau, 0] \\ &p(x,t,0) = \beta S(x,t) I(x,t) \end{aligned} \tag{A.3}$$

where the original non-local integral term in (2.6) has been replaced by the solution of $p(x,t,s)$ with $s = T$.

Now if we let $u(x,t,s) = p(x, t-T+s, s)$. Then for a fixed time $t > 0$

$$\begin{aligned} \frac{\partial u}{\partial s} &= \left(\frac{\partial p}{\partial t} + \frac{\partial p}{\partial a}\right)\Big|_{a=s, t=t-T+s} \\ &= D_2 \frac{\partial^2 p}{\partial x^2} - bp \\ &= D_2 \frac{\partial^2 u}{\partial x^2} - bu \end{aligned}$$

with

$$u(x,t,0) = p(x, t-T, 0) = \beta S(x, t-T) I(x, t-T).$$

Now we can rewrite again the system (A.3) as

$$\begin{aligned}
&\frac{\partial S}{\partial t} = rS\left(1-\frac{S}{K}\right) - \beta SI \\
&\frac{\partial I}{\partial t} = -\mu I + D_1\frac{\partial^2 I}{\partial x^2} + u(x,t,s)|_{s=T} \\
&\frac{\partial u}{\partial s} = D_2\frac{\partial^2 u}{\partial x^2} - bu \\
&S(x,t) = S^\circ(x,t), \qquad t \in [-\tau, 0] \\
&I(x,t) = I^\circ(x,t), \qquad t \in [-\tau, 0] \\
&u(x,t,0) = \beta S(x,t-T)I(x,t-T).
\end{aligned} \tag{A.4}$$

System (A.4) is easier to solve than (A.3) because u equation is a reaction diffusion one that is relatively easy to implement, given that we consider a fixed time t.

Then we truncate the one-dimensional domain $(-\infty, \infty)$ to $[-M, M]$ with M sufficiently large. Let

$$-M = x_1 < x_2 < \cdots < x_{N+1} = 0 < x_{N+2} < \cdots < x_{2N} < x_{2N+1} = M.$$

There are $L = 2N + 1$ grid points and $2N$ intervals. Let $h = \frac{2M}{2N} = \frac{M}{N}$ be the spatial step size.

In our simulation, we choose $M = 100, N = 1000$.

Now let $S_j(t), I_j(t), u_j(t,s)$ be approximation of S, I, u at x_j at time $t > 0, s \in [0, T]$. Let the termination time be tf. We discretize the simulation time interval so that the time step size Δt satisfies

$$\frac{T}{\Delta t} = B$$

where B is an integer. Here we choose $tf = 20, B = 40$.

Let the simulation time interval be discretized as

$$0 = t_1 < t_2 < \cdots t_{P+1} = tf$$

where $t_j = (j-1)\Delta t$ with $j = 1, \cdots, P+1$.

Now central difference for spatial derivatives in (A.4) yields

$$\begin{aligned}
&S_j' = rS_j\left(1-\frac{S_j}{K}\right) - \beta S_j I_j \\
&I_j' = -\mu I_j + D_1\frac{I_{j+1} - 2I_j + I_{j-1}}{h^2} + u_j(t,T) \\
&u_j'(t,s) = D_2\frac{u_{j+1}(t,s) - 2u_j(t,s) + u_{j-1}(t,s)}{h^2} - bu_j(t,s), \quad s \in [0,T] \\
&u_j(t,0) = \beta S_j(t-T)I_j(t-T) \\
&S_j(s) = S^\circ(x_j,s),\ I_j(s) = I^\circ(x_j,s), \quad s \in [-T, 0]
\end{aligned} \tag{A.5}$$

for $j = 1, 2, \cdots, L$.

For ease of simulation we equip the system (A.4) with the homogeneous Neumann boundary conditions. This implies that

$$S_0 = S_2,\ S_{L+1} = S_{L-1},\ I_0 = I_2,\ I_{L+1} = I_{L-1},\ I_0 = S_2,\ I_{L+1} = I_{L-1}.$$

To advance in time, we use the embedded pair of continuous Runge-Kutta method of order 4 and discrete Runge-Kutta method of order 3 which is used for local error estimation. See Jackiewicz *et al.* (2012) for a recent implementation example of this method.

Now we are ready to iteratively solve system (A.4). For $j = 1, \cdots, L$ and $k = 1, \cdots, P$. First we initialize $u_j(t_k, 0)$ using $S_j(t_k - T)$ and $I_j(t_k - T)$. Then numerically solving u equation in (A.5) yields $u_j(t_k, T)$. Subsequently we can use $u_j(t_k, T)$ to solve for $S_j(t_{k+1})$ and $I_j(t_{k+1})$.

Since T is an integer multiple of Δt, for any t_k with $k = 1, \cdots, P$, we can always find numerical approximation of $S_j(t_k - T)$ and $I_j(t_k - T)$ for $j = 1, \cdots, L$. In the case of $t_k - T \leq 0$, they are determined by the initial conditions for S, I.

For simplicity in simulations we let the initial conditions be

$$S_j = K,\ j = 1, \cdots, N \quad S_j = \hat{S},\ j = N+1, \cdots, L$$

$$I_j = 0,\ j = 1, \cdots, N \quad I_j = \hat{I},\ j = N+1, \cdots, L$$

where $\hat{S}, \hat{I}$ are defined in (2.27).

A.5 Implementation details for (4.11)

A.5.1 Time advancement

To solve the ODE for $\mathbf{v}_u$ we still need to apply some numerical scheme to advance it in time. To do that we first discretize the time interval $[0, T]$ into L subintervals of equal length $\Delta t = \frac{T}{L}$. So now we want to advance (4.11) from t_n to t_{n+1} with

$$t_n = n\Delta t = n\frac{T}{L}$$

where $n = 0, 1, \cdots, L-1$. Also let

$$\mathbf{v}_u^n = [u_1^n\, u_2^n\, \cdots\, u_N^n]^T$$

where $u_j^n = u_j(t_n)$ and $j = 1, \cdots, N$.

Now we can discretize the time derivative in (4.11) at $t = t_n$ by

$$\frac{\mathrm{d}\mathbf{v}_u}{\mathrm{d}t}(t_n) \approx \frac{\mathbf{v}_u^n - \mathbf{v}_u^{n-1}}{\Delta t}$$

Since the right hand side of (4.11) involves nonlinearity when computing $\mathbf{f}^u$ at $t = t_n$, it will cause great computational complexity if we use complete implicit schemes to advance (4.11) in time. So as an alternative, we opt to use a implicit-explicit scheme that uses backward Euler approximation of time derivative, as indicated above, and is implicit at the term correpsonding to the diffusion operator but explicit on the right hand side.

Now equation (4.11) becomes

$$M\frac{\mathbf{v}_u^n - \mathbf{v}_u^{n-1}}{\Delta t} + H(u)\mathbf{v}_u^n = M\mathbf{f}^{u,n-1} \tag{A.6}$$

where

$$\mathbf{f}^{u,n} = [f^u(\mathbf{u}^n(x_1, y_1))\, f^u(\mathbf{u}^n(x_2, y_2)) \cdots f^u(\mathbf{u}^n(x_N, y_N))]^T$$

where $\mathbf{u}^n(x_j, y_j)$ is an approximation of $\mathbf{u}(t_n, x_j, y_j)$ with $n = 1, \cdots, L$, and $j = 1, \cdots, N$.

It follows from (A.6) that to compute $\mathbf{v}_u^n$ for all $u = S_s, E_s, I_s, S_b, E_b, I_b, R_b$ we should take these steps

(1) let $i = 0$. For $t_0 = 0$ use (4.5) to initialize $\mathbf{v}_u^0$ and $\mathbf{f}^{u,0}$ for all $u = S_s, E_s, I_s, S_b, E_b, I_b, R_b$

(2) if $i = L$ go to step 5 otherwise go to step (3)

(3) solve for $\mathbf{v}_u^{i+1}$ in the equation

$$(M + H(u)\Delta t)\, \mathbf{v}_u^{i+1} = M\left(\Delta t\, \mathbf{f}^{u,i} + \mathbf{v}_u^i\right) \tag{A.7}$$

for all $u = S_s, E_s, I_s, S_b, E_b, I_b, R_b$

(4) add i by 1 and go to step (2)

(5) visualize $\mathbf{v}_u^L$ for all u

Now that we have derived a numerical scheme in the finite element method framework, what is left is to establish an appropriate triangulation mesh $\mathscr{T}_N$, find the set of basis functions $\{\phi_i\}_{i=1}^N$ for the piecewise continuous linear polynomial space $\mathscr{P}_1$ over $\mathscr{T}_N$, compute matrices M and $H(u)$ for all $u = S_s, E_s, I_s, S_b, E_b, I_b, R_b$, perform simulations and display simulation results.

A.5.2 Assembling mass and stiffness matrices

Now we have generated a triangulation $\mathscr{T}_N$ that consists of N nodes $\{(x_i, y_i)\}_{i=1}^N$ and L triangular elements $\{K_i\}_{i=1}^L$. The piecewise continuous linear polynomial space $\mathscr{P}_1$ over $\mathscr{T}_N$ has N basis functions $\{\phi_i\}_{i=1}^N$ such that

$$\phi_i(x_j, y_j) = \begin{cases} 1 & i = j \\ 0 & i \neq j \end{cases}$$

Let's see first what exactly these basis functions are. Consider a node (x_i, y_i) and its corresponding basis function $\phi_i(x, y) \in \mathscr{P}_1$. Since $\mathscr{P}_1$ is piecewise continuous linear polynomial space, every function f in this space can be defined as

$$f = a_1 x + a_2 y + a_3$$

over any triangular element with a_1, a_2, a_3 constant.

Consider again a triangular element K that has a vertex at (x_i, y_i). Let the other two vertices be (x_{i-1}, y_{i-1}) and (x_{i+1}, y_{i+1}). We want to find the expression of ϕ_i defined over K. Suppose that

$$\phi_i = a_1 x + a_2 y + a_3.$$

Then it follows from the definition of basis functions that

$$\begin{aligned}
&\phi_i(x_i, y_i) = 1 \Rightarrow a_1 x_i + a_2 y_i + a_3 = 1 \\
&\phi_i(x_{i-1}, y_{i-1}) = 0 \Rightarrow a_1 x_{i-1} + a_2 y_{i-1} + a_3 = 0 \\
&\phi_i(x_{i+1}, y_{i+1}) = 0 \Rightarrow a_1 x_{i+1} + a_2 y_{i+1} + a_3 = 0
\end{aligned}$$

In matrix form this is equivalent to solving for $[a_1\, a_2\, a_3]^T$ in

$$\begin{pmatrix} x_i & y_i & 1 \\ x_{i-1} & y_{i-1} & 1 \\ x_{i+1} & y_{i+1} & 1 \end{pmatrix} \begin{pmatrix} a_1 \\ a_2 \\ a_3 \end{pmatrix} = \begin{pmatrix} 1 \\ 0 \\ 0 \end{pmatrix} \tag{A.8}$$

Note that the matrix

$$\begin{pmatrix} x_i & y_i & 1 \\ x_{i-1} & y_{i-1} & 1 \\ x_{i+1} & y_{i+1} & 1 \end{pmatrix}$$

has a determinant equal to $2|K| > 0$ where $|K|$ is the area of triangle K, since

$$|K| = \frac{1}{2} \det \begin{pmatrix} x_{i-1} - x_i & y_{i-1} - y_i \\ x_{i+1} - x_i & y_{i+1} - y_i \end{pmatrix}$$

So (A.8) has a unique nonzero solution $[a_1\, a_2\, a_3]^T$. And every basis function ϕ_i is uniquely defined in each triangular element containing vertex (x_i, y_i), while it equals zero over trianglular element K that does not contain vertex (x_i, y_i).

However we are not going to compute the coefficients in (A.8) explicitly to assemble mass and stiffness matrices, because it leads to cumbersome and messy expressions. Instead we first seek to transform any triangular element K under consideration to a reference triangle K_0, where K_0 is spanned by its three vertices $(\hat{x}_1, \hat{y}_1) = (1, 0)$, $(\hat{x}_2, \hat{y}_2) = (0, 1)$ and $(\hat{x}_3, \hat{y}_3) = (0, 0)$. And we use $\hat{\mathbf{x}} = (\hat{x}, \hat{y})^T$ as a vector in the reference triangle's coordinate.

For any such triangular element K in xy-coordinates, we can treat it as the image of K_0 in $\hat{x}\hat{y}$-coordinates under an affine map $F : K_0 \to K$

$$\begin{aligned}
F(1, 0) &= (x_{i-1}, y_{i-1})^T \\
F(0, 1) &= (x_{i+1}, y_{i+1})^T \\
F(0, 0) &= (x_i, y_i)^T
\end{aligned}$$

where

$$F(\hat{\mathbf{x}}) = Q^T \hat{\mathbf{x}} + c$$

with

$$Q = \begin{pmatrix} x_{i-1} - x_i & y_{i-1} - y_i \\ x_{i+1} - x_i & y_{i+1} - y_i \end{pmatrix}, \qquad \text{and} \qquad c = (x_i, y_i)^T$$

Let u be arbitrary function of x, y. If we define $\hat{u}(\hat{\mathbf{x}}) = u(F(\hat{\mathbf{x}}))$, then

$$\hat{\nabla} \hat{u} = \begin{pmatrix} \dfrac{\partial \hat{u}}{\partial \hat{x}} \\ \dfrac{\partial \hat{u}}{\partial \hat{x}} \end{pmatrix} = \begin{pmatrix} \dfrac{\partial \hat{u}}{\partial x}\dfrac{\partial x}{\partial \hat{x}} + \dfrac{\partial \hat{u}}{\partial y}\dfrac{\partial y}{\partial \hat{x}} \\ \dfrac{\partial \hat{u}}{\partial x}\dfrac{\partial x}{\partial \hat{y}} + \dfrac{\partial \hat{u}}{\partial y}\dfrac{\partial y}{\partial \hat{y}} \end{pmatrix} = \begin{pmatrix} \dfrac{\partial x}{\partial \hat{x}} & \dfrac{\partial y}{\partial \hat{x}} \\ \dfrac{\partial x}{\partial \hat{y}} & \dfrac{\partial y}{\partial \hat{y}} \end{pmatrix} \begin{pmatrix} \dfrac{\partial \hat{u}}{\partial x} \\ \dfrac{\partial \hat{u}}{\partial y} \end{pmatrix} = Q \nabla u$$

and $\mathrm{d}x\,\mathrm{d}y = |\det(Q)|\,\mathrm{d}\hat{x}\,\mathrm{d}\hat{y}$.

First consider assembling mass and stiffness matrices over an arbitrary triangular element K consisting of (x_{i-1}, y_{i-1}), (x_i, y_i) and (x_{i+1}, y_{i+1}). We convert xy-coordinates to $\hat{x}\hat{y}$-coordinates to get

$$M^K_{jk} = \int_K \phi_j \phi_k \,\mathrm{d}x\,\mathrm{d}y = \int_{K_0} \hat{\phi_j}\hat{\phi_k} |\det Q|\,\mathrm{d}\hat{x}\,\mathrm{d}\hat{y}$$

and

$$H^K_{jk}(u) = \int_K (\hat{\Phi}_u \nabla\phi_j)\cdot\nabla\phi_k \,\mathrm{d}x\,\mathrm{d}y = \int_{K_0} (\hat{\Phi}_u Q^{-1}\hat{\nabla}\hat{\phi_j})\cdot(Q^{-1}\hat{\nabla}\hat{\phi_k})|\det Q|\,\mathrm{d}\hat{x}\,\mathrm{d}\hat{y}$$

where these terms are nonzero only if $j,k = i-1, i, i+1$ and $\hat{\phi_j}$'s are basis functions in $\hat{x}\hat{y}$-coordinates defined over the reference triangle K_0. Since under the affine map F

$$(x_{i-1}, y_{i-1}) \to (1,0), \qquad (x_i, y_i) \to (0,0) \quad \text{and} \quad (x_{i+1}, y_{i+1}) \to (0,1)$$

$\hat{\phi_{i-1}}$ in $\hat{x}\hat{y}$-coordinates will be

$$\hat{\phi_{i-1}} = a_1\hat{x} + a_2\hat{y} + a_3$$

where a_1, a_2, a_3 are constant and satisfy

$$\begin{pmatrix} 1 & 0 & 1 \\ 0 & 1 & 1 \\ 0 & 0 & 1 \end{pmatrix} \begin{pmatrix} a_1 \\ a_2 \\ a_3 \end{pmatrix} = \begin{pmatrix} 1 \\ 0 \\ 0 \end{pmatrix}$$

which yields $a_1 = 1, a_2 = a_3 = 0$. Hence $\hat{\phi_{i-1}} = \hat{x}$.

Also $\hat{\phi_i}$ in $\hat{x}\hat{y}$-coordinates will be

$$\hat{\phi_i} = b_1\hat{x} + b_2\hat{y} + b_3$$

where b_1, b_2, b_3 are constant and satisfy

$$\begin{pmatrix} 1 & 0 & 1 \\ 0 & 1 & 1 \\ 0 & 0 & 1 \end{pmatrix} \begin{pmatrix} b_1 \\ b_2 \\ b_3 \end{pmatrix} = \begin{pmatrix} 0 \\ 0 \\ 1 \end{pmatrix}$$

which yields $b_1 = -1, b_2 = -1, b_3 = 1$. Hence $\hat{\phi_i} = 1 - \hat{x} - \hat{y}$.

Similarly we have that $\hat{\phi_{i+1}} = \hat{y}$.

It is readily shown that

$$\int_{K_0} \hat{x}\,\mathrm{d}\hat{x}\,\mathrm{d}\hat{y} = \int_{K_0} \hat{y}\,\mathrm{d}\hat{x}\,\mathrm{d}\hat{y} = \frac{1}{6}$$

$$\int_{K_0} \hat{x}^2\,\mathrm{d}\hat{x}\,\mathrm{d}\hat{y} = \int_{K_0} \hat{y}^2\,\mathrm{d}\hat{x}\,\mathrm{d}\hat{y} = \frac{1}{12}$$

$$\int_{K_0} \hat{x}\hat{y}\,\mathrm{d}\hat{x}\,\mathrm{d}\hat{y} = \frac{1}{24}, \quad \int_{K_0} \mathrm{d}\hat{x}\,\mathrm{d}\hat{y} = \frac{1}{2}.$$

Now we can define a 3×3 local mass matrix M_K such that

$$(M_K)_{jk} = M^K_{i-2+j,i-2+k}$$

with $j, k = 1, 2, 3$. Then

$$M_K = \begin{pmatrix} M^K_{i-1,i-1} & M^K_{i-1,i} & M^K_{i-1,i+1} \\ M^K_{i,i-1} & M^K_{i,i} & M^K_{i,i+1} \\ M^K_{i+1,i-1} & M^K_{i+1,i} & M^K_{i+1,i+1} \end{pmatrix} = \frac{|\det Q|}{24} \begin{pmatrix} 2 & 1 & 1 \\ 1 & 2 & 1 \\ 1 & 1 & 2 \end{pmatrix}$$

From the above discussions it is also readily seen that all the gradients in $\hat{x}\hat{y}$-coordinates are

$$\hat{\nabla}\hat{\phi_{i-1}} = \begin{pmatrix} 1 \\ 0 \end{pmatrix}, \qquad \hat{\nabla}\hat{\phi}_i = \begin{pmatrix} -1 \\ -1 \end{pmatrix} \quad \text{and} \quad \hat{\nabla}\hat{\phi}_{i+1} = \begin{pmatrix} 0 \\ 1 \end{pmatrix}$$

Also we can define a local stiffness matrix $H_K(u)$ such that

$$\begin{aligned} (H_K(u))_{jk} &= H^K_{i-2+j,i-2+k}(u) \\ &= \int_{K_0} (\hat{\Phi}_u Q^{-1} \hat{\nabla}\hat{\phi}_{i-2+j}) \cdot (Q^{-1}\hat{\nabla}\hat{\phi}_{i-2+k}) |\det Q| \, \mathrm{d}\hat{x} \, \mathrm{d}\hat{y} \end{aligned} \tag{A.9}$$

with $j, k = 1, 2, 3$ and $Q, \hat{\nabla}\hat{\phi}_{i-1}, \hat{\nabla}\hat{\phi}_i, \hat{\nabla}\hat{\phi}_{i+1}$ are constant and defined as above.

Note that Φ_u is a function of x, y and $\hat{\Phi}_u$ is a function of $\hat{x}, \hat{y}$. To compute exactly what the integral in (A.9) is, we let the integrand be $p(\hat{x}, \hat{y})$ and use the following quadrature rule

$$\int_{K_0} p \, \mathrm{d}\hat{x} \, \mathrm{d}\hat{y} \approx \frac{1}{3} \left(p(\frac{1}{2}, \frac{1}{2}) + p(\frac{1}{2}, 0) + p(0, \frac{1}{2}) \right)$$

where in $\hat{x}\hat{y}$-coordinates $(\frac{1}{2}, \frac{1}{2}), (\frac{1}{2}, 0), (0, \frac{1}{2})$ correspond to the midpoints of three sides of triangle K_0. This scheme is third order accurate, i.e. the error is $O(h^3)$ where h is the longest distance within triangle.

With each triangular element K of the triangulation $\mathscr{T}_N$, we can find out its corresponding local mass matrix M_K and local stiffness matrix $H_K(u)$. These, in turn, help in assembling the mass matrix M and $H(u)$. We follow the steps below to compute M and H_u.

Suppose initially $i = 1$ and $M, H(u)$ are zero matrices.

(1) If $i > L$ quit, else consider triangle K_i. Let its three vertices be respectively $(x_{j_1}, y_{j_1}), (x_{j_2}, y_{j_2})$ and (x_{j_3}, y_{j_3}), and let them be mapped by F to $(\hat{x}_1, \hat{y}_1) = (1, 0), (\hat{x}_2, \hat{y}_2) = (0, 1)$ and $(\hat{x}_3, \hat{y}_3) = (0, 0)$ in the reference triangle K_0.

(2) Compute M_{K_i} and $H_{K_i}(u)$.

(3) Let $M_{j_l,j_k} = M_{j_l,j_k} + (M_{K_i})_{lk}$ and $H_{j_l,j_k}(u) = H_{j_l,j_k}(u) + (H_{K_i})_{lk}(u)$ with $l, k = 1, 2, 3$.

(4) Add i by 1 and go to step (1).